

PROCESSING AND TRIBOLOGICAL BEHAVIOUR OF FLYASH-ILLMENITE COATING

A

**THESIS SUBMITTED IN PARTIAL FULFILLMENT
OF THE REQUIREMENT FOR THE DEGREE OF**

MASTER OF TECHNOLOGY

in

Metallurgical & Materials Engineering

By

SATYABATI DAS



**DEPARTMENT OF METALLURGICAL & MATERIALS ENGINEERING
NATIONAL INSTITUTE OF TECHNOLOGY, ROURKELA**

2008

PROCESSING AND TRIBOLOGICAL BEHAVIOUR OF FLYASH-ILLMENITE COATING

A

**THESIS SUBMITTED IN PARTIAL FULFILLMENT
OF THE REQUIREMENT FOR THE DEGREE OF**

MASTER OF TECHNOLOGY

in

Metallurgical & Materials Engineering

By

SATYABATI DAS

Under the Guidance of

Prof. S.C.Mishra

&

Under the Co-Guidance of

Prof. S.Sarkar



**DEPARTMENT OF METALLURGICAL & MATERIALS ENGINEERING
NATIONAL INSTITUTE OF TECHNOLOGY, ROURKELA**

2008



Department of Metallurgical and Materials Engineering

National Institute of Technology

Rourkela - 769008

CERTIFICATE

This is to certify that thesis entitled, “**PROCESSING AND TRIBOLOGICAL BEHAVIOUR OF FLYASH-ILLMENITE COATING**” submitted by **Miss SATYABATI DAS** in partial fulfillment of the requirements for the award of **Master of Technology Degree in Metallurgical and Materials Engineering** at National Institute of Technology, Rourkela (Deemed University) is an authentic work carried out by her under our supervision and guidance.

To the best of our knowledge, the matter embodied in this thesis has not been submitted to any other university/ institute for award of any Degree or Diploma.

Prof. S.Sarkar

Asst.professor

Dept.of Metallurgical& Materials Engg.

National Institute of Technology

Rourkela

Prof. S.C. Mishra

Professor

Dept.of Metallurgical &Materials Engg

National Institute of Technology

Rourkela

Acknowledgement

I avail this opportunity to extend my hearty indebtedness to my guide **Prof. S. C. Mishra** for his invaluable guidance, untiring efforts and meticulous attention at all stages during my course of work. I would also like to convey my deep regards to my co-guide **Prof.S.Sarkar** for his patience, constant motivation and regular monitoring of the work and inputs, for which this work has come to fruition.

I express my grateful thanks to **Prof. G. S. Agarwal, Head of the Department** for providing me the necessary facilities in the department. I am also grateful to **Prof.B.B.Verma & Prof.A.K.Panda, M. Tech. co-ordinators**, for their constant concern and encouragement for execution of this work.

I also express my sincere gratitude to **Prof. Alok Satapathy, Dept. of Mechanical Engineering** for his timely help during the course of work.

I am thankful to **Ms Tabasum ara Begum , Sri Hemram, Sri Udayanath Sahu, Sri Rajesh Pattnaik, and Sri Samir Pradhan**, Metallurgical & Materials Engineering, Technical assistants, for their co-operation in experimental work.

Special thanks to **Ms Sangeeta Pattanaik & Sri Nadiya Bihari Nayak** department of Metallurgical and Materials Engineering for being so supportive and helpful in every possible way.

SATYABATI DAS

CONTENTS

	Page No.
CERTIFICATE.....	i
ACKNOWLEDGEMENT.....	ii
CONTENTS.....	iii
ABSTRACT.....	ix
LIST OF FIGURES.....	xi
LIST OF TABLES.....	xiv
INTRODUCTION.....	1
1.1 Background	2
1.2 Objectives of the present piece of investigation.....	7
LITERATURE SURVEY.....	8
2.1 Preamble.....	9
2.2 Surface Engineering.....	9
2.3 Surface modification.....	10

2.4 Techniques of surface modification.....	10
2.5 Thermal spraying	11
2.6 Plasma spraying.....	15
2.7 Industrial applications of plasma spraying.....	20
2.7 i) Textile Industry.....	21
2.7 ii) Paper and printing industry.....	21
2.7 iii) Automotive Industry and the production of Combustion engines	22
2.7 iv) Glass Industry	22
2.7 v) Electrochemical Industry.....	22
2.7 vi) Hydraulic machines and mechanisms.....	23
2.7 vii) Rolling mills and foundry	23
2.7 viii) High Temperature wears resistance coatings on Slide Gate Plates.....	23
2.8 ix) Chemical Plants.....	24
2.8 x) Aircraft Jet engines.....	24
2.8 Wear.....	24

2.9 Types of wear.....	25
2.9.1 Abrasive wear	25
2.9.2 Adhesive wear	26
2.9.3 Erosive wear	26
2.9.4 Surface fatigue wear.....	27
2.9.5 Corrosive wear.....	28
2.10 Symptoms of wear	28
2.11 Recent trends in metal wear research.....	30
2.12 Wear resistant coatings.....	32
2.11.1 Oxide Coatings	32
2.12.1a) Chromia (Cr_2O_3) Coatings.....	32
2.12.2b) Zirconia (ZrO_2) Coatings.....	33
2.12.2c) Titania (TiO_2) Coatings.....	34
2.12.2d) Alumina (Al_2O_3) Coatings.....	35
2.12.2e) Alumina Titania Coatings.....	37
2.12.2f) Flyash coating.....	40

2.13 Erosion wear of ceramic coatings.....	41
--	----

EXPERIMENTAL SET UP & METHODOLOGY.....45

3.1 Introduction.....	46
-----------------------	----

3.2 Development of the coatings.....	46
--------------------------------------	----

3.2.1. Preparation of powders.....	46
------------------------------------	----

3.2.2. Preparation of substrate.....	46
--------------------------------------	----

3.2.3 Plasma spray coating deposition.....	47
--	----

3.3 Characterization of powder.....	51
-------------------------------------	----

3.3.1 Particle Size Analysis	51
------------------------------------	----

3.4 Characterization of coatings.....	51
---------------------------------------	----

3.4.1 Evaluation of Coating Deposition Efficiency.....	51
--	----

3.4.2 Evaluation of Coating Interface Bond Strength.....	52
--	----

3.4.3 Coating Thickness Measurement.....	53
--	----

3.4.4 Porosity Measurement.....	53
---------------------------------	----

3.4.5 Microhardness Measurement.....	53
3.4.6 X-Ray Diffraction Studies.....	54
3.4.7 Scanning Electron Microscopic Studies.....	54
3.5 Erosion wear behaviour of coatings.....	54
RESULTS AND DISCUSSION.....	57
4.1 Introduction.....	58
4.2 Particle size analysis.....	58
4.3 Coating deposition efficiency.....	59
4.4 Coating adhesion strength.....	61
4.5 Coating thickness.....	63
4.6 Coating porosity.....	64
4.7 Coating hardness.....	65
4.8 XRD phase composition analysis.....	67
4.9 Erosion wear behaviour of coatings	68
4.10 Microstructural Investigation.....	78

4.10.1 Powder morphology.....	78
4.10.2 Microstructure of coating surface.....	79
4.10.3 Interface Morphology.....	80
4.10.4 Morphology of the Erodent.....	82
4.10.5 Worn surfaces.....	82
CONCLUSIONS.....	85
Scope for Future Work	88
REFERENCES.....	89
PUBLICATIONS.....	103

ABSTRACT

A unique way to tailor the surface properties of a component, suit to a specific operating environment without sacrificing the bulk characteristics of the structure, is by deposition of a surface coating. Thermal spraying processes have been known for producing hard overlay coatings especially ceramic coatings, to improve tribological properties. Amongst the thermal spray techniques conventional atmospheric plasma spray technique is widely used to develop coatings of ceramic materials. Though plasma spray coatings deposition is very promising and drawn extensive attention, a major hindrance to its wide spread application is due to high cost of spray grade powders. To overcome this problem, research has been carried out to find the possibility of using some low grade ore mineral and industrial wastes as coating material so that the cost of raw material used for coating can be minimized. In this work plasma spray deposition of alumino-silicate composite coatings onto metal substrates is done using industrial waste i.e. fly ash with addition of illmenite, a titanium bearing ore mineral. To overcome the poor interface mechanical properties arising due to the mismatch of thermal expansion coefficients of ceramics and metals, generally metallic bond coat is provided onto the substrate for better interface adherence of ceramic coating. An improvement of coating properties when pre-mixed metal–ceramic powders are used (instead of using a bond coat), has already been reported . It is well established that, addition of titania to alumina provide dense coating & better adherence on substrate. Therefore, illmenite a low grade ore mineral plentifully available in India, is premixed with fly ash so as to further reduce the raw material cost.

Using atmospheric plasma spraying system coatings are deposited on metal substrates at different operating power levels of the plasma torch and then characterization of the coatings is carried out. The particle sizes of the raw materials used for coating are characterized using Laser particle size analyzer. Deposition efficiency is an important factor that determines the techno-economics of the process. It is evaluated for the deposited coatings. Coating interface bond strength is evaluated using coating pull out method, confirming to ASTM C-633 standard. In view of tribological applications, hardness is one of the most required mechanical properties. Micro-hardness measurement is done on the polished cross section of the samples (on the optically distinguishable phases of the coating), using Leitz Micro-Hardness Tester. Coating

porosity is measured by image analysis technique. For ascertaining the phases present and phase changes / transformation taking place during plasma spraying, XRD analysis is made. Coating surface & interface morphology is studied with Scanning Electron Microscope. To study the suitability of the coatings for wear resistance application, wear properties of these coatings are studied. The erosion wear behaviour of these coatings is evaluated with solid particle erosion tests under various operating conditions. In order to control the wear loss in such a process, one of the challenges is to recognize parameter interdependencies; correlations and their individual effects on wear so that the coating can be useful for tribological application. Statistical analysis of the experimental results using Taguchi experimental design is presented. Spraying parameters such as impact angle, impact velocity, stand off distance, size of the erodent are identified as the significant factors affecting the coating erosion wear. This work establishes that, Flyash-illmenite mixture can be used as a potential coating material suitable for depositing plasma spray coating. It also opens up a new pathway for value added utilization of this industrial waste and low grade ore mineral.

LIST OF FIGURES

- 2.1** Various forms of surface modification technologies
- 2.2** Schematic of coating formation
- 2.3** Two basic ways of generating heat in thermal spray processes
- 2.4** Schematic of Plasma spraying
- 2.5** Schematic representations of the abrasion wear mechanism
- 2.6** Schematic representations of the adhesive wear mechanism
- 2.7** Schematic representations of the erosive wear mechanism
- 2.8** Schematic representations of the surface fatigue wear mechanism
- 2.9** Model of the effects of impact parameters on exponents k_2 and k_3
- 2.10** Schematic diagram of Model of erosion wear (a) at 90° (b) at 30°
- 3.1** General arrangement of the plasma spraying equipment
- 3.2** The schematic of coating development by plasma spraying
- 3.3** Jig used for the test
- 3.4** Specimen under tension

3.5 Adhesion test with Instron 1195 UTM

3.6 Schematic diagram of the erosion test rig

3.7 Erosion test set up

4.1 Particle size distribution of fly ash-illmenite feed stock

4.2 Deposition efficiency of fly ash-illmenite coatings made at different power level on mild steel substrate.

4.3 Adhesion strength of fly ash-illmenite coatings on different substrates

4.4 Variation of fly ash-illmenite coating thickness values with torch input power for mild steel substrate

4.5 Variation of coating porosity of fly ash-illmenite with torch input power

4.6 X-Ray Diffractogram of fly ash-illmenite raw powder and coating deposited at 11kW, 15kW, 18kW, 21kW power level.

4.7 Erosion wear rate of coatings under different test conditions

4.8 Relative effect of main factors on erosion rate of the coatings made at 11kW.

4.9 Relative effect of main factors on erosion rate of the coatings made at 18 Kw

4.10 Variation of Coating mass loss with time, for 400 μm size (dry silica sand) erodent.

4.11 Variation of Coating mass loss with time; for 200 μm size (SiC) erodent.

4.12 Variation of Erosion rate with time for the sample eroded with sand

4.13 Variation of Erosion rate with time for the sample eroded with silicon carbide

4.14 SEM micrograph of flyash-illemnite raw powders (i.e. feed stock)

4.15 Surface Morphology of fly ash-illmenite coatings deposited at different power level i.e. (a) 11kW (b) 15kW(c) 18kW, (d) 21kW

4.16 Interface morphology of fly ash-illmenite coatings deposited on mild steel substrates, at (a) 11kW (b) 15kW (c) 18 kW (d) 21kW power level

4.17 Surface morphology of (a) dry silica sand and (b) silicon carbide erodent

4.18 Micrographs of eroded surfaces of coatings deposited at (a) 11kW and (b) 18kW for 90° angle of impact; (c)11 kW and (d)18kW for 60° angle of impact and (e)11kW and (f)18kW for 30° angle of impact

LIST OF TABLES

2.1 Thermal-spraying processes

2.2 Symptoms and appearance of different types of wear

2.3 Priority in wears research

2.4 Type of wear in industry

2.5 Physical properties of Titania

2.6 Physical properties of Alumina

3.1 Operating parameters during coating deposition

4.1 Coating deposition efficiency of fly ash-illmenite coatings and mildsteel substrates

4.2 Adhesion strength values of fly ash-illmenite coating at different power levels

4.3 Thickness values of fly ash-illmenite coatings made at different power level for mild steel substrates

4.4 Porosity of coating for different power levels

4.5 Hardness on the coating cross section for the coating

4.6 Control factors and selected test levels

4.7 Experimental layout and erosion wear rate under different test conditions for coatings at 11kW and 18kW power levels

4.8 S/N ratios for coating erosion wear rate at 11kW

4.9 S/N ratios for coating erosion wear rate at 18kW

4.10 Response Table for Signal to Noise Ratios (for 11 kW)

4.11 Response Table for Signal to Noise Ratios (for 18 kW)

Chapter 1

INTRODUCTION

CHAPTER 1

INTRODUCTION

1.1 BACKGROUND

Modern technology has placed increasing stresses on the material used for a variety of technological uses. Both the uses and the stresses have probably grown at a greater rate than the number of materials that can be used to meet them. This is particularly true for structural materials which are almost entirely metallic. Although much has been done by producing new alloys with improved properties, there is a limit to the protection that can be afforded by this means alone. For this reason coatings have played an increasing role in protecting the structural metals from environmental attack.

It can be conveniently be classified into a few types-

(i)Wear: Wear occurs when material is removed from a surface by abrasion, i.e, the moving of one surface over another which, in severe cases, may result in detachment of the coating, and by erosion, the loss of material from the impact of high velocity particles.

(ii)Chemical attack: This may occur both in gaseous and liquid phase, particularly at high temperatures and includes attack by ambient oxygen. Corrosive liquids include acids and bases, molten salts and slags, i.e. molten oxides and silicates. Chemical attack may include a combination of these, such as occurs in marine gas turbines when ambient oxygen droplets of sea salt and sulfur impurities in the fuel combine to form molten sodium sulfate which attacks the metallic turbine blade coating.

(iii)High Temperatures: Structural materials may undergo undesirable changes when their temperature is raised, such as mechanical weakening or increased susceptibility to other kinds of attack. One approach to this problem is the application of thermal barrier coatings which reduce the substrate temperature. Another is the use of ablation coatings which reduce the surface temperature of space vehicles reentering the earth's atmosphere by removing excess heat as the heat of vaporization of the coating material.

The types of materials used for coatings are relatively few-metals and a few classes of inorganic (ceramic) compound (oxides, carbides, borides and nitrides) singly or

in combination. In selecting a coating material it is necessary to consider the uses to which it will be put. Factors to be considered include:

- (a) the properties of the coating material itself-its melting point, hardness, vapor pressure, density and thermal expansion coefficient
- (b) the resistance of the coating material to the attack expected
- (c) the compatibility of the coating and substrate over the temperature range of the expected application. This includes the minimizing of thermal stresses, by matching thermal expansion coefficients, and the provision of good coating-substrate adhesion. Some interdiffusion may be desirable, but an excessive amount, such as may occur with silicon plating at high temperatures, may only lead to bulk diffusion and alloy formation; and
- (d) the cost ultimately whether or not a particular coating will be used, depends on the trade-off between the benefits to be gained and the additional cost to be incurred.

Driven by technological need and fuelled by exciting possibilities, novel methods for applying coatings, improvements in existing methods and new applications have proliferated in recent years. Surface modification technologies have grown rapidly, both in terms of finding better solutions and in the number of technology variants available, to offer a wide range of quality and cost. The significant increase in the availability of coating process of wide ranging complexities that are capable of depositing a plethora of coatings and handling components of diverse geometry today ensures that components of all imaginable shape and size can be coated economically. A protective coating deposited to act as a barrier between the surfaces of the component and the aggressive environment that it is exposed to during operation is now, globally acknowledged to be an attractive means to significantly reduce/suppress damage to the actual component by acting as the first line of defense. Coating is a layer of material formed naturally or synthetically or deposited artificially on the surface of an object made of another material with the aim of obtaining required technical or decorative properties. Existing surface treatment processes fall under three broad categories:

(a) Overlay Coatings:

This category incorporates a very wide variety of coating processes wherein a material different from the bulk is deposited on the substrate. The coating is distinct from the substrate in the as-coated condition and there exists a clear boundary at the substrate/coating interface. The adhesion of the coating to the substrate is a major issue.

(b) Diffusion Coatings:

Chemical interaction of the coating-forming element(s) with the substrate by diffusion is involved in this category. New elements are diffused into the substrate surface, usually at elevated temperatures so that the composition and properties of outer layers are changed as compared to those of the bulk.

(c) Thermal or Mechanical Modifications of Surfaces:

In this case, the existing metallurgy of the component surface is changed in the near-surface region either by thermal or mechanical means, usually to increase its hardness. The type of coating to be provided depends on the application. There are many techniques available, e.g. electroplating, vapor depositions, thermal spraying etc.

Of all these techniques, thermal spraying is popular for its wide range of applicability, adhesion of coating with the substrate and durability. It has gradually emerged as the most industrially useful method of developing a variety of coatings, to enhance the quality of new components as well as to reclaim worn/wrongly machined parts. The type of thermal spraying depends on the type of heat source employed and consequently flame spraying (FS), high velocity oxy-fuel spraying (HVOF), plasma spraying (PS) etc. come under the umbrella of thermal spraying. Plasma spraying utilizes the exotic properties of the plasma medium to impart new functional properties to conventional and non-conventional materials and is considered as one highly versatile and technologically sophisticated thermal spraying technique instead of having relatively high price of the sprayable consumables.

Plasma spraying, one of the thermal spraying processes, is increasingly popular owing to its versatility in spraying a large number of materials and is being researched well. It is a very large industry with applications in corrosion, abrasion and temperature resistant coatings and the production of monolithic and near net shapes [1]. The process can be applied to coat on variety of substrates of complicated shape and size using

metallic, ceramic and /or polymeric consumables. The production rate of the process is very high and the coating adhesion is also adequate. Since the process is almost material independent, it has a very wide range of applicability, e.g., as thermal barrier coating, wear resistant coating etc. Thermal barrier coatings are provided to protect the base material, e.g., internal combustion engines, gas turbines etc. at elevated temperatures. Zirconia (ZrO_2) is a conventional thermal barrier coating material. As the name suggests, wear resistant coatings are used to combat wear especially in cylinder liners, pistons, valves, spindles, textile mill rollers etc. alumina (Al_2O_3), titania (TiO_2), and zirconia (ZrO_2) are some of the conventional wear resistant coating materials [2].

One major limitation of the process is a relatively high price of the plasma sprayable consumables. Plasma spraying has certain unique advantages over other competing surface engineering techniques. By virtue of the high temperature (10,000-15,000°K) and high enthalpy available in the thermal plasma jet, any powder, which melts without decomposition or sublimation, can be coated keeping the substrate at room temperature. The coating process is fast and the thickness can go from a few tens of microns to a few mm. Very intricate shapes of the materials can be coated by this method. Plasma spraying is extensively used in hi-tech industries like aerospace, nuclear energy as well as conventional industries like textiles, chemicals, plastics and paper mainly as wear resistant coatings in crucial components.

Plasma spraying is a surface modification technique that combines particle melting, rapid solidification and consolidation in a single process. Because of their higher strength-to-weight ratio and superior wear-resistant properties, ceramics are preferred in most tribological applications. The ceramic materials can be applied for the overlay coating due to the higher gas enthalpy of the thermal plasma jet. The suitability of a ceramic coating on metal substrates depends on (i) the adherence strength at coating-substrate interface, and (ii) stability at operating conditions.

Silica and alumino-silicate bricks have been preferred as refractory materials in many industrial applications due to their high wear resistance and high load bearing capacity at high temperatures. In the present case the plasma spray deposition of alumino-silicate composite coatings onto metal substrates is done using industrial waste such as fly ash so that the limitation in applications/adoption of plasma spray coatings

due to the high cost of the spray grade powders required for coating can be addressed, but the adherence of the coating was not satisfactory [3]. To overcome difficulties such as poor interface mechanical properties, arising due to the mismatch between the thermal expansion coefficients of ceramics and metals, metallic bond coat is provided onto the substrate for better interface adherence of the coating [4]. Studies have shown an improvement of coating properties when pre-mixed metal– ceramic powders are used [5]. In this case ilmenite, a low grade ore mineral which is also plentifully available in India, is used as the premixed metal so as to further decrease the cost of raw material of coating. Conventional atmospheric plasma spray technique has been used to develop coatings of these materials [6,7]. Coatings of various operating parameters were prepared and characterized. .

Here the coatings (fly ash-ilmenite) have been characterized for their hardness, porosity, adhesion strength and microstructure. The significant phase changes associated with the plasma processing during the coating deposition have been studied. In addition, the coating deposition efficiencies at various operating conditions have also been evaluated.

To study the suitability of the coatings for wear resistance application, wear properties of these coatings is evaluated. The erosion wear behavior is one of the less studied areas in case of ceramic coatings. This aspect is studied in the present work using a solid particle erosion test and the capabilities of the coatings to sustain the erosive attack have been assessed. Erosion wear tests were carried out on the coatings to ensure its applicability under various operating conditions. In order to control the wear loss in such a process, one of the challenges is to recognize parameter interdependencies; correlations and their individual effects on wear so that the coating can be useful for tribological application. A qualitative analysis of the experimental results with regard to erosion wear rate using statistical techniques is presented. The analysis is aimed at identifying the operating variables/factors significantly influencing the erosion wear rate of fly ash-ilmenite on metals. Factors are identified in accordance to their influence on the coating erosion wear rate.

1.2 OBJECTIVES OF THE PRESENT PIECE OF INVESTIGATION

The objective of the present investigation is as follows:

- To explore the coating potential of fly ash-illmenite on metal substrates by plasma spraying.
- To develop a series of plasma sprayed coatings from fly ash-illmenite on metal substrates and to find coating deposition efficiency, porosity and thickness etc.
- X-ray diffraction studies for phase analysis.
- Micro-structural characterization to evaluate the soundness of the coatings.
- Mechanical properties viz. to evaluate the micro-hardness and interface bond strength of the coatings.
- To assess the capabilities of the coatings to combat wear with a special reference to solid particle erosion wear.
- To analyze the experimental results using statistical techniques so as to identify the significant factors/interactions influencing the coating erosion wear rate.

Chapter 2

LITERATURE SURVEY

CHAPTER 2

LITERATURE SURVEY

2.1 PREAMBLE

This chapter deals with the literature survey of the broad topic of interest namely the development of surface modification technology for tribological applications. This treatise embraces various coating techniques with a special reference to plasma spraying, the coating materials and their characteristics. The performances of wear resistant coatings under various conditions have been reviewed critically along with the corresponding failure mechanisms. It also presents a review of the wear, types of wear, symptoms of wear and recent trends in metal wear research along with erosion wear behaviour of ceramic coatings, which is the material of interest in this work.

2.2 SURFACE ENGINEERING

Surface engineering is the sub-discipline of materials science which deals with the surface of solid matter. The surface phase of a solid interacts with the surrounding environment. This interaction can degrade the surface phase over time. Environmental degradation of the surface phase over time can be caused by wear, corrosion, fatigue and creep. Surface engineering involves altering the properties of the Surface Phase in order to reduce the degradation over time. This is accomplished by making the surface robust to the environment in which it will be used.

Surface engineering techniques are being used in the automotive, aerospace, missile, power, electronic, biomedical, textile, petroleum, petrochemical, chemical, steel, power, cement, machine tools, construction industries. Surface engineering techniques can be used to develop a wide range of functional properties, including physical, chemical, electrical, electronic, magnetic, mechanical, wear-resistant and corrosion-resistant properties at the required substrate surfaces. Almost all types of materials, including metals, ceramics, polymers, and composites can be coated on similar or dissimilar materials. In 1995, surface engineering was a £10 billion market in the United Kingdom. Coatings, to make surface life robust from wear and corrosion, was approximately half the market.

2.3 SURFACE MODIFICATION

Surface modification is a relatively new term that has come up in the last two decades or so to describe interdisciplinary activities aimed at tailoring the surface properties of engineering materials. The object of surface engineering is to upgrade their functional capabilities keeping the economic factors in mind [8]. 'Surface Engineering' is the name of the discipline - surface modification is the philosophy behind it. To elucidate the matter an example can be taken. Tungsten carbide cobalt composite is a very popular cutting tool material, and is well known for its high hardness and wear resistance. If a thin coating of TiN is applied on to the WC-Co insert, its capabilities increase considerably [9]. Actually a cutting tool, in action, is subjected to a high degree of abrasion, and TiN is more capable of combating abrasion. On the other hand, TiN is extremely brittle, but the relatively tough core of WC-Co composite protects it from fracture. Thus through a surface modification process we assemble two (or more) materials by the appropriate method and exploit the qualities of both [10]. It is a very versatile tool for technological development provided it is applied judiciously keeping the following restrictions in mind:

- (i) The technological value addition should justify the cost.
- (ii) The choice of technique must be technologically appropriate.
- (iii) The coating-surface treatment should not impair the properties of the bulk material.

2.4 TECHNIQUES OF SURFACE MODIFICATION

In recent years, there has been a paradigm shift in surface engineering from age-old electroplating to processes such as vapor phase deposition, diffusion, thermal spray & welding using advanced heat sources like plasma, laser, ion, electron, microwave, solar beams, pulsed arc, pulsed combustion, spark, friction and induction. Hence, today a large number of commercially available technologies are present in the industrial scenario. An overview of such technologies is presented below (Fig 2.1).

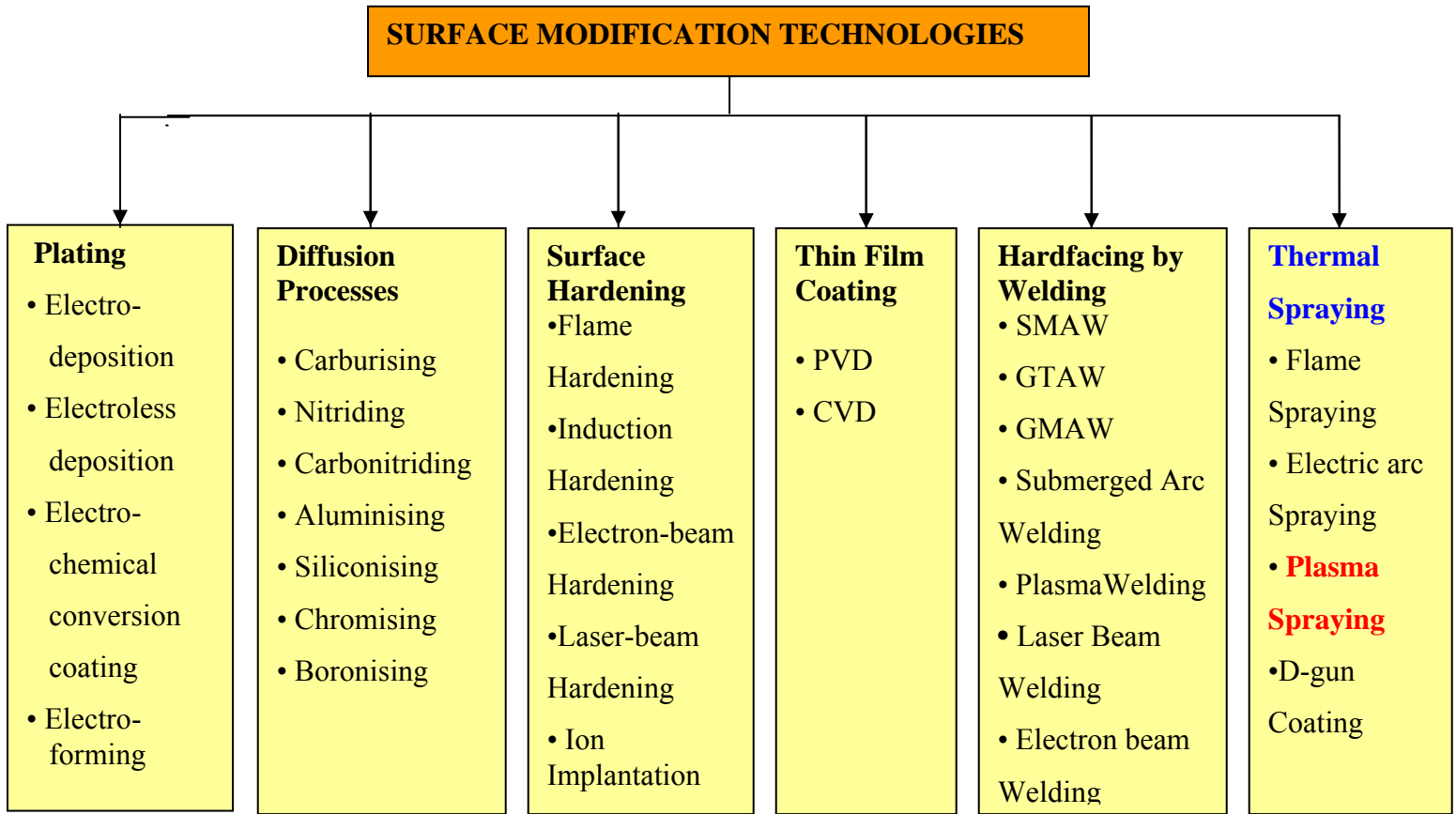


Fig 2.1 Various forms of surface modification technologies

2.5 THERMAL SPRAYING

Thermal spray processing is uniquely important to an ever-increasing engineering community, for its (i) improved spray footprint definition versus wide spray beam; (ii) high throughput versus competitive techniques; (iii) significantly improved process control; (iv) lower cost-per-mass of applied material, together with overall competitive economics. Thermal spray coatings have been produced for at least 40 years, but the last decade has seen a virtual revolution in the capability of the technology to produce truly high performance coatings of a great range of materials on many different substrates [11]. The principle behind thermal spray is to melt material feedstock (wire or powder) to accelerate the melt to impact on a substrate where rapid solidification and deposit build up occur. Thus, a heat source and a means of accelerating the material are required. Any material can be sprayed as long as it can be melted by the heat source employed and does not undergo degradation during heating [12]. This is pictured

schematically in Fig2.2 [13]. Here the feedstock material, in the form of a powder, is melted and propelled in the effluent of a flame. The high temperature for melting is achieved chemically (through combustion) or electrically (in arc); these melting methods also accelerate the molten particles to the target substrate, where the material solidifies, forming a deposit. The deposit is built up by successive impingement of these individual flattened particles or splats.

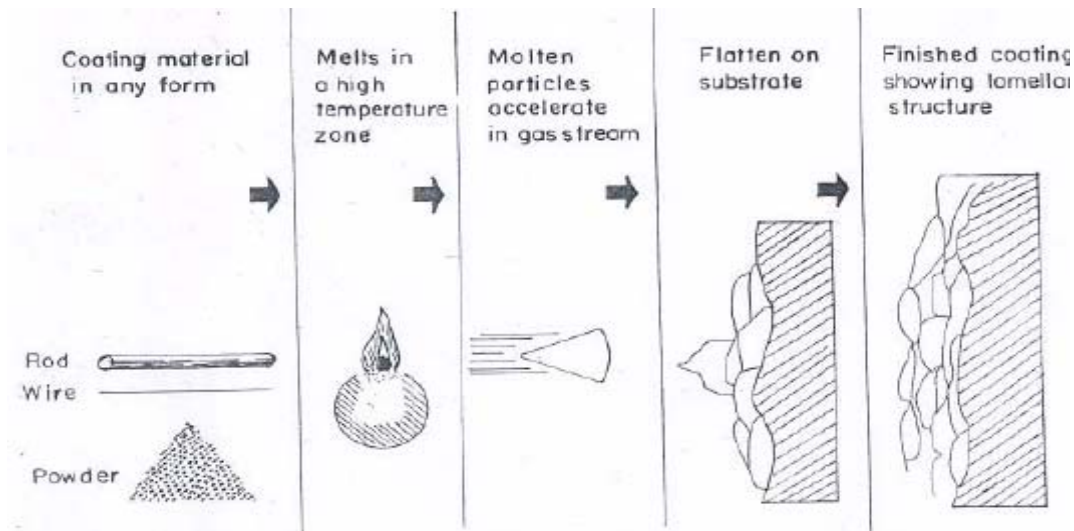
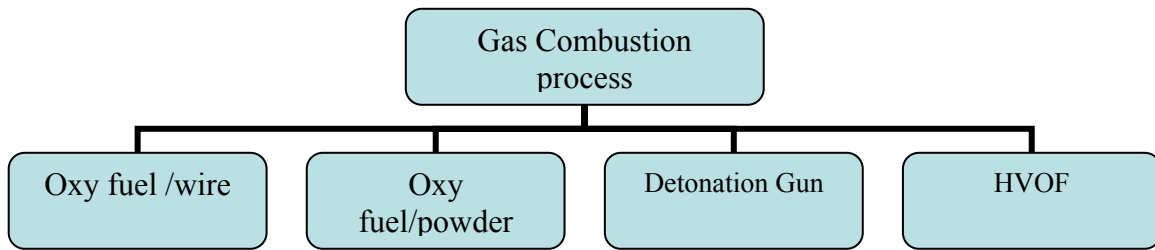
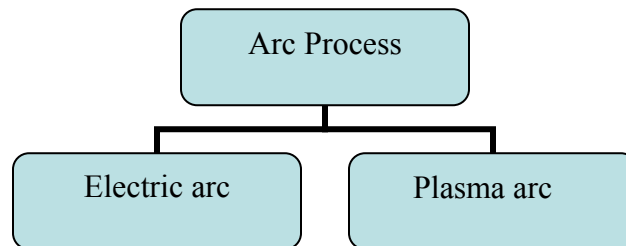


Fig 2.2 Schematic of coating formation

The nature of bonding at the coating-substrate interface is not completely understood. It is normally assumed that bonding occurs by the mechanical interlocking. Under this circumstance it is generally possible to ignore the metallurgical compatibility [12]. This is an extremely significant feature of thermal spraying. Another interesting aspect of thermal spraying is that the surface temperature seldom exceeds 200°C. Hard metal or ceramic coating can be applied to thermosetting plastics. Stress related distortion problems are also not so significant. The spraying action is achieved by the rapid expansion of combustion gases (which transfer the momentum to the molten droplets) or by a separate supply of compressed air. There are two basic ways of generating heat required for melting the consumables [14, 15]. They are (i) combustion of a fuel gas and (ii) high energy electric arc, shown in Fig.2.3.



(i)



(ii)

Fig. 2.3 Two basic ways of generating heat in thermal spray processes

Processes available for thermal spraying have been developed specifically for a purpose and fall into two categories-high and low energy processes. The key processes and their energy sources are summarized in Table 2.1 [15].

Table 2.1 Thermal-spraying processes

Processes		Energy sources	Different nomenclature
Low energy processes	Flame spraying	Chemical	Oxyfuel gas-powder spraying
			Oxyfuel gas-wire spraying
			Metallizing
	Arc spraying	Electrical	Electric arc spraying
			Twin-wire arc spraying
			Metallizing
High energy processes	Plasma spraying	Electrical	Air plasma spraying (APS)
			Vacuum plasma spraying (VPS)
			Low pressure plasma spraying (LPPS)
			Water stabilized plasma spraying (UWS)
			Inductive plasma spraying
	Detonation flame spraying	Chemical	D-gun
	High velocity oxyfuel spraying	Chemical	HVOF spraying
			High velocity oxygen fuel spraying
			High velocity flame spraying (HVFS)
			High velocity air fuel

2.6 PLASMA SPRAYING

Plasma spraying is the most versatile thermal spraying process as shown in Fig.2.4. An arc is created between thoria-tungsten cathode and an annular copper anode (both water cooled). Plasma generating gas is forced to pass through the annular space between the electrodes. While passing through the arc, the gas undergoes ionization in the high temperature environment resulting plasma. The plasma protrudes out of the electrode encasement in the form of a flame. The consumable material, in the powdered form, is poured into the flame in metered quantity. The powders melt immediately and absorb the momentum of the expanding gas and rush towards the target to form a thin deposited layer.

The next layer deposits onto the first immediately after and thus the coating builds up layer by layer [10, 12]. The temperature in the plasma arc can be as high as 10,000°C and it is capable of melting anything.

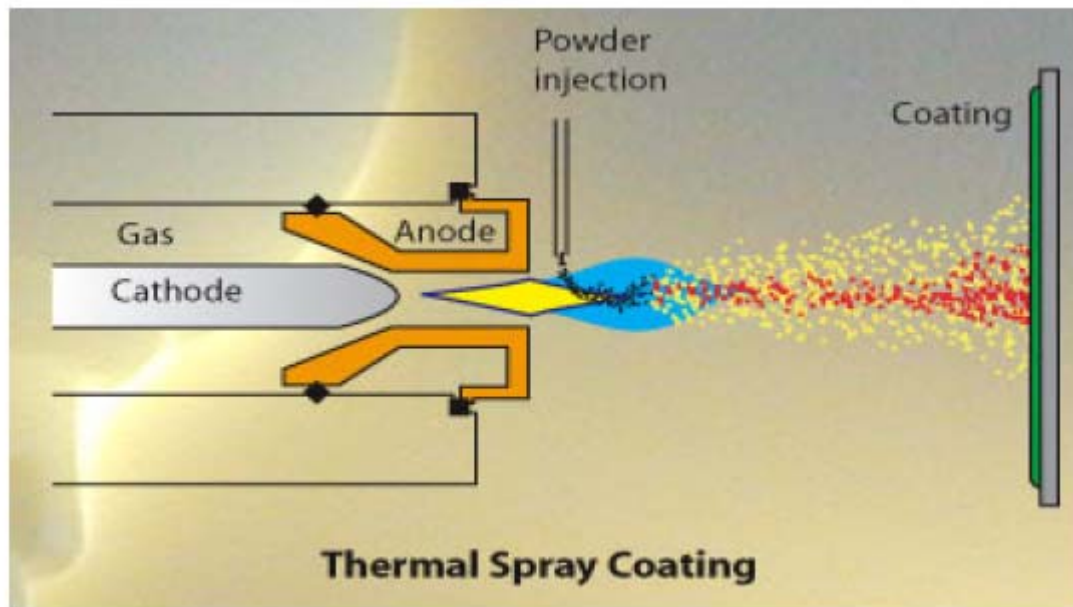


Fig. 2.4 Schematic of Plasma spraying

The key features of plasma spraying are:

- Deposits metals, ceramics or any combinations of these materials.
- Forms microstructures with fine, equiaxed grains and without columnar boundaries
- Produces deposits that do not change in composition with thickness (length of deposition time)

- Can change from depositing a metal to a continuously varying mixture of metals and ceramics(i.e. functionally graded materials)
- High deposition rates (>4kg/h)
- Fabricates freestanding forms of virtually any material or any materials combinations
- Process materials in virtually any environment, e.g. air, reduced pressure inert gas, high pressure.

2.6.1 Requirements for Plasma Spraying

Roughness of the substrate surface:

A rough surface provides a good coating adhesion. A rough surface provides enough room for anchorage of the splats facilitating bonding through mechanical interlocking. A rough surface is generally created by shot blasting technique. The shots are kept inside a hopper, and compressed air is supplied at the bottom of the hopper. The shots are taken afloat by the compressed air stream into a hose and ultimately directed to an object kept in front of the exit nozzle of the hose. The shots used for this purpose are irregular in shape, highly angular in nature, and made up of hard material like alumina, silicon carbide, etc. Upon impact they create small craters on the surface by localized plastic deformation, and finally yield a very rough and highly worked surface. The roughness obtained is determined by shot blasting parameters, i.e., shot size, shape and material, air pressure, standoff distance between nozzle and the job, angle of impact, substrate material etc. [16]. The effect of shot blasting parameters on the adhesion of plasma sprayed alumina has been studied [17]. Mild steel serves as the substrate material. The adhesion increases proportionally with surface roughness and the parameters listed above are of importance. A significant time lapse between shot blasting and plasma spraying causes a marked decrease in bond strength [18].

Cleanliness of the substrates:

The substrate to be sprayed on must be free from any dirt or grease or any other material that might prevent intimate contact of the splat and the substrate. For this purpose the substrate must be thoroughly cleaned (ultrasonically, if possible) with a solvent before spraying. Spraying must be conducted immediately after shot blasting and cleaning. Otherwise on the nascent

surfaces, oxide layers tend to grow quickly and moisture may also affect the surface. These factors deteriorate the coating quality drastically [18].

Bond coat:

Materials like ceramic cannot be sprayed directly onto metals, owing to a large difference between their thermal expansion coefficients. Ceramics have a much lower value of α and hence undergo much less shrinkage as compared to the metallic base to form a surface in compression. If the compressive stress exceeds a certain limit, the coating gets peeled off. To alleviate this problem a suitable material, usually metallic of intermediate value is plasma sprayed onto the substrate followed by the plasma spraying of ceramics. Bond coat may render itself useful for metallic topcoats as well. Molybdenum is a classic example of bond coat for metallic topcoats. Molybdenum adheres very well to the steel substrate and develops a somewhat rough top surface ideal for the topcoat spraying. The choice of bond coats depends upon the application. For example, in wear application, an alumina and Ni-Al top and bond coats combination can be used [19]. In thermal barrier application, CoCrAlY or Ni-Al bond coat [20] and zirconia topcoat are popular. Ceramic coatings when subjected to hertzian loading deform elastically and the metallic substrate deforms plastically. During unloading, elastic recovery of the coating takes place, whereas for the metallic substrate a permanent set has already taken place. Owing to this elastoplastic mismatch the coating tends to spall off at the interface. A bond coat can reduce this mismatch as well.

Cooling water:

For cooling purpose distilled water was used, whenever possible. Normally a small volume of distilled water is recirculated into the gun and it is cooled by an external water supply from a large tank. Sometime water from a large external tank is pumped directly into the gun [12].

2.6.2 Process parameters in plasma spraying

In plasma spraying one has to deal with a lot of process parameters, which determine the degree of particle melting, adhesion strength and deposition efficiency of the powder. Deposition

efficiency is the ratio of amount of powder deposited to the amount fed to the gun. An elaborate listing of these parameters and their effects are reported in the literature [21]

Some important parameters and their roles are listed below:

Arc power:

It is the electrical power drawn by the arc. The power is injected into the plasma gas, which in turn heats the plasma stream. Part of the power is dissipated as radiation and also by the gun cooling water. Arc power determines the mass flow rate of a given powder that can be effectively melted by the arc. Deposition efficiency improves to a certain extent with an increase in arc power, since it is associated with an enhanced particle melting [18,21,22]. However, increasing power beyond a certain limit may not cause a significant improvement. On the contrary, once a complete particle melting is achieved, a higher gas temperature may prove to be harmful. In the case of steel, at some point vaporization may take place lowering the deposition efficiency.

Plasma gas:

Normally nitrogen or argon doped with about 10% hydrogen or helium is used as a plasma gas. The major constituent of the gas mixture is known as primary gas and the minor is known as the secondary gas. The neutral molecules are subjected to the electron bombardment resulting in their ionization. Both temperature and enthalpy of the gas increase as it absorbs energy. Since nitrogen and hydrogen are diatomic gases, they first undergo dissociation followed by ionization. Thus they need higher energy input to enter the plasma state. This extra energy increases the enthalpy of the plasma. On the other hand, the mono-atomic plasma gases, i.e. argon or helium, approach a much higher temperature in the normal enthalpy range. Good heating ability is expected from them for such high temperature [23]. In addition, hydrogen followed by helium has a very high specific heat, and therefore is capable of acquiring very high enthalpy. When argon is doped with helium the spray cone becomes quite narrow which is especially useful for spraying on small targets.

Carrier gas:

Normally the primary gas itself is used as a carrier gas. The flow rate of the career gas is an important factor. A very low flow rate cannot convey the powder effectively to the plasma jet,

and if the flow rate is very high then the powders might escape the hottest region of the jet. There is an optimum flow rate for each powder at which the fraction of unmelted powder is minimum and hence the deposition efficiency is maximum [21].

Mass flow rate of powder:

Ideal mass flow rate for each powder has to be determined. Spraying with a lower mass flow rate keeping all other conditions constant results in under utilization and slow coating buildup. On the other hand, a very high mass flow rate may give rise to an incomplete melting resulting in a high amount of porosity in the coating. The un-melted powders may bounce off from the substrate surface as well keeping the deposition efficiency low [21].

Torch to base distance:

It is the distance between the tip of the gun and the substrate surface. A long distance may result in freezing of the melted particles before they reach the target, whereas a short standoff distance may not provide sufficient time for the particles in flight to melt [18,21]. The relationship between the coating properties and spray parameters in spraying alpha alumina has been studied in details. It is found that the porosity increases and the thickness of the coating (hence deposition efficiency) decreases with an increase in standoff distance. The usual alpha-phase to gamma-phase transformation during plasma spraying of alumina has also been restricted by increasing this distance. A larger fraction of the un-melted particles go in the coating owing to an increase in torch to base distance.

Spraying angle:

This parameter is varied to accommodate the shape of the substrate. In coating alumina on mild steel substrate, the coating porosity is found to increase as the spraying angle is increased from 30° to 60°. Beyond 60°, the porosity level remains unaffected by a further increase in spraying angle. The spraying angle also affects the adhesive strength of the coating. The influence of spraying angle on the cohesive strength of chromia, zirconia 8-wt% yttria and molybdenum has been investigated, and it has been found that the spraying angle does not have much influence on the cohesive strength of the coatings [24].

Substrate cooling:

During a continuous spraying, the substrate might get heated up and may develop thermal-stress related distortion accompanied by a coating peel-off. This is especially true in situations where thick deposits are to be applied. To harness the substrate temperature, it is kept cool by an auxiliary air supply system. In addition, the cooling air jet removes the unmelted particles from the coated surface and helps to reduce the porosity [18].

Powder related variables:

These variables are powder shape, size and size distribution, processing history, phase composition etc. They constitute a set of extremely important parameters. For example, in a given situation if the powder size is too small it might get vaporized. On the other hand a very large particle may not melt substantially and therefore will not deposit. The shape of the powder is also quite important. A spherical powder will not have the same characteristics as the angular ones, and hence both could not be sprayed' using the same set of parameters [25].

Angle of powder injection:

Powders can be injected into the plasma jet perpendicularly, coaxially, or obliquely. The residence time of the powders in the plasma jet will vary with the angle of injection for a given carrier gas flow rate. The residence time in turn will influence the degree of melting of a given powder. For example, to melt high melting point materials a long residence time and hence oblique injection may prove to be useful. The angle of injection is found to influence the cohesive and adhesive strength of the coatings as well [12].

2.7 INDUSTRIAL APPLICATIONS OF PLASMA SPRAYING

There has been a steady growth in the number of applications of thermally sprayed coatings. Availability of hardware and adaptability of the technique are the most important factors for this growth. Plasma spraying has been successfully applied to a wide range of industrial technologies. Automotive industry, aerospace industry, nuclear industry, textile industry, paper industry and iron and steel industry are some of the sectors that have successfully exploited thermal plasma spray technology [26].

2.7 i) Textile Industry

Plasma spraying was for the first time employed in textile industry in Czechoslovakia. Plasma spraying has replaced the classical technologies of chrome plating, anodization and chemical surface hardening. Advantages of this technique are a lot, all of which add to the quality and quantity of textile production.

- **Critical machinery parts:** Different thread guiding & distribution rollers, ridge thread brakes, distribution plates, driving & driven rollers, gallets, tension rollers, thread brake caps, lead-in bars etc.

- **Coatings and advantages:** High wear resistance coatings are required on textile machinery parts, which are in contact with synthetic fibers. For this purpose especially $\text{Al}_2\text{O}_3 + 3\% \text{TiO}_2$, $\text{Al}_2\text{O}_3 + 13\% \text{TiO}_2$, Cr_2O_3 , $\text{WC} + \text{Co}$ are applied. These coatings with hardness ranging from 1800 to 2600 HRV are extraordinarily dense, have high wear resistance and provide excellent bonding with the substrate. Plasma spraying has following advantages in textile industries:

- Replacement of worn out parts is minimized and hence reduces the idle times.
- Physical and mechanical properties of fibers are improved.
- Revolution speed of these lighter parts can be increased.
- Shelf life of the textile machinery parts with plasma sprayed coating last 5 to 20 times longer than parts coated by chrome plating or another classical technique.
- Economic savings are realized considerably by substituting heavy steel or cast iron parts with aluminum or durable ones with wear- resistant coatings.

2.7 ii) Paper and printing industry

The machinery in the paper and printing industry is usually quite large and is subjected to considerable wear from the sliding and friction contact with the paper products.

- **Critical machinery parts:** Paper drying rolls, sieves, filters, roll pins etc.in paper machines, printing rolls, tension rolls and other parts of printing machines.
- **Coatings and advantages:** Spraying of oxide layers is an available economical solution which can be employed right in place in the production shop. Here again oxide layers composed of Al_2O_3 with 3 to 13 % additions of TiO_2 , Cr_2O_3 or MnO_2 are applied. Cast iron rolls are

typically first sprayed with NiCr 80/20, 50 µm thick and then over it 0.2mm thick $\text{Al}_2\text{O}_3 + 13\% \text{TiO}_2$ layer is coated. The special advantages are mentioned below:

- Ensures corrosion resistance of rolls i.e. the base metal
- Resistance of oxide layers against printing inks extends the life of machine parts
- Production cost is reduced considerably
- Coating resulted to the so-called “orange peel” phenomena, surface finishing obtainable that prevents paper foil, dyes etc. from sticking and allows their proper stretching.

2.7 iii) Automotive Industry and the production of Combustion engines

Plasma sprayed coatings used, in automotive industries of many industrially advanced countries, endure higher working pressure and temperature to improve wear resistance, good friction properties, resistance against burn-off and corrosion due to hot combustion products and resistance against thermal loading. Some of the several applications developed for the automotive industry at the Slovak Academy of Sciences (SAV) in Bratislava are spraying torsion bars with aluminium coatings against corrosion. The plasma spraying technology is introduced in the production of gearshift forks for gear boxes in fiat car factory and on the critical parts of big Diesel engines.

2.7 iv) Glass Industry

Molten glass quickly wears the surface of metal which comes in contact with it. In order to protect the metal tools, plasma sprayed coatings are made on to it.

2.7 v) Electrochemical Industry

In the electromechanical and computer industries the electrically conductive Cu, Al, W and the semi-conductive and insulating ceramic layers are widely used. Some contacts of electrodes, e.g. the spark gaps of nuclear research equipment, are produced of massive tungsten. Such electrodes can be replaced by modern electrodes with a sprayed tungsten coating about 0.5mm thick. This electrode ensures short- time passages of 300,000A current with a life of several hundred switching.

2.7 vi) Hydraulic machines and mechanisms

The range of possible applications in this field is very extensive, mainly in water power plants, in production and work of pumps, where many parts are subjected to combined effects of wear, corrosion, erosion and cavitations.

2.7 vii) Rolling mills and foundry

In Rolling mills and pressing shops the wear resistant coatings are used to renovate the heavy parts of heavy duty machines whose replacement would be very costly. Several applications in this field are presented herewith:

- Rolling strand journals being repaired by giving a coating layer of stainless steel. Blooming roll mill journal renovated with a NiCrBSi layer.
- Gears of rolling mill gear box being renovated by a wear resistance coating.
- To repair a rolling mill slide and the plungers of a forging press a hard wear resistance is applied.
- Heat resistant plasma coating is widely used for foundry and metallurgical equipment where molten metal or very high temperatures are encountered. This equipment includes the sliding plugs of steel ladles with alumina or zirconia coatings.
- Conveyer rollers in plate production with zirconia based refractory coatings.
- Oxygen tubes, cast iron moulds in continuous casting of metals, with $\text{Al}_2\text{O}_3 + \text{TiO}_2$, $\text{ZrSiO}_4 + \text{ZrO}_2 + \text{MgO}$.

2.7 viii) High Temperature wears resistance coatings on Slide Gate Plates

In steel plants severe erosion of refractory teeming plates (slide gate plates) and generation of macro-micro cracks during teeming of steel is observed, rendering the plates unstable for reuse. Plasma sprayed ceramic coatings on refractory plates is made to minimize the damage and hence increase the life of slide gate plate. Al_2O_3 , MgZrO_3 , ZrO_2 , TiO_2 , Y_2O_3 and calcia stabilized. Zirconia can also be coated.

2.7 ix) Chemical Plants

The base metal of machine parts is subjected to different kind of wear in chemical plants. In such cases plasma sprayed coatings are applied to protect the base metal. They can be used for various blades, shafts, bearing surfaces, tubes, burners, parts of cooling equipments etc.

2.7 x) Aircraft Jet engines

The working parts of Aircraft jet engines are subjected to serve mechanical, chemical and thermal stresses. A jet engine has a number of construction nodes where plasma coating is employed with much success in order to protect them. There are for example, face of the blower box, compressor box and disc, guide bearing, fuel nozzles, blades, combustion chambers.

2.8 WEAR

Wear occurs as a natural consequence when two surfaces with a relative motion interact with each other. Wear may be defined as the progressive loss of material from contacting surfaces in relative motion. Scientists have developed various wear theories in which the Physico-Mechanical characteristics of the materials and the physical conditions (e.g. the resistance of the rubbing body and the stress state at the contact area) are taken in to consideration. In 1940 Holm [27] starting from the atomic mechanism of wear, calculated the volume of substance worn over unit sliding path.

Wear of metals is probably the most important yet at least understood aspects of tribology. It is certainly the youngest of the tri of topics, friction, lubrication and wear, to attract scientific attention, although its practical significance has been recognizes throughout the ages.

Wear is not an intrinsic material property but characteristics of the engineering system which depend on load, speed, temperature, hardness, presence of foreign material and the environmental condition [28]. Widely varied wearing conditions causes wear of materials. It may be due to surface damage or removal of material from one or both of two solid surfaces in a sliding, rolling or impact motion relative to one another. In most cases wear occurs through surface interactions at asperities. During relative motion, material on contacting surface may be removed from a surface, may result in the transfer to the mating surface, or may break loose as a wear particle. The wear resistance of materials is related to its microstructure may take place during the wear process and hence, it seems that in wear research emphasis is placed on

microstructure [29]. Wear of metals depends on many variables, so wear research programs must be planned systematically. Therefore researchers have normalized some of the data to make them more useful. The wear map proposed by Lim and Ashby [28] is very much useful in this regard to understand the wear mechanism in sliding wear, with or without lubrication.

2.9 TYPES OF WEAR

In most basic wear studies where the problems of wear have been a primary concern, the so-called dry friction has been investigated to avoid the influences of fluid lubricants. Dry friction' is defined as friction under not intentionally lubricated conditions but it is well known that it is friction under lubrication by atmospheric gases, especially by oxygen [30]. A fundamental scheme to classify wear was first outlined by Burwell and Strang [31]. Later Burwell [32] modified the classification to include five distinct types of wear, namely (1) Abrasive (2) Adhesive (3) Erosive (4) Surface fatigue (5) Corrosive.

2.9.1 Abrasive wear

Abrasive wear can be defined as wear that occurs when a hard surface slides against and cuts groove from a softer surface. It can account for most failures in practice. Hard particles or asperities that cut or groove one of the rubbing surfaces produce abrasive wear. This hard material may be originated from one of the two rubbing surfaces. In sliding mechanisms, abrasion can arise from the existing asperities on one surface (if it is harder than the other), from the generation of wear fragments which are repeatedly deformed and hence get work hardened for oxidized until they became harder than either or both of the sliding surfaces, or from the adventitious entry of hard particles, such as dirt from outside the system. Two body abrasive wear as shown in Fig. 2.5 occurs when one surface (usually harder than the second) cuts material away from the second, although this mechanism very often changes to three body abrasion as the wear debris then acts as an abrasive between the two surfaces. Abrasives can act as in grinding where the abrasive is fixed relative to one surface or as in lapping where the abrasive tumbles producing a series of indentations as opposed to a scratch. According to the recent tribological survey, abrasive wear is responsible for the largest amount of material loss in industrial practice [33].

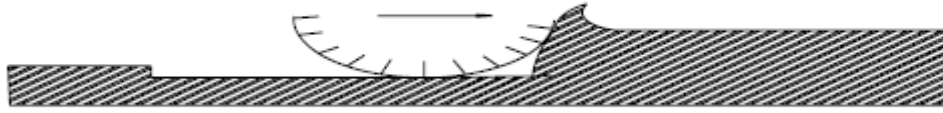


Fig. 2.5 Schematic representations of the abrasion wear mechanism.

2.9.2 Adhesive wear

Adhesive wear can be defined as wear due to localized bonding between contacting solid surfaces leading to material transfer between the two surfaces or the loss from either surface. For adhesive wear as shown in Fig. 2.6 to occur it is necessary for the surfaces to be in intimate contact with each other. Surfaces, which are held apart by lubricating films, oxide films etc. reduce the tendency for adhesion to occur.

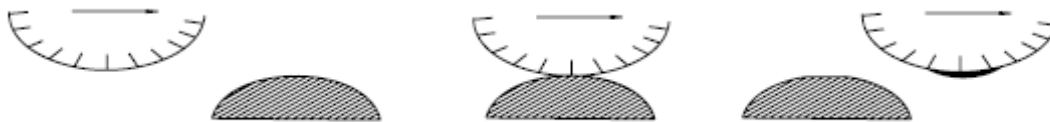


Fig. 2.6 Schematic representations of the adhesive wear mechanism.

2.9.3 Erosive wear

Erosive wear can be defined as the process of metal removal due to impingement of solid particles on a surface. Erosion is caused by a gas or a liquid, which may or may not carry, entrained solid particles, impinging on a surface. When the angle of impingement is small, the wear produced is closely analogous to abrasion. When the angle of impingement is normal to the surface, material is displaced by plastic flow or is dislodged by brittle failure. The schematic representation of the erosive wear mechanism is shown in Fig.2.7.



Fig. 2.7 Schematic representations of the erosive wear mechanism.

2.9.4 Surface fatigue wear

Wear of a solid surface caused by fracture arising from material fatigue. The term ‘fatigue’ is broadly applied to the failure phenomenon where a solid is subjected to cyclic loading involving tension and compression above a certain critical stress. Repeated loading causes the generation of micro cracks, usually below the surface, at the site of a pre-existing point of weakness. On subsequent loading and unloading, the micro crack propagates. Once the crack reaches the critical size, it changes its direction to emerge at the surface, and thus flat sheet like particles is detached during wearing. The number of stress cycles required to cause such failure decreases as the corresponding magnitude of stress increases. Vibration is a common cause of fatigue wear. The schematic representation of the surface fatigue wear mechanism is shown in Fig. 2.8.

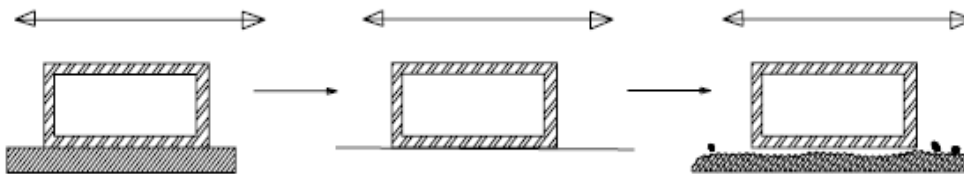


Fig. 2.8 Schematic representations of the surface fatigue wear mechanism.

2.9.5 Corrosive wear

Most metals are thermodynamically unstable in air and react with oxygen to form an oxide, which usually develop layer or scales on the surface of metal or alloys when their interfacial bonds are poor. Corrosion wear is the gradual eating away or deterioration of unprotected metal surfaces by the effects of the atmosphere, acids, gases, alkalis, etc. This type of wear creates pits and perforations and may eventually dissolve metal parts.

2.10 SYMPTOMS OF WEAR

Literature available on the rate controlling wear mechanism demonstrated that it may change abruptly from one another at certain sliding velocities and contact loads, resulting in abrupt increases in wear rates. The conflicting results in the wear literature arise partly because of the differences in testing conditions, but they also make clear that a deeper understanding of the wear mechanism is required if an improvement in the wear resistances of the coating is to be achieved. This in turn requires a systematic study of the wear under different stresses, velocities and temperatures. It is generally recognized that wear is a characteristic of a system and influenced by many parameters. Laboratory scale investigation if designed properly allows careful control of the tribo system where by the effects of different variables on wear behaviour of the coating can be isolated and determined. The data generated through such investigation under controlled conditions may help in correct interpretation of the results. A summary of the appearance and symptoms of different wear mechanism is indicated in Table 2.2 [34] and the same is a systematic approach to diagnose the wear mechanisms.

Table 2.2 Symptoms and Appearance of different types of wear.

Types of wear	Symptoms	Appearance of the worn-out surface
Abrasive	Presence of clean furrows cut out by abrasive particles	Grooves
Adhesive	Metal transfer is the prime symptoms	Seizure, catering rough and torn-out surfaces.
Erosion	Presence of abrasives in the fast moving fluid and short abrasion furrows	Waves and troughs.
Corrosion	Presence of metal corrosion products.	Rough pits or depressions.
Fatigue	Presence of surface or subsurface cracks accompanied by pits and spalls	Sharp and angular edges around pits.
Impacts	Surface fatigue, small sub micron particles or formation of spalls	Fragmentation, peeling and pitting.
Delamination	Presence of subsurface cracks parallel to the surface with semi-dislodged or loose flakes	Loose, long and thin sheet like particles
Fretting	Production of voluminous amount of loose debris	Roughening, seizure and development of oxide ridges
Electric attack	Presence of micro craters or a track with evidence of smooth molten metal	Smooth holes

A typical model, exemplifying the rate of erosion depending on size and velocity of particle on impacting the substrate is shown in Fig.2.9. The increase in impact velocity or particle diameter clearly accelerates erosion damage. From the fact that an increase in particle velocity or size leads to larger or deeper indentations as schematically shown in Fig. 2.7, deviations in k_2 and k_3 values from the theoretical ones ($k_2=2$, $k_3=0$) indicate the true effects of impact velocity and particle diameter which are connected with the relative aggressiveness of indentation. The larger or deeper is the indentation the greater amount of material is removed from the rim of the indentation.

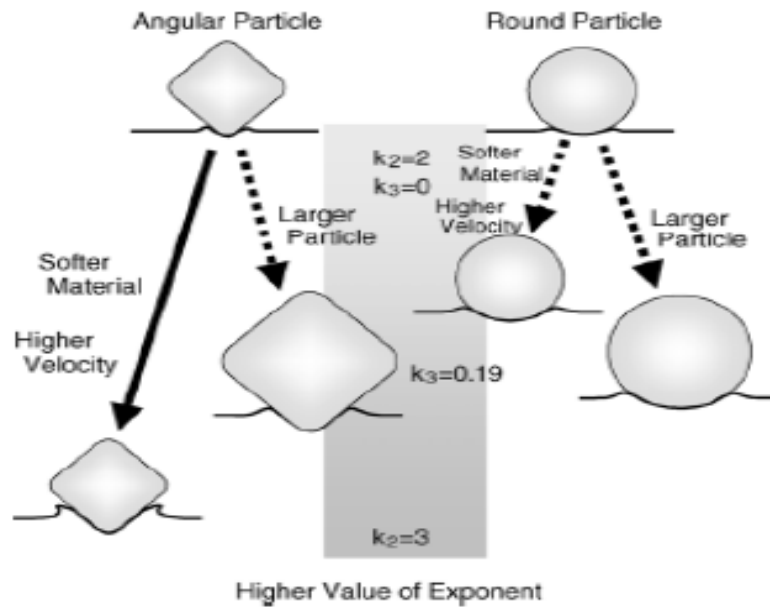


Fig. 2.9 Model of the effects of impact parameters on exponents k_2 and k_3 .

2.11 RECENT TRENDS IN METAL WEAR RESEARCH

Much of the wear researches carried out in the 1940's and 1950's were conducted by mechanical engineers and metallurgists to generate data for the construction of motor drive, trains, brakes, bearings, bushings and other types of moving mechanical assemblies [35].

It became apparent during the survey that wear of metals was a prominent topic in a large number of the responses regarding some future priorities for research in tribology. Some 22 experienced technologists in this field, who attended the 1983 'Wear of Materials Conference' in Reston, prepared a ranking list [37]. Their proposals with top priority were further investigations of the mechanism of wear and this no doubt reflects the judgments that particular effects of wear should be studied against a background of the basic physical and chemical processes involved in surface interactions. The list proposed is shown in Table 2.3. [36]

Peterson [37] reviewed the development and use of tribo-materials and concluded that metals and their alloys are the most common engineering materials used in wear applications. Grey cast iron for example has been used as early as 1388. Much of the wear research conducted over the past 50 years is in ceramics, polymers, composite materials and coatings [38].

Table 2.3 Priority in wears research

Ranking	Topics
1.	Mechanism of Wear
2.	Surface Coatings and treatments
3.	Abrasive Wear
4.	Materials
5.	Ceramic Wear
6.	Metallic Wear
7.	Polymer Wear
8.	Wear with Lubrication
9.	Piston ring-cylinder liner Wear
10.	Corrosive Wear
11.	Wear in other Internal Combustion Machine Components

Wear of metals encountered in industrial situations can be grouped into categories shown in Table 2.4. Though there are situations where one type changes to another or where two or more mechanism plays together.

Table 2.4 Type of wear in industry [25].

Type of wear in Industry	Approximate percentage involved
Abrasive	50
Adhesive	15
Erosion	8
Fretting	8
Chemical	5

2.12 WEAR RESISTANT COATINGS

The choice of a material depends on the application. However, the ceramic coatings are very hard and hence on an average offer more abrasion resistance than their metallic counterparts. Today a variety of materials, e.g., carbides, oxides, metallic, etc., belonging to the above category are available commercially. The coatings with these materials can be grouped into the following categories: [10]

- (i) Carbides: WC, TiC, SiC, ZrC, Cr_2C_3 etc.
- (ii) Oxides: Al_2O_3 , Cr_2O_3 , TiO_2 , ZrO_2 etc.
- (iii) Metallic: NiCrAlY, Triballoy etc.
- (iv) Diamond

2.12.1 Oxide Coatings

Metallic coatings and metal containing carbide coatings sometime are not suitable in high temperature environments in both wear and corrosion applications. Often they fail owing to oxidation or decarburization. In such case the material of choice can be an oxide ceramic coating, e.g., Al_2O_3 , Cr_2O_3 , TiO_2 , ZrO_2 or their combinations. However, a high wear resistance, and chemical and thermal stability of these materials are counterbalanced by the disadvantages of low values of thermal expansion coefficient, thermal conductivity, mechanical strength, fracture toughness and somewhat weaker adhesion to substrate material. The thickness of these coatings is also limited by the residual stress that grows with thickness. Therefore, to obtain a good quality coating it is essential to exercise proper choice of bond coat, spray parameters and reinforcing additives [10].

2.12.1 (a) Chromia (Cr_2O_3) Coatings

These coatings are applied when corrosion resistance is required in addition to abrasion resistance. It adheres well to the substrate and shows an exceptionally high hardness 2300 HV [10]. Chromia coatings are also useful in ship and other diesel engines, water pumps, and printing rolls [3]. A Cr_2O_3 , - 40 wt% TiO_2 coating provides a very high coefficient of friction (0.8), and hence can be used as a brake liner [39]. The wear mode of chromia coatings has been investigated under various conditions. Depending on experimental conditions, the wear mode can be abrasive [39], plastic deformation [40], micro fracture [41] or a conglomerate of all of

these [42]. This material has also been tested under lubricated conditions, using inorganic salt solutions (NaCl , NaNO_3 , Na_3PO_4) as lubricants and also at a high temperature. The wear rate of self-mated chromia is found to increase considerably at 450°C , and plastic deformation and surface fatigue are the predominant wear mechanisms [43]. Under lubricated condition, the coatings exhibit tribochemical wear [44]. It has also been tested for erosion resistance [45].

2.12.2 (b) Zirconia (ZrO_2) Coatings

Zirconia is widely used as a thermal barrier coating. However, it is endowed with the essential qualities of a wear resistant material, i.e., hardness, chemical inertness, etc. and shows reasonably good wear behaviour. In the case of a hot pressed zirconia mated with high chromium containing iron (martensitic, austenitic, or pearlitic), it has been found that in course of rubbing the iron transfers on to the ceramic surface and the austenitic material adheres well to the ceramic as compared to their martensitic or pearlitic counterparts [46]. The thick film improves the heat transfer from the contact area keeping the contact temperature reasonably low; thus the transformation of ZrO_2 is prevented. On the other hand with the pearlitic or martensitic iron the material transfer is limited. The contact temperature is high enough to bring about a phase transformation and related volume change in ZrO_2 causing a stress induced spalling. In a similar experiment the wear behaviour of sintered, partially stabilized zirconia (PSZ) with 8 wt% yttria against PSZ and steels has been tested at 200°C . When metals are used as the mating surface, a transferred layer soon forms on the ceramic surface (coated or sintered) [47]. In ceramic-ceramic system the contact wear is abrasive in nature. However, similar worn particles remain entrapped between the contact surfaces and induce a polishing wear too. In the load range of 10 to 40 N, no transformation of ZrO_2 occurs [47,48]. However, similar tests conducted at 800°C show a phase transformation from monoclinic ZrO_2 to tetragonal ZrO_2 [49]. The wear debris of ZrO_2 sometimes get compacted in repeated loading and gets attached to the worn surface forming a protective layer [50]. During rubbing, pre-existing or newly formed cracks may grow rapidly and eventually interconnect with each other, leading to a spallation of the coating [51]. The worn particles get entrapped between the mating surfaces and abrade the coating. The wear performance of ZrO_2 -12 mol% CeO_2 and ZrO_2 -12 mol% CeO_2 -10 mol% Al_2O_3 coatings against a bearing steel under various loads has been studied [52]. Introduction of alumina as a dopant, has been found to improve the wear performance of the ceramic significantly. Here plastic deformation is the main wear mode. The wear performance of zirconia at 400°C and 600°C has

been reported in the literature [53]. At these temperatures the adhesive mode of wear plays the major role.

Table 2.5 Physical properties of Titania.

Properties	TiO ₂
Composition	TiO ₂ (Rutile)
Density, g/c.c.	4.10
Melting point, °C	1900
Hardness, HV. Kg/mm ²	942
Co-efficient of thermal expansion, µm/m. °C	7.5

2.12.2(c) Titania (TiO₂) Coatings

Titania coating is known for its high hardness, density, and adhesion strength. It has been used to combat abrasive, erosive and fretting wear either in essentially pure form or in association with other compounds [54,55]. The mechanism of wear of TiO₂ at 450°C under both lubricated and dry contact conditions has been studied. It has been found to undergo a plastic smearing under lubricated contact, where as it fails owing to the surface fatigue in dry condition. TiO₂-stainless steel couples in various speed load conditions have also been investigated in details [56]. At a relatively low load, the failure is owing to the surface fatigue and adhesive wear, whereas at a high load the failure is attributed to the abrasion and delamination associated with a back and forth movement [57]. At low speed the transferred layer of steel oxidizes to form Fe₂O₃ and the wear progresses by the adhesion and surface fatigue. At a high speed, Fe₃O₄ forms instead of Fe₂O₃ [58]. The TiO₂ top layer also softens and melts owing to a steep rise in temperature, which helps in reducing the temperature subsequently [59]. The performance of the plasma sprayed pure TiO₂ has been compared with those of Al₂O₃ – 40 wt% TiO₂ and pure Al₂O₃ under both dry and lubricated contact conditions [60]. TiO₂ shows the best results. TiO₂ owing to its relatively high porosity can provide good anchorage to the transferred film and also can hold the lubricants effectively [61]. Table 2.5 shows some physical properties of Titania.

2.12.2 (d) Alumina (Al_2O_3) Coatings

Alumina is obtained from a mineral called bauxite, which exists in nature as a number of hydrated phases, e.g., boehmite ($\gamma\text{-Al}_2\text{O}_3 \cdot \text{H}_2\text{O}$), hydrargillate, diaspor ($\alpha\text{-Al}_2\text{O}_3 \cdot 3\text{H}_2\text{O}$). It also exists in several other metastable forms like β , δ , θ , η , κ and X [62]. $\alpha\text{-Al}_2\text{O}_3$ is known to be a stable phase and it is available in nature in the form of corundum. In addition, $\alpha\text{-Al}_2\text{O}_3$ can be extracted from the raw materials by fusing them.

Boehmite $\rightarrow 450^\circ\text{C} \rightarrow \gamma\text{-Al}_2\text{O}_3 \rightarrow 750^\circ\text{C} \rightarrow \delta\text{-Al}_2\text{O}_3 \rightarrow 1000^\circ\text{C} \rightarrow \nu\text{-Al}_2\text{O}_3 \rightarrow 1200^\circ\text{C} \rightarrow \alpha\text{-Al}_2\text{O}_3$

Bayererite $\rightarrow 230^\circ\text{C} \rightarrow \eta\text{-Al}_2\text{O}_3 \rightarrow 850^\circ\text{C} \rightarrow \nu\text{-Al}_2\text{O}_3 \rightarrow 1200^\circ\text{C} \rightarrow \alpha\text{-Al}_2\text{O}_3$

The phase transformation during freezing of the plasma sprayed alumina droplets has been studied in details [63,64]. From the molten particles, $\gamma\text{-Al}_2\text{O}_3$ tends to nucleate, since liquid to γ transformation involves a low interfacial energy. The phase finally formed upon cooling depends on the particle diameter. For particle diameter less than $10\text{ }\mu\text{m}$, the metastable form is retained (γ , δ , β or θ). Plasma spraying of alumina particles having a mean diameter of $9\text{ }\mu\text{m}$ results in the development of the gamma phases in the coating after cooling [65]. The α form is found in the large diameter particle. In fact larger is the diameter; greater is the fraction of $\alpha\text{-Al}_2\text{O}_3$ in the cooled solid. This form is desirable for its superior wear properties. Other than the cooling rate, one way to achieve the phase finally formed is to vary the temperature of the substrate. If the substrate temperature is kept at 900°C , the δ phase forms. The $\alpha\text{-Al}_2\text{O}_3$ can be formed by raising the temperature of the substrate to 1100°C resulting a slow cooling. During freezing the latent heat of solidification is absorbed in the still molten pool. If this heat generation is balanced by the heat transfer to the substrate, columnar crystals grow. On the other hand, if the aforesaid heat transfer is faster than the heat injection rate from the growing solidification front, equi-axed crystals are supposed to form. In reality columnar crystals are generally found. Table 2.6 shows some physical properties of Alumina

Table 2.6 Physical properties of Alumina.

Properties	Alumina (99.9%)
Composition	Al_2O_3 (corundum)
Density, g/c.c.	3.90
Melting point, °C	2015
Thermal conductivity, J/kg. K	35.60
Hardness, HV. Kgf/mm ²	1500
Flexural strength, MPa	380
Tensile strength, MPa	262
Poisson's ratio	0.26
Young's modulus, Gpa	370
Co-efficient of thermal expansion, $\mu\text{m/m. } ^\circ\text{C}$	8
Heat capacity, J/kg.K	880

There are several advantages of alumina as a structural material, e.g., availability, hardness, high melting point, resistance to wear and tear etc. It bonds well with the metallic substrates when applied as a coating on them. Some of the applications of alumina are in bearings, valves, pump seals, plungers, engine components, rocket nozzles, shields for guided missiles, vacuum tube envelops, integrated circuits, etc. Plasma sprayed alumina-coated railroad components are presently being used in Japan [66]. Properties of alumina can be further complemented by the particulate (TiO_2 , TiC) or whisker (SiC) reinforcement [67]. TiC reinforcement limits the grain growth, improves strength and hardness, and also retards crack propagation through the alumina matrix [68]. The sliding wear behaviour of both monolithic and SiC whisker reinforced alumina has been studied [69]. The whisker reinforced composite has been found to have good wear resistance. The monolithic alumina has a brittle response to sliding wear, whereas the worn surface of the composite reveals signs of plastic deformation along with fracture. The whiskers also undergo pullout or fracture.

The sliding wear behaviour of plasma sprayed alumina against AISI-D2 steel under different speed load conditions has been reported. Within the load range used (45N-133N), the wear vs. load plot shows a maxima. In the initial phase, the wear volume increases with the load

for a given number of sliding cycles. Beyond a certain load, owing to both load and frictional heating, a major plastic flow occurs on the coating surface. The plastic flow leads to an increase in real area of contact and a corresponding reduction of normal stress, though the normal load increases. As a result, wear decreases with an increase in load beyond a critical normal load. On the other hand, the wear vs. sliding speed plot also displays maxima within the speed range used (0.31 to 8 m/s). At a low speed range, the asperities move against each other and deform each other in the process. As the speed is increased, the asperities are subjected to heavy impacts and tend to get fractured from the root producing a higher volume of debris. At a very high velocity the friction related temperature rise becomes high enough to soften the asperities and thereby to protect them from fracture. The wear rate keeps low under such circumstances. Therefore, the plastic deformation and brittle fracture form the failure mechanisms.

2.12.2 (e) Alumina Titania Coatings

TiO₂ is a commonly used additive in plasma sprayable alumina powder. TiO₂ has a relatively low melting point and it effectively binds the alumina grains. However, a success of an Al₂O₃ - TiO₂ coating depends upon a judicious selection of the arc current, which can melt the powders effectively. This results in a good coating adhesion along with high wear -50 wt% TiO has been reported in the literature [69]. In dry sand abrasion testing, alumina outperformed others presumably owing to its high hardness. In dry sliding at low velocity range, the tribocouple (ceramic and hardened stainless steel) exhibits stick-slip. At relatively high speed range, the coefficient of friction drops owing to the thermal softening of the interface [60]. The wear of alumina is found to increase appreciably beyond a critical speed and a critical load. Alumina has been found to fail by plastic deformation, shear and grain pullout. In dry and lubricated sliding as well, the mixed ceramic has been found to perform better than pure alumina. A coating of AlO-50 wt% TiO is quite porous and hence is quite capable of holding the transferred metallic layer which protects the surface [61]. Wear performance of such coatings can further be improved by a sealing of the pores by polymeric substances. A low thermal diffusivity of the alumina coatings results in a high localized thermal stress on the surface. The mode of wear of alumina is mainly abrasive. The pore size and pore size distribution also play a vital role in determining the wear properties. The wear performance of Al₂O₃ and Al₂O₃-TiO₂ coating has a high thermal diffusivity and hence it is less prone to wear.

Alumina-Titania coatings are excellent candidates for providing protection against abrasive wear, and are resistant to high temperature erosion. Such coatings are desirable in electrical insulation and anti-wear applications, for example in protective coatings for sleeve shafts, thermo-couples jackets, pump shafts e.t.c. These coatings exhibit wear, corrosion and thermal shock resistance. Alumina-Titania powder is deposited on graphite using vacuum spraying to minimize porosity of the sprayed coating. With addition of titania wear resistance increases, adhesion strength increases but hardness decreases [70]. TiO_2 is the most wear resistance, with least friction coefficient and is less hard than Al_2O_3 coating. Wear resistance is measured by POD test [71]. The erosion, abrasion rates increased by three orders of magnitude when increasing the size of the erodent from 75 to 600 μm and wearing particles, with increasing titania erosion and abrasion rate decreases [72]. Porosity of Al_2O_3 -40% TiO_2 ranges within 4 to 6%, an agglomerated powder allows to improve the homogeneity of the coating, with the formation of a new compound, Al_2TiO_5 . In ball on disc situation wear resistance of an agglomerated powder coating is more improved, thermal expansion coefficient of alumina and titania are 8 and $7.5(10^{-6} \text{ K}^{-1})$ [73]. Nanostructured alumina–titania coatings exhibits superior wear resistance adhesion, toughness. Post treated deposits exhibit higher resistance to indentation; post treatment induces spray deposit properties with high densification. An improvement in surface properties of treated deposits by way of reduced indentation diameter due to enhanced surface hardness and densification of microstructure [74]. The coatings deposited by HVOF are significantly harder and tougher, and their abrasion resistance is two–threefold higher with less porosity. Bead width and thickness increases with increasing hydrogen fraction in the plasma gas, argon gas fraction increases the bead symmetry. Bond strength of the coating, coating thickness, micro hardness, and porosity depend on gas enthalpy i.e. on H_2 . At lower power levels, titania particles are melted, where as alumina particles remain unmelted. As the power is increased, the aluminium oxide content in the coating increases and the coating composition progressively approaches that of the feedstock powder, hardness and wear resistance increase with the torch power [75]. The friction coefficient determination from POD (Pin-On-Disk) test is 0.5-0.6 [76]. XRD, SEM, TEM results showed that Nanostructured coating exhibits a bimodal microstructure. So, mechanical properties increases, the splat lamellae consisted of γ - Al_2O_3 grains and most of them were less than 200 nm in diameter. Equiaxed grains took the modification of α - Al_2O_3 and ranged from 150 to 800 nm in size. The micro hardness of both kinds of coating was similar and about 820 HV. However, the adhesion strength of the Nan

structured coating increased by 33 %, as compared with those of the conventional coating. The wear rate of the nanostructured coating was lower than that of the conventional coating [77]. Wear behaviour of atmospheric plasma sprayed (APS) alumina–titania coating is investigated using Pin-On-Disc (POD), friction coefficient decreases with increase of sliding velocity and applied load. In the running-in period, the friction coefficient increases because of the contact surface increase as low roughness. Then, the value of the friction coefficient stabilizes representing the wear behavior of the considered material couple [78]. Porosity decreases with increase of arc current, hydrogen fraction, with decrease of powder feed rate micro structural observations showed that the multilayers contain some inhomogeneities such as porosity, crack-like defects, unmelted particles, oxides and inclusions, which decreases the microhardness, it decreases from surface to substrate. The porosity content of the ceramic top coating and bond layer were approximately 6% and 2%. The HV values on the cross section of as-sprayed deposits varied over the range of 490T84 HVN for the bond coat and of 666 T68 HVN for the ceramic top layer. The hardness values of $\text{Al}_2\text{O}_3\text{--TiO}_2/\text{Mo}$ layers are higher than that of substrate. The elastic modulus of the as-sprayed Mo and $\text{Al}_2\text{O}_3\text{--TiO}_2$ coating layers are 180 and 236 GPa. The corresponding average strength for the Mo bond layer and $\text{Al}_2\text{O}_3\text{--TiO}_2$ coating were 40 and 31MPa respectively [79]. Coating is having low density, with increasing titania porosity, hardness, melting point decrease, abrasive wear resistance increases with hardness [80].

2.12.2(f) Flyash coating

Fly ash is generated in dry form in large quantities as a by-product of thermal power generation plants and thus is a major source for environment pollution. Currently, large quantities of fly ash are landfilled. Research is in progress to find out the various ways to utilize this by-product to prevent any environmental problems as well as effectively use them. Flyash particles are generally spherical in shape and range in size from 0.5 μm to 100 μm . They consist mostly of silicon dioxide (SiO_2), aluminium oxide (Al_2O_3) and iron oxide (Fe_2O_3), and are hence a suitable source of aluminum and silicon. For a long time, silica and alumino-silicate bricks have been preferred as refractory materials in many industrial applications due to their high wear resistance and high load bearing capacity at high temperatures. During the last decade, although a large number of investigations have been carried out for development of plasma spray ceramic coatings, not much effort has been made to use low-grade raw materials for plasma spray purposes. [81] Recently, attempts have been made to develop the plasma spray deposition of

alumino-silicate composite coatings onto metal substrates using industrial waste, but the adherence of the coating was not satisfactory. [82] The properties of fly ash has been studied by Tiwari S. and Saxena M. and coatings that were developed have shown improved corrosion and abrasion resistance and also better resistance to chemicals (5% Na_2CO_3 , 1% NaOH , and 2% H_2SO_4) and organic solvents (toluene and mineral spirit). Fly ash can be a cost effective substitute for conventional extenders in high performance industrial coatings [83]. It can be utilized to develop ceramic coatings on metal substrate. Good quality coating and homogeneously distributed phases are observed in the coatings made at power levels between 12 to 20 kW [84]. Fly ash with aluminium additions can be used to provide plasma spray ceramic composite coating on metal substrates and it is found that the coating quality and properties are improved with higher aluminium content in the feed material and are affected by the operating power level of the plasma [85]. Buta singh et al have investigated the fly ash coating obtained by shrouded plasma spray process on carbon steel and found it to be effective to increase the oxidation and salt corrosion resistance of the given carbon steel [86]. The work done by Mishra et al established Redmud-Flyash mixture as a potential coating material, suitable for plasma spraying and for wear resistant applications and also opened up a new pathway for value added utilization of these industrial wastes [87].

2.13 EROSION WEAR OF CERAMIC COATINGS

Surface damage can result in changes in surface condition and dimension of a mechanical component, and this may sometimes cause disastrous failure of an entire mechanical system. One of cost-effective approaches against surface failure is coating. Various coating techniques have been successfully applied in industry to protect machinery and equipment from surface damage respectively caused by corrosion, oxidation and wear. However, when used in a harsh environment involving two or more damage modes, such as corrosion-wear or corrosion-erosion, many coatings perform poorly due to the synergistic action of wear and corrosion. Considerable efforts have been continuously made to develop high-performance coatings that can resist corrosive wear encountered in various industries such as mining, oilsand, petroleum and chemical industries [88]. It has been reported that the thermal spray is a technique that produces a wide range of coatings for diverse applications [89]. Coatings of a wide variety of materials are commonly applied to substrates for many purposes. Often, coatings are applied to improve tribological performance. These may include the enhancement of mechanical properties, visual

appearance or corrosion resistance or may provide special magnetic and optical properties [90]. Plasma sprayed coatings are used today as thermal barriers and abrasion, erosion or corrosion resistant coatings in a wide variety of applications [91]. Plasma spraying is the most flexible and versatile thermal spray process with respect to the sprayed materials. Almost any material can be used for plasma spraying on almost any type of substrate. The high temperatures of plasma spray processes permit the deposition of coatings for applications in areas of liquid and high temperature corrosion and wear protection and also special applications for thermal, electrical and biomedical purposes [92,93].

The loss of material caused by the impingement of tiny, solid particles, which have a high velocity and impact on the material surface at defined angles, is called erosive wear [94]. Particulates ingested into the engine or formed as a result of incomplete combustion are known to cause erosion problems in gas turbines [95,96]. Erosion is a serious problem in many engineering systems, including steam and jet turbines, pipelines and valves used in slurry transportation of matter, and fluidized bed combustion systems [97]. Gas and steam turbines operate in environments where the ingestion of solid particles is inevitable. In industrial applications and power generation, such as coal-burning boilers, fluidized beds, and gas turbines, solid particles are produced during the combustion of heavy oils, synthetic fuels, and pulverized coal and causes erosion of materials. In such environments, protective coatings on the surface of superalloys are frequently used [98,99]. Erosion tests on coatings have been widely reported. However, the mechanisms of coating damage in this type of test depend on the coating material and its thickness, the properties of the interface, the substrate material and the test conditions [100].

Liquid impact erosion is a well known phenomenon in hydro and low-pressure steam turbine blades, and also in aircraft or missiles traveling at high speed through rain [101–103]. The material damage is caused mainly by the high pressure caused by the impact of liquid droplets and the micro-jetting action due to the asymmetrical collapse of bubbles on or near the surface. The surface damage can be minimized by heat treatment or surface modification and substantial advances have been made in this field. Lee et al. [104] investigated the liquid impact erosion resistance of 12Cr steel and stellite 6B coated with TiN by reactive magnetron sputter ion plating. The stresses generated by droplet impact were stated to have been decreased by the TiN as a result of stress attenuation and stress wave interactions.

Solid Particle Erosion (SPE) is a wear process where particles strike against surfaces and promote material loss. During flight a particle carries momentum and kinetic energy, which can be dissipated during impact, due to its interaction with a target surface. Different models have been proposed that allow estimations of the stresses that a moving particle will impose on a target [105]. It has been experimentally observed by many investigators that during the impact the target can be locally scratched, extruded, melted and/or cracked in different ways. The imposed surface damage will vary with the target material, erodent particle, impact angle, erosion time, particle velocity, temperature and atmosphere.

Plasma sprayed coatings are used today as erosion or abrasion resistant coatings in a wide variety of applications. Extensive research shows that the deposition parameters like energy input in the plasma and powder properties affect the porosity, splat size, phase composition, hardness etc. of plasma sprayed coatings [106]. These in turn, have an influence on the erosion wear resistance of the coatings. Quantitative studies of the combined erosive effect of repeated impacts are very useful in predicting component lifetimes, in comparing the performance of materials and also in understanding the underlying damage mechanisms involved.

Resistance of engineering components encountering the attack of erosive environments during operation can be improved by applying ceramic coatings on their surfaces. Alonso et. al. [107] experimented with the production of plasma sprayed erosion- resistant coatings on carbon-fiber-epoxy composites and the studied of their erosion behaviour. The heat sensitivity of the composite substrate requires a specific spraying procedure in order to avoid its degradation. In addition, several bonding layers were tried to allow spraying of the protective coatings. Two different functional coatings; a cermet (WC-12 Co) and a ceramic oxide (Al_2O_3) were sprayed onto an aluminium-glass bonding layer. The microstructure and properties of these coatings were studied and their erosion behaviour determined experimentally in an erosion-testing device. Tabakoff and Shanov [108] designed a high temperature erosion test facility to provide erosion data in the range of operating temperatures experienced in compressors and turbines. In addition to the high temperatures, the facility properly simulates all the erosion parameters important from the aerodynamics point of view. These include particle velocity, angle of impact, particle size, particle concentration and sample size. They reported the erosion behavior of titanium carbide coating exposed to fly ash and chromite particles. Chemical vapor deposition technique (CVD) was used to apply a ceramic coating on nickel and cobalt based super-alloys (M246 and

X40). The test specimens were exposed to particle-laden flow at velocities of 305 and 366 ms⁻¹ and temperatures of 550°C and 815°C.

A good number of reports are available on erosion behaviour of alumina coatings. The resistance to erosion of such coatings depends upon intersplat cohesion, shape, size, and hardness of erodent particles, particle velocity, angle of impact and the presence of cracks and pores [109]. The slurry (SiC and SiO₂) and airborne particle (Al₂O₃ and SiO₂) erosions of flame sprayed alumina coatings have also been reported in the literature. SiC and Al₂O₃ are found to cause significant amount of erosion in slurry and airborne erosion testing respectively. High particle velocity enhances the erosion rate and the erosion rate is maximum for an impact angle of 90°. The failure is by the progressive removal of splats and can be attributed to the presence of defects and pores in the inter-splat regions. Similar observation has been made for the plasma sprayed alumina coatings subjected to an erosive wear caused by the SiO₂ particles [110].

Branco et. al. [111] examined room temperature solid particle erosion of zirconia and alumina-based ceramic coatings, with different levels of porosity and varying microstructure and mechanical properties. The erosion tests were carried out by a stream of alumina particles with an average size of 50 µm at 70 m/s, carried by an air jet with impingement angle of 90°. The results indicate that there is a strong relationship between the erosion rate and the coating porosity.

The erosion wear behaviour and mechanism of several kinds of middle temperature seal coatings were investigated by Yi Maozhong et al. The results show that the relationship between the erosion mass loss and the erosion time is linear, the coatings hold a maximum erosion rate at 60° impact angle, and the relation between the erosion rate and the impact speed is an exponential function. The speed exponent increases with the increase of the impact angle. At 90° impact, the abrasive particles impinging on the coating surface produce indentations and extruded lips, and then the lips are work-hardened and fall off; and flattened metal phase grains are impacted repeatedly, loosened and debonded. At 30° impact, the micro-cutting, plowing and tunneling via pores and non-metal phase are involved. The model of the erosion mechanism is advanced on the basis of the above-mentioned erosion wear behaviour, as shown in Fig 2.10.

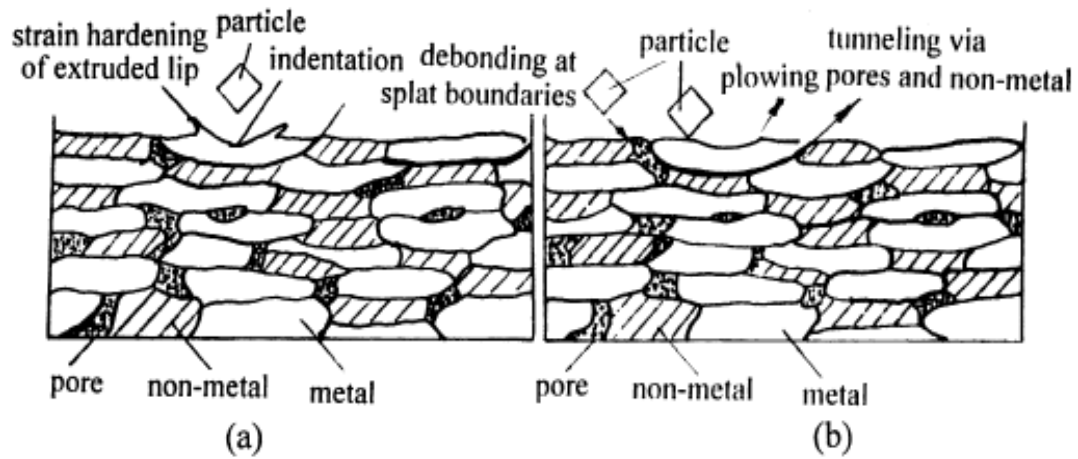


Fig.2.10 Schematic diagram of Model of erosion wear (a) at 90° (b) at 30°

Against with this few backgrounds, the present research work has been undertaken, with an objective to explore the coating potential of flyash-illmenite.

Chapter 3

EXPERIMENTAL SET UP AND METHODOLOGY

CHAPTER 3

EXPERIMENTAL SET UP & METHODOLOGY

3.1 INTRODUCTION

This chapter deals with the details of the experimental procedures followed in this study. The coating procedure itself requires some basic preparation, i.e., shot blasting and cleaning. After plasma spraying, the coated materials have been subjected to a series of tests, e.g., microstructural characterization of the surfaces and cross sections, microhardness measurement, X - ray diffraction studies, adhesion test, erosion wear test etc. The details of each process are described here.

3.2 DEVELOPMENT OF THE COATINGS

3.2.1 Preparation of powders

In this study, fly ash-illmenite powders (fly ash with 40%illmenite) were mechanically milled in a FRITSCH-Planetary ball mill for 3 hours to get a homogeneous mixture. The planetary ball mill has 8 numbers of zirconia balls (20g) and 20 numbers of zirconia balls (2g) for milling. The powders obtained were sieved to proper particle size range with the help of a roto-tap sieve shaker machine by using Laboratory test sieves (ISO R565). The particle size the powders considered in the study range between 40 to 100 micrometer mostly about 50 micrometer was used as raw materials for coating deposition on various substrates.

3.2.2 Preparation of substrate

Commercially available copper and mild steel have been chosen as different substrate materials. The specimens were circular i.e. 1 inch dia disc, 3mm thick. The specimens were grit blasted at a pressure of 3 kg/cm² using alumina grits having a grit size of 60. The standoff distance in shot blasting was kept between 120-150 mm. The average roughness of the substrates was ~ 6.8 µm. The grit blasted specimens were

cleaned with acetone in an ultrasonic cleaning unit. Spraying was carried out immediately after cleaning.

3.2.3 Plasma spray coating deposition

The plasma spraying was done at the Laser and Plasma Technology Division, Bhaba Atomic Research Center, Mumbai. Conventional 40kW atmospheric plasma spraying (APS) set up was used. The plasma input power was varied from 11 to 21 kW by controlling the gas flow rate, voltage and the arc current. The powder feed rate was kept constant at 15 gm/min, using a turntable type volumetric powder feeder. The general arrangement of the plasma spraying equipment is shown in Fig.3.1.

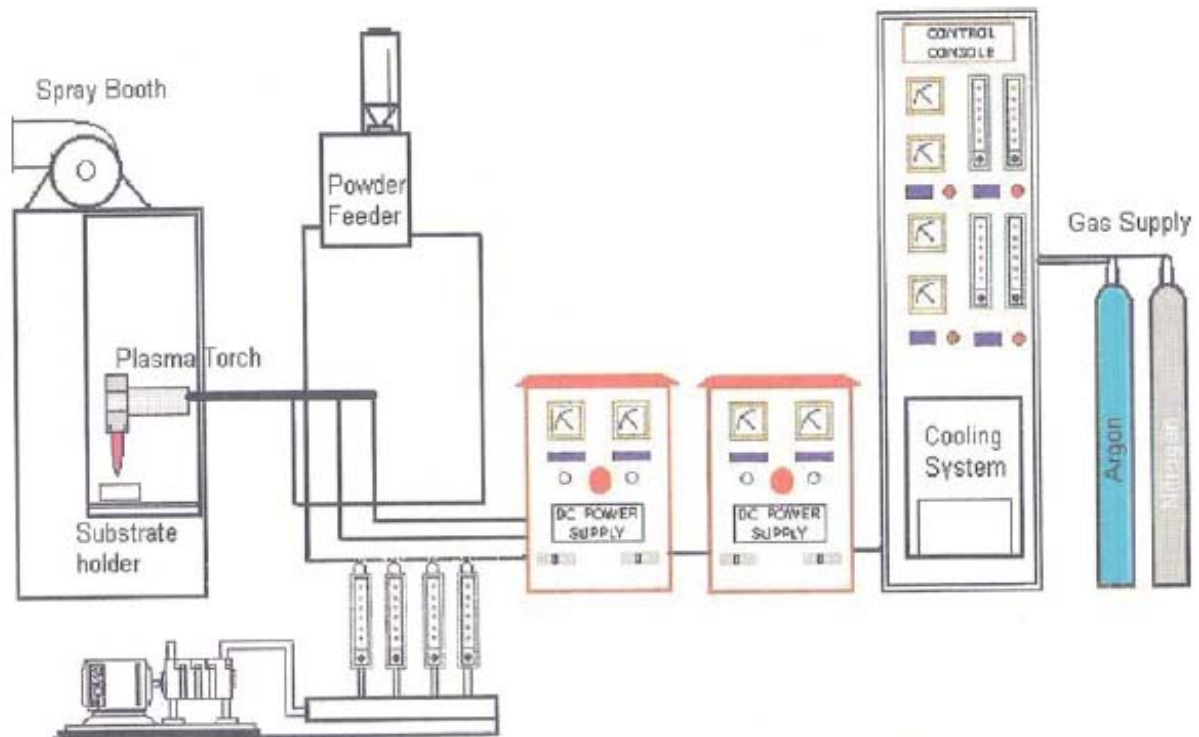


Fig. 3.1 General arrangement of the plasma spraying equipment.

The equipment consists of the following units :

1. Plasma torch
2. Control console

3. Powder feeder
4. Power supply unit
5. Water cooling system
6. Gas cylinders and accessories

- **The plasma torch:**

It is the device which houses the electrodes and in which the plasma reaction takes place. It has the shape of a torch and it is connected to the water-cooled power supply cables, powder supply hose and gas supply hose.

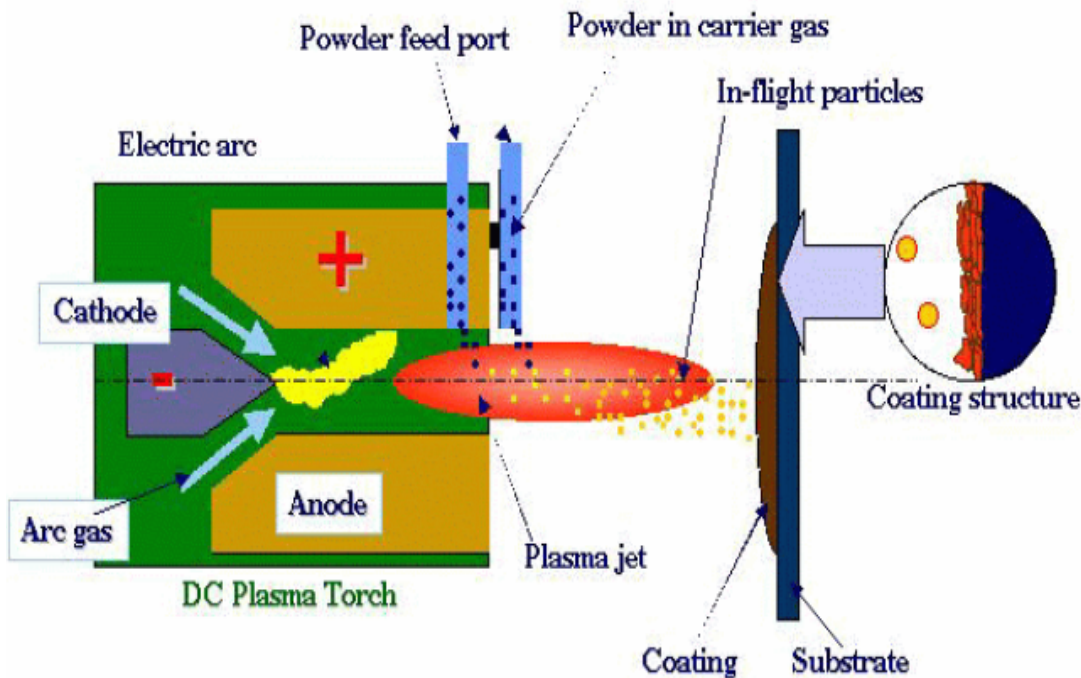


Fig. 3.2 The schematic of coating development by plasma spraying.

The plasma torch as shown in Fig.3.2 consists of a cathode, made of thoriated tungsten for better thermo-ionic emission and a nozzle shaped copper anode for high velocity plasma jet. The dimensions are: nozzle diameter: 6 mm, gap between the cathode and anode fixed at 12 mm and cathode length: 50 mm. Both the electrodes are water-cooled. The electrodes are separated by an insulating block made of teflon that has provision for gas injection. Powder to be spray deposited was injected through an

injection port located at the nozzle exit. An arc was created between cathode and anode (both water cooled). Plasma generating gas was forced to pass through the annular space between the electrodes. While passing through the arc, the gas ionized in the high temperature environment resulting plasma. The ionization was achieved by collisions of electrons of the arc with the neutral molecules of the gas. The plasma protrudes out of the electrode encasement in the form of a flame. The consumable material, in the powdered form, was poured into the flame in metered quantity. The powders melted immediately and absorbed the momentum of the expanding gas and rushed towards the target with velocity 100 m/sec to form a thin deposited layer. The next layer deposited onto the first immediately after, and thus the coating build up layer by layer. The temperature in the plasma arc can be as high as 10,000°C, velocity 600-800 m/sec and it is capable of melting anything. Elaborate cooling arrangement was required to protect the plasma torch (i.e., the plasma generator) from excessive heating.

- **The control unit:**

Important functions (current control, gas flow rate control etc.) are performed by the control unit. It also consists of the relays and solenoid valves and other interlocking arrangements essential for safe running of the equipment. For example the arc can only be started if the coolant supply is on and water pressure and flow rate is adequate.

- **The powder feeder:**

A turntable type powder feeder, designed and developed at the L&PT Division, BARC was used for injecting the powders into the plasma jet. The powder was kept inside a hopper. Powder flow rate was varied by motor speed. The flow rate of the powder was controlled precisely. A separate gas line directs the carrier gas which fluidizes the powder and carries it to the plasma arc. The carrier gas flow rate was chosen such that the powder particles enter the plasma core. This is because at lower flow rate, the particles may not be able to enter the core of the plasma leading to poor coating quality. On the other hand, if the carrier gas flow is very large, the powder particles will cross the central plasma zone without proper melting leading to poor quality of coating. So, the carrier gas flow rate was optimized for the powder.

- **The power supply unit :**

Normally plasma arc works in a low voltage (30-60 volts) and high current (300-700 Amperes), DC ambient. The available power (AC, 3 phase, 440 V) was transformed and rectified to suit the reactor. This was taken care of by the power supply unit. The power supply has a full control HF unit consisting of a HF (1 MHz) transformer.

- **The coolant water supply unit:**

It circulates water into the plasma torch, the power supply unit, and the power cables. Units capable of supplying refrigerated water are also available.

- **The Gas feeding system:**

The gas feeding system consists of gas cylinders, pressure gauges and gas tubes. The cylinders each have 7m³ capacities. The pressure was maintained at 75 kg/cm². There is a gas feeding arrangement for primary gas, secondary gas and carrier gas. Appropriate gas flow rates can be selected depending on the operating power and nature of the material to be coated. A four stage closed loop centrifugal pump at a pressure of 10 kgf/cm² supplies cooling water for the system. Argon was used as the primary plasma-gas and nitrogen as the secondary gas. The primary plasma gas (argon) and the secondary gas (nitrogen) were taken from normal cylinders at an outlet pressure of 4 kgf/cm². The powders were deposited at spraying angle of 90°. The powder feeding is external through a turntable type powder feeder. The properties of the coatings are dependent on the spray process parameters. The operating parameters during coating deposition process are listed in Table 3.1.

Table 3.1 Operating parameters during coating deposition.

Plasma Arc Current (amp)	280, 360, 425, 500
Arc Voltage (volt)	40, 40 , 44 , 44
Torch Input Power (kW)	11,15,18,21
Plasma Gas (Argon) Flow Rate (lpm)	28
Secondary Gas (N ₂) Flow Rate (lpm)	3
Carrier Gas (Argon) Flow Rate (lpm)	12
Powder Feed Rate (gm/min)	15
Torch to Base Distance TBD (mm)	100

3.3 CHARACTERIZATION OF POWDER

3.3.1 Particle Size Analysis

The particle sizes of the raw materials used for coating (fly ash-illmenite powder) were characterized using Laser particle size analyzer of Malvern Instruments make.

3.4 CHARACTERIZATION OF COATINGS

3.4.1 Evaluation of Coating Deposition Efficiency

Deposition efficiency is defined as the ratio of the weight of coating deposited on the substrate to the weight of the expended feedstock. Weighing method is accepted widely to measure this. Each specimen is weighed before and after coating deposition. The difference is the weight (G_c) of coating deposited on the substrate. From the powder feed rate and time of deposition the weight of expended feed stock (G_p) is determined. The deposition efficiency (η) is then calculated using the equation $\eta = (G_c / G_p \times 100) \%$. Weighing of samples was done using a precision electronic balance with ± 0.1 mg accuracy.

3.4.2 Evaluation of Coating Interface Bond Strength

To evaluate the coating adhesion strength, a special type jig (Fig.3.3) was fabricated. Cylindrical mild steel dummy samples (length 25 mm, top and bottom diameter 12 mm) were prepared. The surfaces of the dummies were roughened by punching. These dummies were then fixed on top of the coating with the help of a polymeric adhesive and pulled with tension after being mounted on the jig (Fig.3.4). The coating pullout test was carried out using the set up Instron 1195 at a crosshead speed of 1 mm/minute.



Fig. 3.3 Jig used for the test



Fig. 3.4 Specimen under tension



Fig. 3.5 Adhesion test with Instron 1195 UTM.

The moment coating got torn off from the specimen, the reading (of the load), which corresponds to the adhesive strength of the coating, was recorded. A typical test set up (during testing) is shown in Fig.3.5 The test was performed as per ASTM C-633.

3.4.3 Coating Thickness Measurement

Thickness of the fly ash-illmenite coatings on different substrates were measured on the polished cross-sections of the samples, using an optical microscope. Five readings were taken on each specimen and the average value is reported as the mean coating thickness.

3.4.4 Porosity Measurement

Measurement of porosity was done using the image analysis technique. The porosity of the coatings was measured by putting polished cross sections of the coating sample under a microscope (Neomate) equipped with a CCD camera (JVC, TK 870E). This system is used to obtain a digitized image of the object. The digitized image is transmitted to a computer equipped with VOIS image analysis software. The total area captured by the objective of the microscope or a fraction thereof can be accurately measured by the software. Hence the total area and the area covered by the pores are separately measured and the porosity of the surface under examination is determined.

3.4.5 Microhardness Measurement

Small specimens were sliced from the coated samples. Samples containing coating cross-sections were mounted and polished for the microhardness measurement. Microscopic observation under optical microscope of the polished section of the coatings exhibited three distinctly different regions/ phases namely grey, dark and spotted/mixed. Vickers Microhardness measurement was made on these optically distinguishable phases using Leitz Microhardness Tester equipped with a monitor and a microprocessor based controller, with a load of 0.245N and a loading time of 20 seconds. About twelve or more readings were taken on each sample and the average value is reported as the data point.

3.4.6 X-Ray Diffraction Studies

X-ray diffraction technique was used to identify the different (crystalline) phases present in the coatings. XRD analysis was done using Ni-filtered Cu-K α radiation in a Philips X-ray diffractometer. The characteristic d-spacing of all possible values are taken from JCPDS cards and were compared with d-values obtained from XRD patterns to identify the various X-ray peaks obtained.

3.4.7 Scanning Electron Microscopic Studies

Plasma sprayed coated specimens and plasma processed powders were studied by JEOL JSM-6480 LV scanning electron microscope mostly using the secondary electron imaging. The surface as well as the interface morphology of all coatings was observed under the microscope. Small specimens were sliced from the coated samples and were mounted using thermosetting molding powders. Coating cross-sections was polished in three stages using SiC abrasive papers of reducing grit sizes and then with diamond pastes on a wheel for coating interface analysis under SEM. These specimens were also utilized for the microhardness measurement.

3.5 EROSION WEAR BEHAVIOUR OF COATINGS

Solid particle erosion (SPE) is usually simulated in laboratory by one of two methods. The ‘sand blast’ method, where particles are carried in an air flow and impacted onto a stationary target; and the ‘whirling arm’ method, where the target is spun through a chamber of falling particles. The schematic diagram of the sand blast type of erosion test rig is shown in Fig.3.6

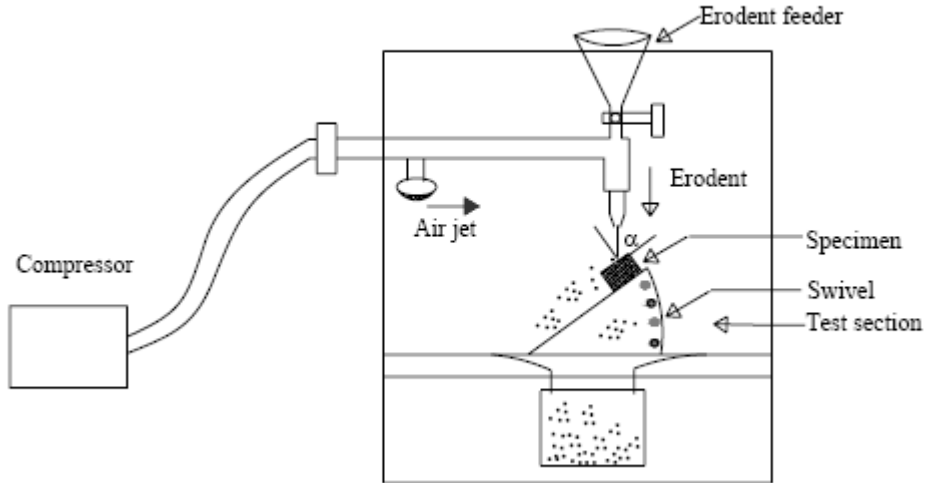


Fig. 3.6 Schematic diagram of the erosion test rig.

In the present investigation, an erosion apparatus (fabricated in laboratory) of the ‘sand blast’ type was used as shown in Fig.3.7. It is capable of creating highly reproducible erosive situations over a wide range of particle sizes, velocities, particles fluxes and incidence angles, in order to generate quantitative data on materials and to study the mechanisms of damage. The test was conducted as per ASTM G76 standards.



(a)



(b)

Fig. 3.7 Erosion test set up

The jet erosion test rig used in this work employs a 300 mm long nozzle of 3 mm bore and 300 mm long. This nozzle size permits a wider range of particle types to be used in the course of testing, allowing better simulations of real erosion conditions. The mass flow rate was measured by conventional method. Particles were fed from a simple hopper under gravity into the groove. Velocity of impact is measured using double disc method. Some of the features of this test set up are:

- Vertical traverse for the nozzle: provides variable nozzle to target standoff distance, which influences the size of the eroded area.
- Different nozzles may be accommodated: provides ability to change the particle plume dimensions and the velocity range.
- Large test chamber with sample mount (typical sample size 25 mm x 25 mm) that can be angled to the flow direction: by tilting the sample stage, the angle of impact of the particles can be changed in the range of 0°– 90° and this will influence the erosion process.

The erosion wear rates were obtained by carrying out experiments as per conditions of a standard Taguchi experimental plan with notation **L9**, for fly ash-illmenite coatings of 18 kW and 11 kW power level. The coatings were eroded at different impact angles (i.e. at 30°, 60°, 90°) at stand of distance of 150 mm; and at a pressure of 6.5kgf/cm² (i.e. at a velocity of 58m/sec) with dry silica sand of 400 µm size and silicon carbide erodent of 200 µm sizes. Amount of wear is determined on ‘mass loss’ basis. It was done by measuring the weight change of the samples at regular time intervals during the test duration. A precision electronic balance with 0.001 mg accuracy was used for weighing. Erosion rate, defined as the coating mass loss per unit erodent mass (gm/gm) was calculated.

Chapter 4

RESULTS AND DISCUSSION

CHAPTER 4

RESULTS AND DISCUSSION

4.1 INTRODUCTION

Plasma sprayed coatings of fly ash-illmenite were developed on two different metal substrates (i.e. copper and mild steel), using a 40 kW atmospheric plasma spray system, at different input power levels to the plasma torch (in the range from 11 kW to 21 kW). Characterizations of the coatings were done and the tribological performances of the coating was evaluated. The results of various tests are presented and discussed in this chapter.

4.2 PARTICLE SIZE ANALYSIS

The particle size distribution of fly ash-illmenite powder (after mixing in ball mill and before plasma spraying) was characterized using Laser particle size analyzer of Malvern Instruments make. Fig 4.1 shows the particle size distribution of the feed stock. It can be seen that, majority of particles are in the range of 40 to 100 micron. Maximum volume fractions of the particles are in the range of 50 micron.

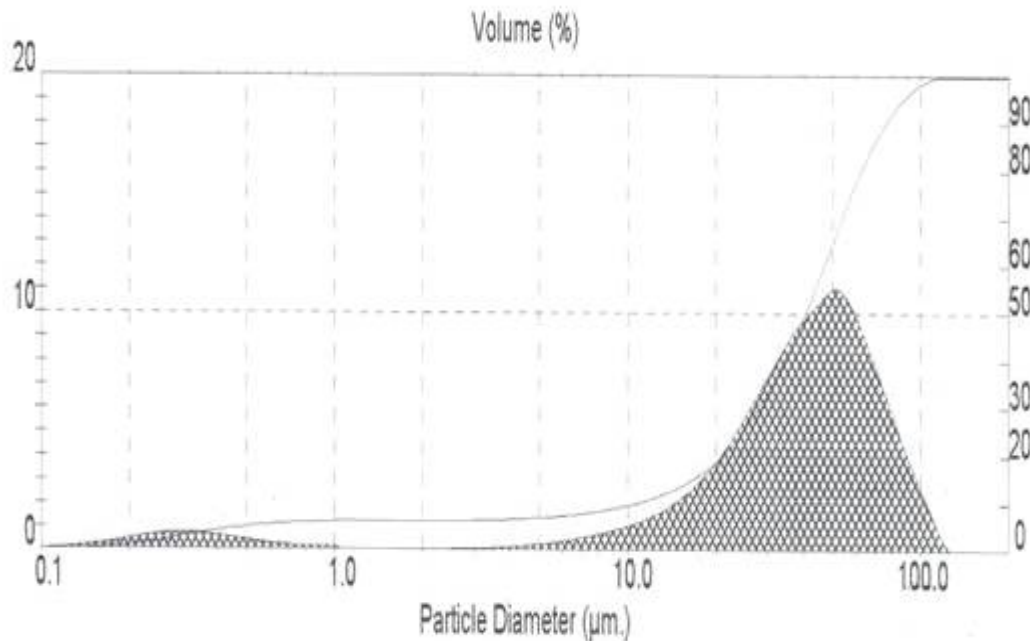


Fig. 4.1 Particle size distribution of fly ash-illmenite feed stock

4.3 COATING DEPOSITION EFFICIENCY

Deposition efficiency is an important factor that determines the techno-economics of the process. Deposition efficiency of coating made within the scope of this investigation is evaluated. Coating deposition efficiency is defined as the ratio of the weight of coating deposited on the substrate to the weight of the expended feedstock. Weighing method is accepted widely to measure this. It can be described by the equation 4.1. [112]

$$\eta = (G_c / G_p) \times 100 \% \quad \text{..... (4.1)}$$

Where, η is the deposition efficiency

G_c is the weight of coating deposited on the substrate

G_p is the weight expended feedstock

Deposition efficiency depends on many factors that include the input power to the plasma torch, material properties, such as melting point, particle size range, heat capacity of the powder being sprayed and stand off distance (torch to substrate distance) etc. For a given stand off distance and given material with specific particle size, torch power appears to be an important factor for the deposition efficiency. The deposition efficiency is a measure of the fraction of the powder that has melted, but that has not vaporized or decomposed into gaseous products. Deposition efficiency values of fly ash-illmenite coating made at different operating power levels (on mild steel substrate) is given in Table 4.1.

Table 4.1 Coating deposition efficiency of fly ash-illmenite coatings.

Sl. No.	Specimen	Power level(kW)	Deposition efficiency (%)
1	Fly ash-Illmenite coating	11	25
2	-do-	15	35
3	-do-	18	45
4	-do-	21	48

Fig. 4.2 shows the variation of deposition efficiency of fly ash-illmenite coating with operating power level on mild steel substrate. It is interesting to note that the deposition efficiency is increased in a sigmoidal fashion with the torch input power. It reveals that efficiency of coating deposition is significantly influenced by the input power to the torch.

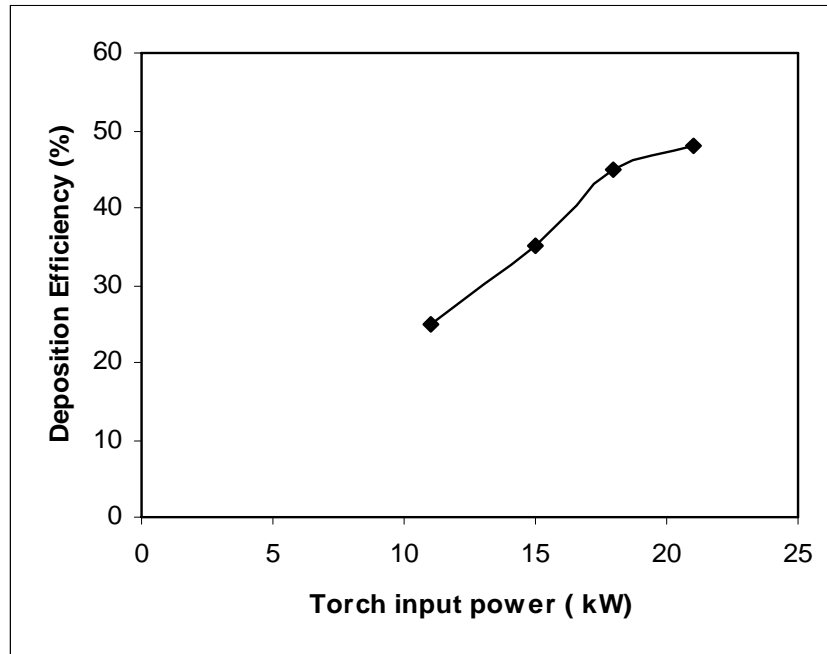


Fig. 4.2 Deposition efficiency of fly ash-illmenite coatings made at different power level on mild steel substrate

Plasma spray deposition efficiency of a given materials depends on its melting point, thermal heat capacity and particle size of the powder. At lower input power to the plasma torch, the plasma jet temperature is not high enough to melt the entire powder particles that enter the plasma jet. As the power is increased, the average plasma temperature increases there by melting a larger fraction of the powder. The spray efficiency therefore increases with input power to the plasma torch. However, beyond a certain power level, the temperature of the plasma is very high, leading to vaporization/dissociation/fragmentation of the powder particles. This causes the deposition efficiency to decrease at higher power levels. This tendency is generally observed in plasma spray depositions. However, the plasma operating power above which the efficiency decrease depends on the chemical nature of the feed material i.e. powder properties.

4.4 COATING ADHESION STRENGTH

Coating adhesion tests have been carried out by many investigators with various coatings. It has been stated that, the fracture mode is adhesive if it takes place at the coating-substrate interface and that the measured adhesion value is the value of practical adhesion, which is strictly an interface property, depending exclusively on the surface characteristics of the adhering phase and the substrate surface condition. [113,114]. From the microscopic point of view, adhesion is due to physico-chemical surface forces (Vander-walls, Covalent, ionic etc.), which are established at the coating-substrate interface [115], and corresponds to the work of adhesion. From the mechanical point of view, adherence can be estimated by the force corresponding interfacial fracture and is macroscopic in nature.

In this work, evaluation of coating interface bond strength is done using coating pullout method, confirming to ASTM C-633 standard. It is found that, in all the samples fracture occurred at the coating-substrate interface. The results are tabulated in Table 4.2. The low value of adhesion strength of fly ash-illmenite may be due to difference in coefficient of thermal expansion of substrate and coating and/or formation of pores, cracks, voids in the coating and along coating-substrate interfaces.

Table 4.2 Adhesion strength values of fly ash-illmenite coating at different power levels

Sl.No	Specimen	Power level (kW)	Substrate	Adhesion strength (MPa)
1	Fly ash-illmenite	11	Mild steel	3.718
2	-do-	15	Mild steel	4.562
3	-do-	18	Mild steel	6.732
4	-do-	21	Mild steel	6.2
5	-do-	11	Copper	3.0208
6	-do-	15	Copper	5.842
7	-do-	18	Copper	6.18
8	-do-	21	Copper	4.86

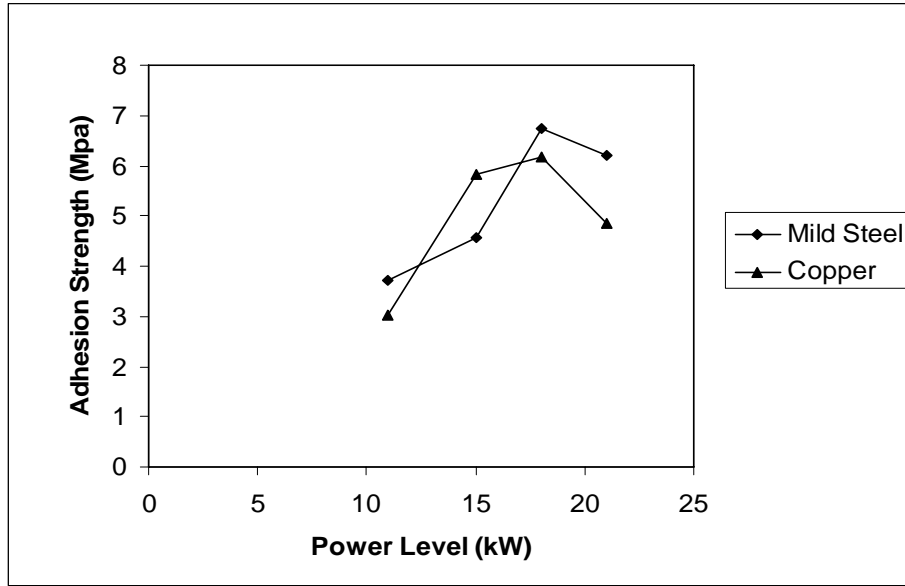


Fig. 4.3 Adhesion strength of fly ash-illmenite coatings on different substrates

The variation of adhesion strength of fly ash-illmenite coating to the mild steel and copper substrates at different power levels is shown in Fig.4.3. From the figure, it is clear that the adhesion strength varies with operating power of the plasma torch. Maximum adhesion strength of 6.732 Mpa on mild steel substrate and of 5.842 Mpa on copper substrate is recorded on the coatings deposited at 18 kW power level. It can be visualized that, the interface bond strength increases with the input power of the torch up to a certain power level and then shows a decreasing trend in coating adhesion, irrespective of the substrate material. This might be due to the fact that, when the operating power level is increased, larger fraction of particles attain molten state as well as the velocity of the particles also increases. Therefore there is better splat formation and mechanical inter-locking of molten particles on the substrate surface leading to increase in adhesion strength [60]. However, at a much higher power level, the amount of fragmentation and vaporization of the particles increases. There is also a greater chance to fly off of smaller particles during in-flight traverse through the plasma jet and results in poor adhesion strength of the coatings. Coating adhesion strength is more in case of mild steel substrate than that of copper substrate, may be due to the dependence of thermal conductivity for melted particle, dissipation of heat at metal interface and also due to thermal expansion coefficient mismatch at the ceramic metal interface [61].

4.5 COATING THICKNESS

To ensure the coating of fly ash-illmenite on different substrates, coating thickness was measured on the polished cross-sections of the samples, using an optical microscope. The thickness values obtained for coatings deposited at different power levels for Mild steel substrates are presented in Table 4.3. Each data point on the curves is the average of at least five readings/measurements. The variation thickness values with torch input power for Mild steel substrate is presented in Fig.4.4.

Table 4.3 Thickness values of fly ash-illmenite coatings made for mild steel substrates.

Sl. No.	Specimen	Power level (kW)	Coating Thickness(Micron)
1	Fly ash-illmenite coating	11	150
2	-do-	15	170
3	-do-	18	200
4	-do-	21	210

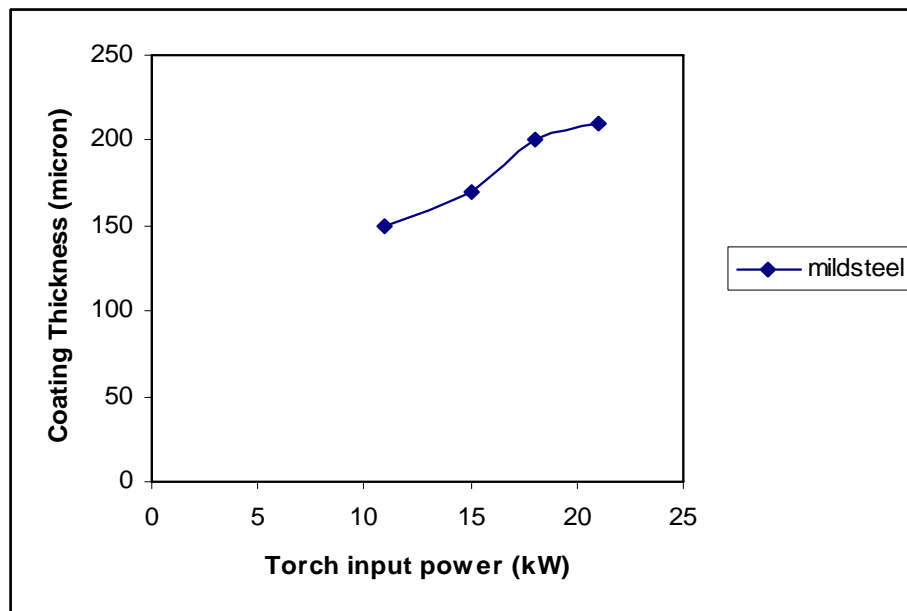


Fig. 4.4 Variation of coating thickness values with torch input power for Mild steel substrate

Maximum coating thickness of ~ 210 micron on mild steel substrates deposited at 21 kW power levels is obtained. From the figure it is evident that there is an increase in coating thickness with increase in input power to the plasma torch. In thermal spray of oxide coatings developed using atmospheric plasma spray (APS) technique; particle deposition is influenced mainly by the input power to the plasma torch. With increase in power level, the plasma density increases leading to a rise in enthalpy and thereby the particle temperature. Hence more number of particles gets melted during in-flight traverse through plasma jet. When these molten species hit the substrate, get flattened and adhere to the surface. The deposition of layers is favored with availability of more number of molten / semi molten particles which is enhanced by increasing the torch input power. This increases the coating thickness. But, beyond certain limit of operating power level; fragmentation and vaporization of sprayed particles do occur simultaneously and some particles fly off during spraying, restricting further increase in coating thickness. Increase of thickness and presence of cavities at inter-lamellar spaces may be the cause of decrease in adhesion strength.

4.6 COATING POROSITY

Porosity measurement was done using the image analysis technique. The polished interfaces of various coatings are studied under optical microscope (Neomate) equipped with a CCD camera (JVC, TK 870E). From the digitized image obtained by this system, coating porosity was determined using VOIS image analysis software. The results are tabulated in Table 4.4.

Table 4.4 Porosity of coating for different power levels

Sl.No	Specimen	Power level (kW)	Porosity (%)
1	Flyash-illmenite coating	11	23.95
2	-do-	15	12.1
3	-do-	18	11.38
4	-do-	21	14.13

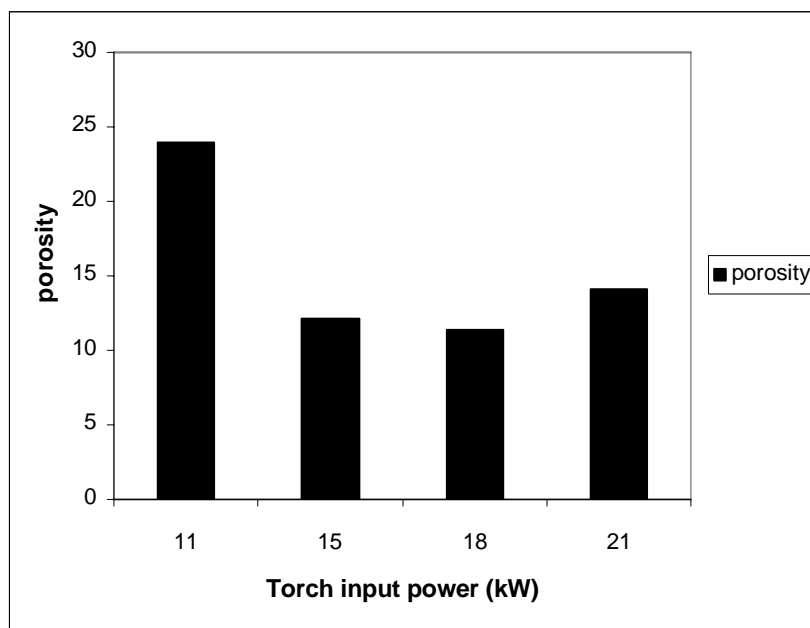


Fig. 4.5 Variation of coating porosity of fly ash-illmenite with torch input power

Variation of coating porosity of fly ash-illmenite with torch input power is shown in fig.4.6. It is observed that the amount of porosity is more in the case of coatings made at lower (11kW) and at higher (21kW) power levels. However, porosity is minimum at 18kW for the coatings made under this study. The increased value of porosity may be the reason of low adhesion strength of the coatings deposited at low and at high power levels.

4.7 COATING HARDNESS

Microscopic observation of the polished cross section of the coatings revealed three distinct different visible regions/ phases namely white, dull and mixed. Micro-hardness measurement is done on these optically distinguishable phases with Leitz Micro-Hardness Tester using 50Pa (0.419N) load, are summarized in Table 4.6. Each data point represents the average of twelve readings.

Table 4.5 Hardness on the coating cross section for the coating

Sl.no	Power level(kW)	Phase	Hardness (Hv)
1	11	White	472.78
2	11	Dull	706.82
3	11	Mixed	160.27
4	15	White	527.82
5	15	Dull	476.18
6	15	Mixed	167.79
7	18	White	617.52
8	18	Dull	437.72
9	18	Mixed	150.66
10	21	White	719.33
11	21	Dull	612.51
12	21	Mixed	145.34

The results show that these three structurally different phases bear three different ranges of hardness. With increase in power level there is an increase in hardness values of some phases, which may be due to the formation/transformation of different allotropic forms and their composition variations during spray deposition.

4.8 XRD PHASE COMPOSITION ANALYSIS

Micro-hardness test shows different hardness values on different optically distinct regions on the coating cross-sections. Therefore, to ascertain the phases present and phase changes / transformation taking place during plasma spraying, X-ray diffractograms are taken on the raw material and on coatings using a Philips X Ray Diffractometer with CuK α radiation. The XRD results are shown in Fig 4.6.

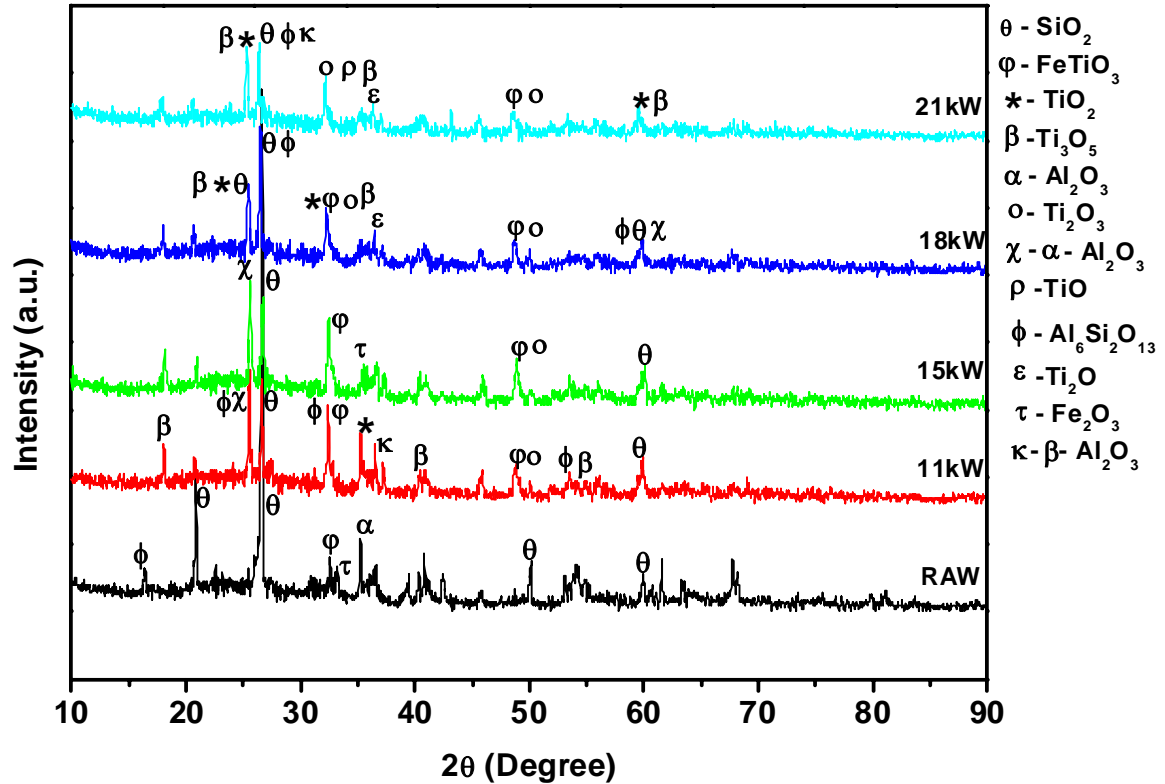


Fig.4.6 X-Ray Diffractogram of fly ash-illmenite raw powder and coating deposited at 11kW, 15kW, 18kW, 21kW power level

The XRD of the feed material shows the presence of SiO₂, FeTiO₃, etc. Coating made at lower power level i.e. at 11kW shows the presence of α - Al₂O₃, SiO₂, FeTiO₃, Ti₂O₃ and some new phases such as TiO₂, Ti₃O₅ & mullite. With increase in power level the percentage of inter-oxide phases i.e. Ti₃O₅, Ti₂O₃ and mullite are found to increase. It may be due to the availability of high temperature which has accelerated the phase transformation, with increase in torch input power during coating deposition. Generally, Al₂O₃ transforms to different allotropic phase (α - Al₂O₃ and β -Al₂O₃) and TiO₂ reduces to Ti₃O₅, Ti₂O₃, Ti₂O, TiO etc. depending on

enthalpy/environment and transformation conditions [116,117]. This trend is also observed in the diffraction patterns (Fig 4.6). During plasma spraying the different phase transformations are taking place, so it is expected that a ceramic composite coating from low grade materials could be made which can have better wear resistance properties. So wear properties of the coatings are studied.

4.9 EROSION WEAR BEHAVIOUR OF COATINGS

Solid particle erosion is a wear process where particles strike against a surface and promote material loss. During flight, a particle carries momentum and kinetic energy, which can be dissipated during impact due to its interaction with a target surface. In case of plasma spray coatings encountering such situations, no specific model has been developed and thus the study of their erosion behavior has been mostly based on experimental data [111]. Erosion is a non-linear process with respect to its variables: either materials or operating conditions. To obtain the best functional output of coatings exhibiting selected in-service properties, the right combinations of operating parameters are to be known. These combinations normally differ by their influence on the erosion wear rate i.e. coating mass loss.

The less erosion wear rate is one the main requirements of the coatings developed by plasma spraying. In order to achieve certain values of erosion rate accurately and repeatedly, the influence parameters of the process have to be controlled accordingly. Since the number of such parameters in plasma spraying is too large and the parameter-property correlations are not always known, statistical methods can be employed for precise identification of significant control parameters for optimization. In recent years, Taguchi method has become a widely accepted methodology for improving productivity. The Taguchi method consists of a plan of experiments with the objective of acquiring data in a controlled way, executing these experiments and analyzing data, in order to obtain information about the behavior of a given process. One of the advantages of the Taguchi method over the conventional experiment design methods is that it minimizes the variability around the target when bringing the performance value to the target value in addition to keeping the experimental cost at the minimum level. Another advantage is that optimum working conditions determined from the laboratory work can also be reproduced in the real production environment [118].

Hence, in this work, Taguchi experimental design method is adopted to investigate the effects of impact angle, velocity, size of the erodent and stand off distance on erosion wear rate.

4.9.1 Experimental design

Experiments are carried out to investigate the influence of the four selected control parameters. The code and levels of control parameters are shown in Table 4.6. This table shows that the experimental plan has three levels. A standard Taguchi experimental plan with notation **L9** is chosen as outlined in Table 4.7 and the erosion wear rates are obtained by carrying out experiments under such conditions for coatings of 11kW and 18kW power level. Fig 4.7 shows erosion wear rate of coatings, under different test conditions, at 11 kW and 18 kW power level are almost same. Experimental results are transformed into a signal-to-noise (S/N) ratio as shown in Table 4.8 and Table 4.9. It uses the S/N ratio as a measure the quality characteristics deviating from or nearing to the desired values. There are three categories of quality characteristics in the analysis of the S/N ratio, i.e. the lower-the-better, the higher-the-better, and the nominal-the-better. To obtain optimal spraying parameters, the lower-the-better quality characteristic for erosion wear rate is taken. Analysis of the influence of each control factor on the coating efficiency is made with a signal-to-noise (S/N) response table, using **MINITAB** computer soft wear package. The response data of the testing process is presented in Table 4.10 and Table 4.11. The S/N response graph for coating erosion wear rate is shown in Fig.4.8 and Fig.4.9. The influence of interactions between control factors is also analyzed in the response table. The control factor with the strongest influence is determined by differences of the obtained values. The higher the difference, the more influential is the control factor or an interaction of two controls.

Table 4.6 Control factors and selected test levels.

Parameter	Code	Level 1	Level 2	Level 3
Erodent Size (μm)	A	300	500	800
Impact Angle (Degree)	B	30	60	90
Impact Velocity (m/sec)	C	32	44	58
Stand Off Distance (mm)	D	120	160	200

Table 4.7 Experimental layout and erosion wear rate under different test conditions for coatings at 11kW and 18kW power levels

Sl.no (Test runs)	A Erodent size (micron)	B Angle of Impact (degree)	C Impact Velocity (m/sec)	D Stand-off Distance (mm)	Er (mg/kg) 11 kW	Er (mg/kg) 18kW
1	300	30	32	120	65.64	67.564
2	300	60	44	160	91.73	94.573
3	300	90	58	200	92.45	96.475
4	500	30	44	200	73.4	67.5
5	500	60	58	120	170.9	176
6	500	90	32	160	129.1	136.463
7	800	30	58	160	80.9	77.765
8	800	60	32	200	111.79	116.4
9	800	90	44	120	148.82	144.5

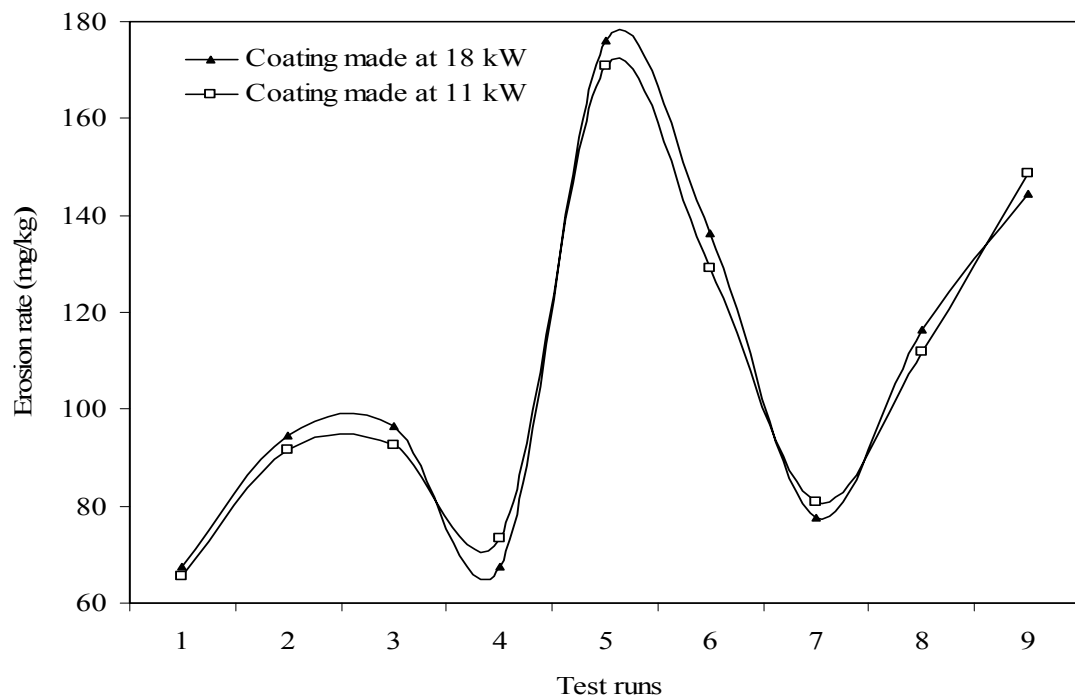


Figure 4.7 Erosion wear rate of coatings under different test conditions

Table 4.8 S/N ratios for coating erosion wear rate at 11kW

Sl. No (Test runs)	A Erodent size (micron)	B Angle of Impact (degree)	C Impact Velocity (m/sec)	D Stand-off Distance (mm)	Er (mg/kg) 11kW	S/N Ratio
1	300	30	32	120	65.64	-36.3434
2	300	60	44	160	91.73	- 39.2502
3	300	90	58	200	92.45	-39.3181
4	500	30	44	200	73.4	-37.3139
5	500	60	58	120	170.9	-44.6548
6	500	90	32	160	129.1	-42.2185
7	800	30	58	160	80.9	-38.159
8	800	60	32	200	111.79	-40.9681
9	800	90	44	120	148.82	-43.4538

Table 4.9 S/N ratios for coating erosion wear rate at 18kW

Sl. No (Test runs)	A Erodent size (micron)	B Angle of Impact (degree)	C Impact Velocity (m/sec)	D Stand-off Distance (mm)	Er (mg/kg) 18kW	S/N Ratio
1	300	30	32	120	67.564	-36.5943
2	300	60	44	160	94.573	-39.515
3	300	90	58	200	96.475	-39.6883
4	500	30	44	200	67.5	-36.5861
5	500	60	58	120	176	-44.9103
6	500	90	32	160	136.463	-42.7003
7	800	30	58	160	77.765	-37.8157
8	800	60	32	200	116.4	-41.3191
9	800	90	44	120	144.5	-43.1974

Table 4.10 Response Table for Signal to Noise Ratios (for 11 kW)

Level	A (Erodent size)	B (Angle of Impact)	C (Impact Velocity)	D (Stand-off Distance)
1	-38.30	-37.27	-39.84	-41.48
2	-41.40	-41.62	-40.01	-39.88
3	-40.86	-41.66	-40.71	-39.20
Delta	3.09	4.39	0.87	2.28
RANK	2	1	4	3

Table 4.11 Response Table for Signal to Noise Ratios (for 18 kW)

Level	A (Erodent size)	B (Angle of Impact)	C (Impact Velocity)	D (Stand-off Distance)
1	-38.60	-37.00	-40.20	-41.57
2	-41.40	-41.91	-39.77	-40.01
3	-40.78	-41.86	-40.80	-39.20
Delta	2.80	4.92	1.04	2.37
RANK	2	1	4	3

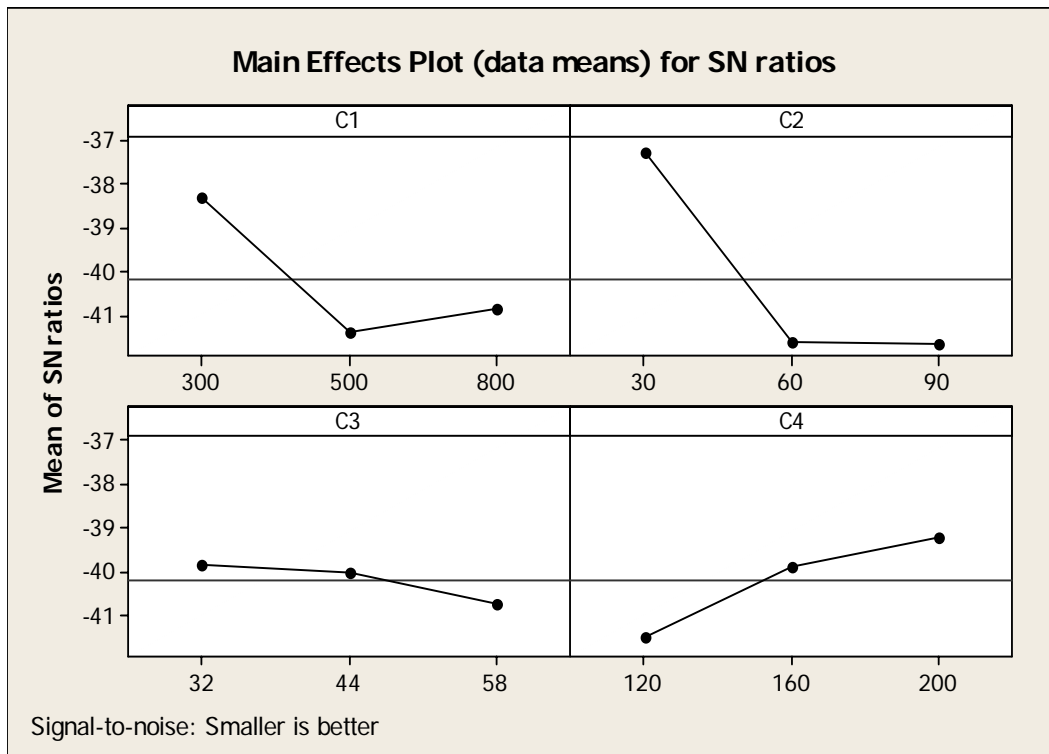


Fig.4.8 Relative effect of main factors on erosion rate of the coatings made at 11 kW

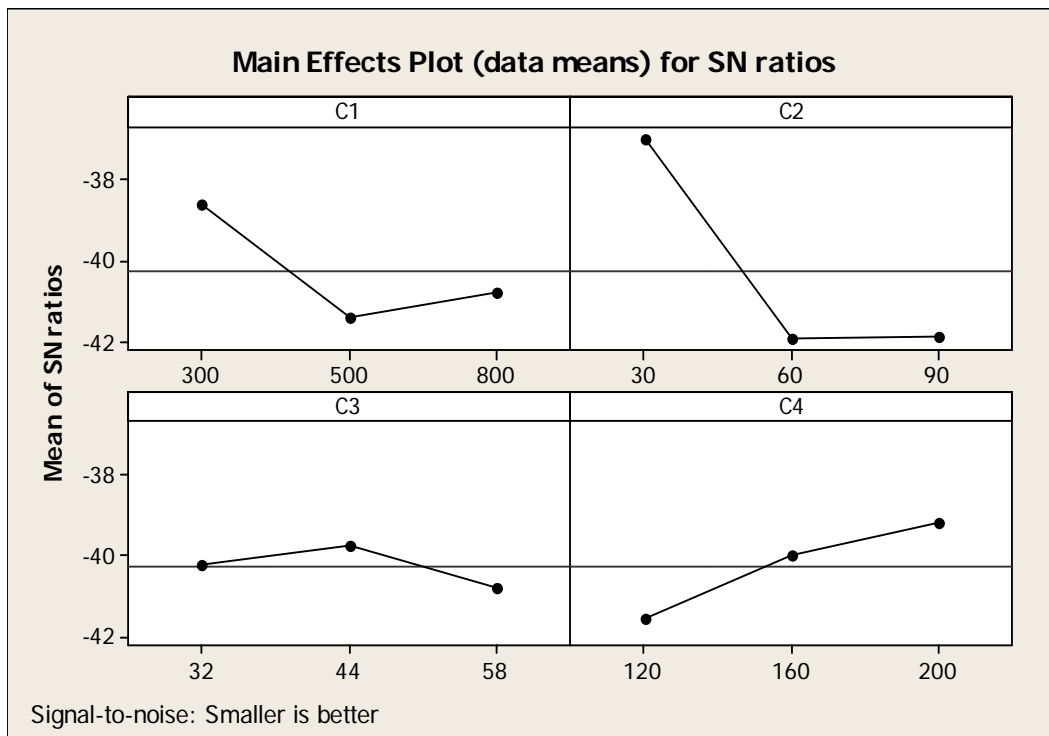


Fig4.9 Relative effect of main factors on erosion rate of the coatings made at 18kW

It is interesting to note that the Taguchi experimental design method identified impact angle and size of the erodent as the most powerful factor influencing the erosion wear rate of the fly ash-illmenite coatings. The stand off distance, velocity impact emerges as the other significant factors affecting the coating erosion wear rate.

Based on the above findings, erosion tests were carried out, on plasma sprayed fly ash-illmenite coatings by a stream of dry silica sand with an average particle size range of $\sim 400\ \mu\text{m}$ and silicon carbide particles of average size of $\sim 200\ \mu\text{m}$; at different impact angles (30° , 60° , 90°) with stand of distance of 150 mm (i.e. exit point of the erodent form the nozzle to the specimen/substrate) and at a velocity of 58 m/sec.

The variation of cumulative mass loss with time, in case of the coating eroded by sand is illustrated in Fig 4.10 & in case of the coating eroded by SiC is illustrated in Fig 4.11.

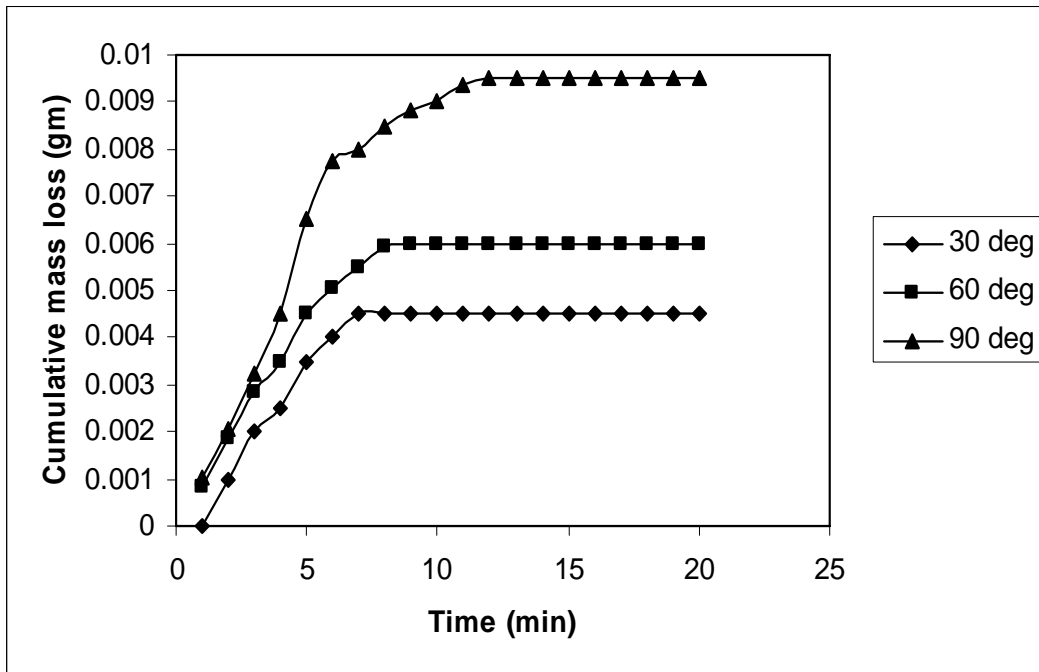


Fig.4.10 Variation of Coating mass loss with time, for $400\ \mu\text{m}$ size (dry silica sand) erodent

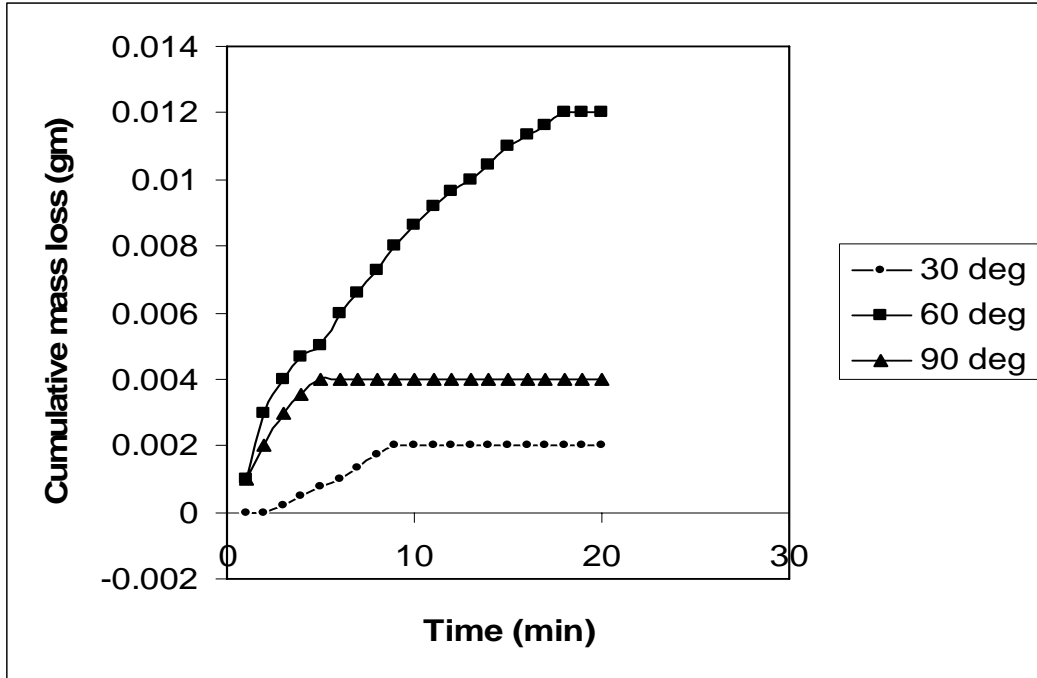


Fig.4.11. Variation of Coating mass loss with time; for 200 μm size (SiC) erodent.

From the figures it is seen that, the coating mass loss increases with increasing the time of attack. The cumulative increment in material loss due to erosion wear of plasma sprayed coatings with time and erodent dose has been studied by Levy [119]. In the present work such a trend is also found in case of all coatings, subjected to erosion test irrespective of angle of impact. This can be attributed to the fact that, the fine protrusions on the top layer of the coatings may be relatively loose and removed with less energy than what would be necessary to remove a similar portion/layer from the bulk of the coating at further time length. Consequently, the initial wear rate is high. With increasing exposure time the rate of wear starts decreasing and in the transient regime, a steady state in the wear rate is obtained.

The variation of erosion rate with time at impact angles of 30°, 60° and 90°, eroded with 400 μm size silica sand is shown in Fig.4.12 and for the sample eroded with 200 μm size silicon carbide erodent is shown in Fig.4.13

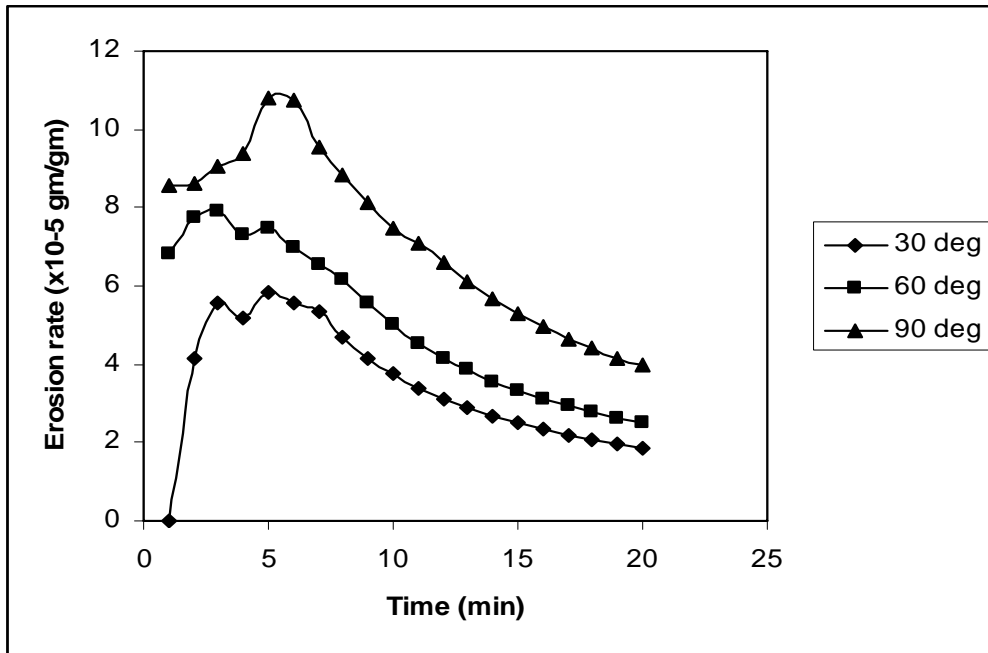


Fig.4.12. Variation of Erosion rate with time for the sample eroded with sand.

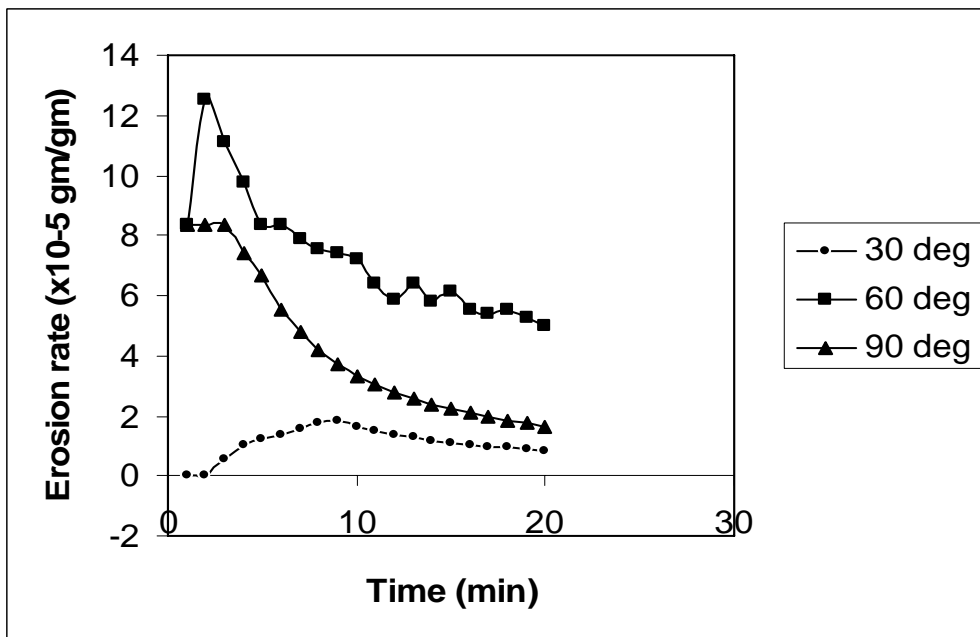


Fig.4.13 Variation of Erosion rate with time for the sample eroded with silicon carbide.

From the above figures it is observed that, the erosion rate increases with increasing the angle of impact and maximum erosion takes place at $\alpha = 90^\circ$, when eroded by sand; and $\alpha = 60^\circ$ when eroded by SiC. Similar to this, a difference in maximum erosion rate was observed in glass [120]. They have also observed the maximum erosion rate at 90° impact angle when eroded by sand and that at 30° impact angle when eroded by silicon carbide. Studies on the effect of the incidence angle on the erosion rate on brittle materials show that, the maximum erosion takes place at normal impact angle where as in case of ductile materials; the material removal is by plastic deformation and reaches its maximum rate at shallow impact angles [121]. According to the common rule of the erosion rate with the change of impact angle α , the erosion wear can be divided into plastic material wear and brittle material wear. The relationship between erosion rate and impact angle as predicted by Lishizhou [122] is;

$$E = A \cos^2 \alpha \sin (m\alpha) + B \sin^2 \alpha \quad \dots\dots\dots (4.2)$$

Where m , A and B are constants.

For typical brittle material, A is equal to zero and the erosion rate is largest at 90° impact angle. For typical plastic material, B is equal to zero and the erosion rate is largest at 20° – 30° impact angle. From the above, the erosion behavior of the fly ash-illmenite coating deposited at 15kW eroded by sand is like the behavior of brittle material. But, the coating eroded by SiC erodent shows some amount of plastically deformed regions and hence maximum amount of material removal occurred at 60° angle of impact. According to I.M. Hutchings [123], the transition in the erosion mechanism from plastic deformation to brittle fracture was explained by the necessary collision energy of the particle to reach a certain threshold. He had proposed the dimensionless expression $(K_{CT}^2 / r.H_T^2)$, in which ‘ r ’ is the radius of the particle, can be used to determine the nature of the dominant erosion mechanism. A lower value of this expression is indicative of brittle fracture. To describe the nature and the mechanism of erosion of different materials, other authors have argued for a new parameter known as the erosion efficiency η , defined as: $\eta = 2E_r.H / \rho V^2$, where E_r is the erosion rate, H the hardness, ρ the density of the specimen and V be the velocity at impact [124]. The variation of erosion wear loss confirms that the angle at which the stream of solid particles impinges the coating surface influences the rate at which the material is removed. It further suggests that, this dependency is also influenced by the nature of the coating material. The angle of impact determines the relative magnitude of the two components of the impact velocity namely, the component normal to the surface and parallel to the surface. The normal component determines/is responsible for the lasting time of impact (i.e.

contact time) and the load. The product of this contact time and the tangential (parallel) velocity component determines the amount of sliding that takes place. The tangential velocity component also provides a shear loading to the surface, which is in addition to the normal load of the normal velocity component. Hence, as this angle changes the amount of sliding that takes place also changes as does the nature and magnitude of the stress system. Both of these aspects influence the way a coating wears. These changes imply that different types of material would exhibit different angular dependency.

4.10 MICROSTRUCTURAL INVESTIGATION

4.10.1 Powder morphology

SEM micrograph of fly ash-illmenite powders prior to coating are shown in Fig.4.14

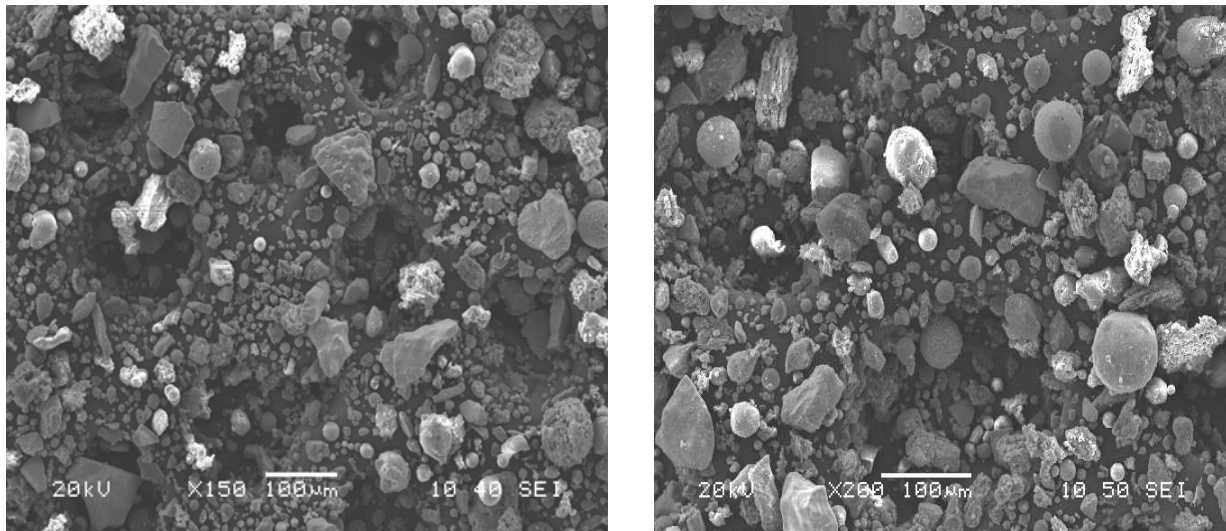


Fig. 4.14 SEM micrograph of fly ash-illmenite raw powders (i.e. feed stock)

It is observed that the Particles are of varied particle sizes, irregular in shape. Some particles are elongated type and some are multifaceted.

4.10.2 Microstructure of Coating Surface

The interface adhesion of the coatings depends on the coating morphology and inter-particle bonding of the sprayed powders. SEM micrograph of fly ash-illmenite coating surfaces are shown in Fig 4.15.

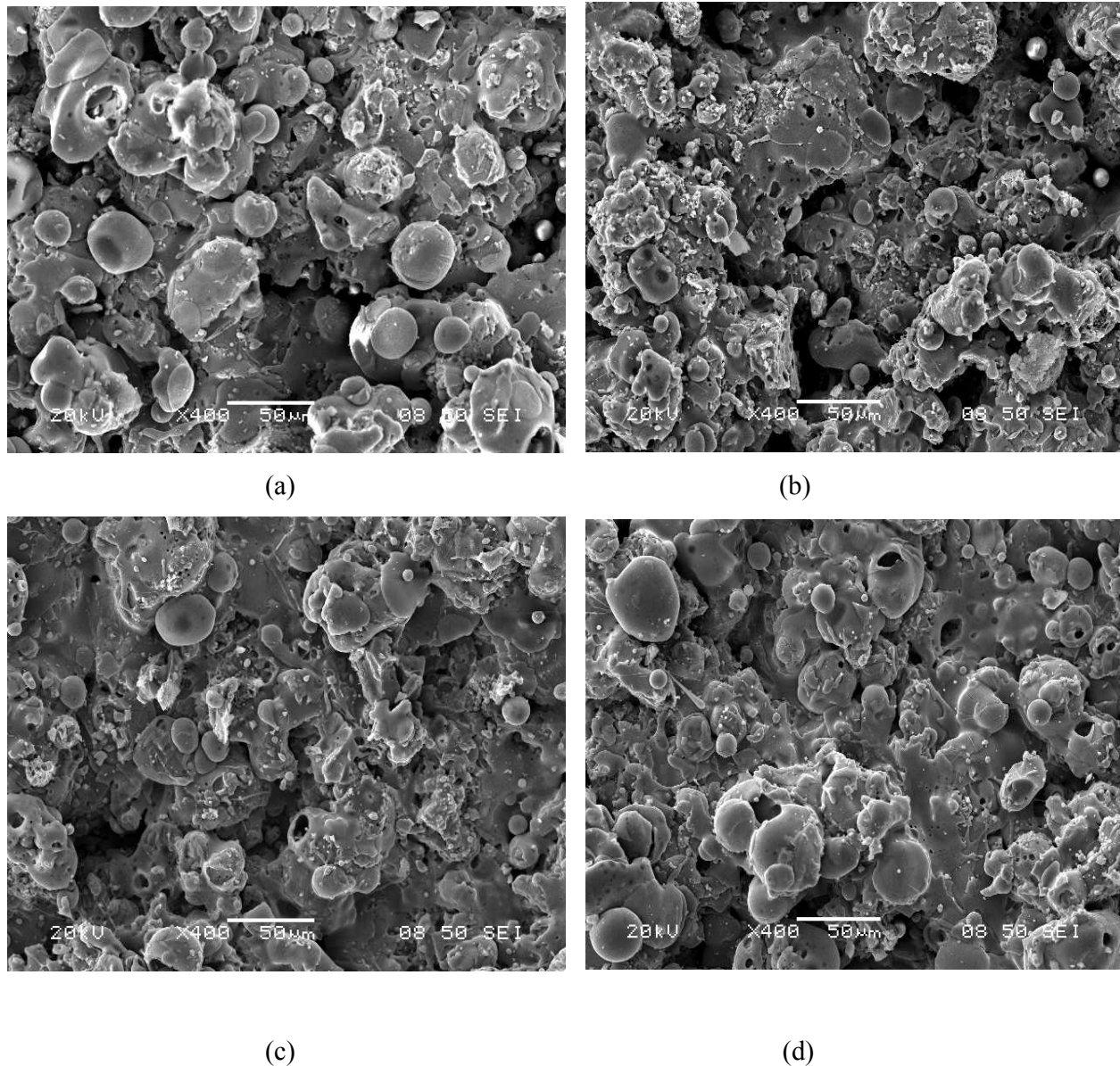


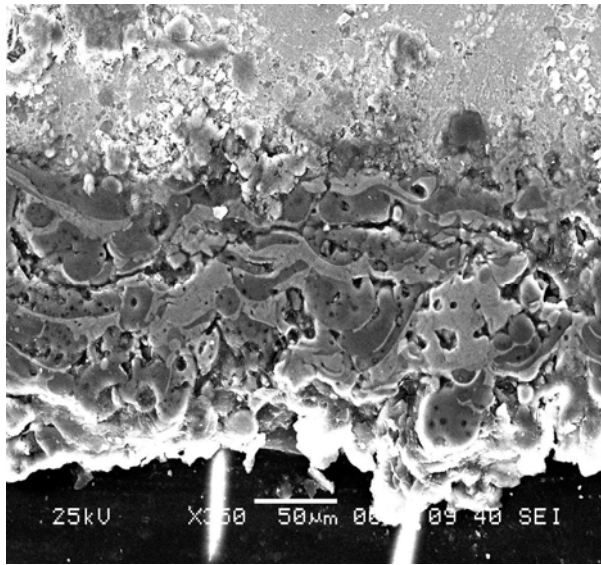
Fig.4.15 Surface Morphology of fly ash-illmenite coatings deposited at different power level i.e. (a) 11kW (b) 15kW(c) 18kW, (d) 21kW.

The coating deposited at 11kW power level on copper substrate [Fig-4.15(a)], shows a uniform distribution of molten/semi molten and un-melted particles. More amounts of cavitations are

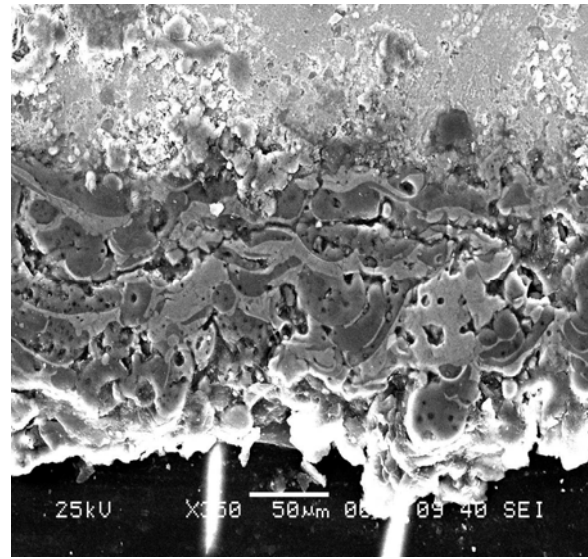
observed. Some large cavities/pores are seen on the inter particle boundaries and triple particle/grain junctions. These may have originated during solidification of particles from molten/semi-molten state. The coating made at 15 kW [Fig-4.15(b)] bears a different morphology. Some flattened regions are observed, indicative of complete melting of particles during coating deposition. The grains/particles are mostly equi-axed type with little boundary mismatch between them. Amount of cavitations is less. Coating deposited at further higher power level i.e. at 18 kW [Fig-4.15(c)] bears a different morphology. Larger portions of the coatings exhibit flattened regions, which have been formed during solidification of molten particles that have fused together in lumps. Less cavitation is observed at inter grain boundaries. This may be the reason for better interface adhesion of the coating onto the substrate that's why improvement of adhesion strength. For the coatings deposited at further higher power level i.e. at 21 kW, [Fig-4.15(d)] the surface morphology is completely different. A large number of spheroidal particles of varied diameters are seen, which might have been formed due to breaking / fragmentation of bigger particles during in flight traverse through the plasma jet and then solidified in form of spheres due to rapid solidification i.e. very fast rate of quenching. Some cracked particles are also seen in [Fig. 4.15 (d)], indicative of thermal quench effect. The amount of porosity appears to have increased again. Amount of cavitations is more than that observed in the previous case i.e. in [Fig. 4.15 (c)]. This might be the cause for the improper inter-particle bonding and poor stacking to the substrate which have resulted in lowering the interface bond strength.

4.10.3 Interface Morphology

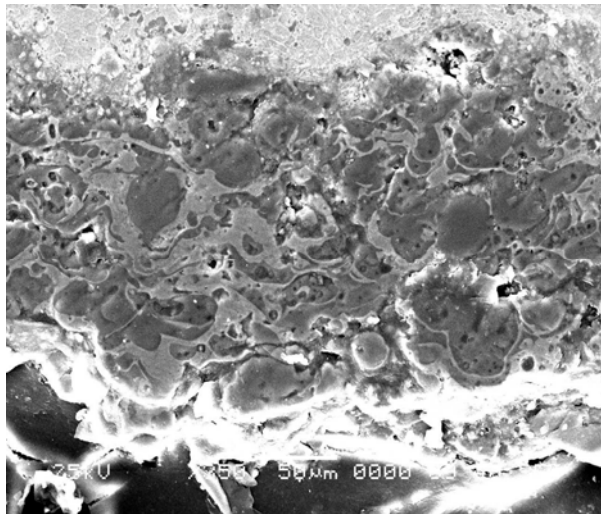
The coating substrate interface plays the most important role on the adhesion of the coating. The surface morphology of the coating cannot predict the interior (layer deposition) structures and their importance/acceptability. The polished cross-sections of the samples are examined under SEM and are shown in Fig. 4.16



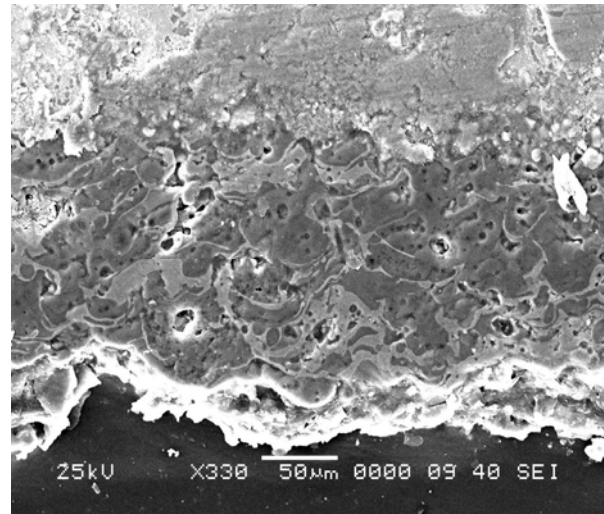
(a)



(b)



(c)



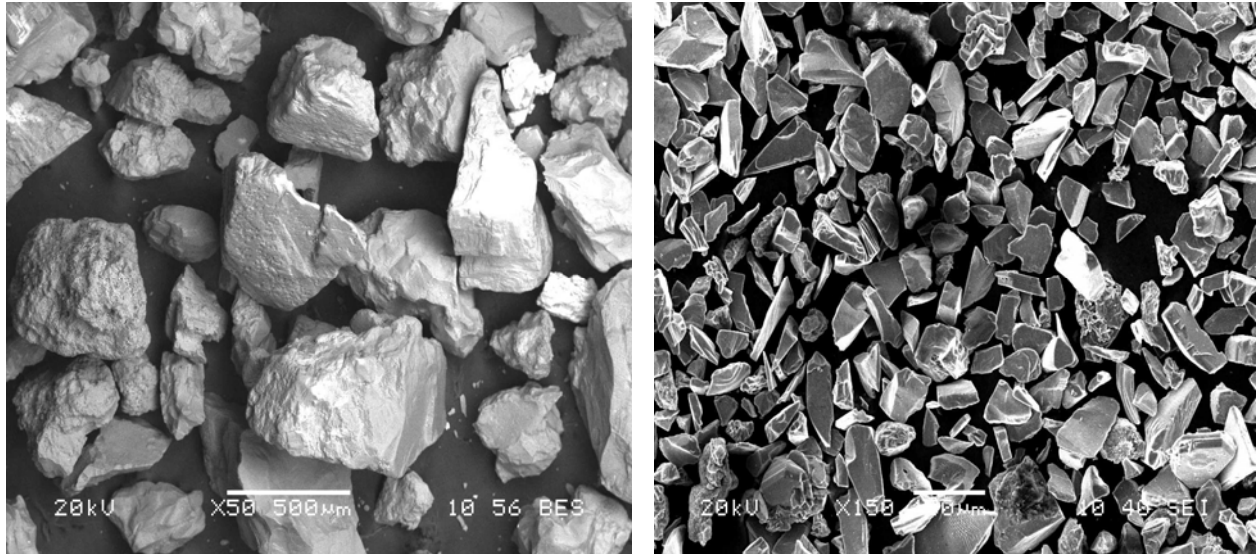
(d)

Fig.4.16 Interface morphology of fly ash-illmenite coatings deposited on mild steel substrates, at (a) 11kW (b) 15kW (c) 18 kW (d) 21kW power level.

From the micrograph good interface matching (mostly mechanical interlocking) of the coatings are seen. Lamellar structure confirms the solidification of molten particles to form splats during coating deposition. The coating is homogenous through out the length for the coating deposited at 18kW than that of other coatings, hence has shown higher adhesion strength.

4.10.4 Morphology of the Erodent

The morphology of the erodents (i.e. Sand and SiC) are shown in Fig. 4.17.



(a)

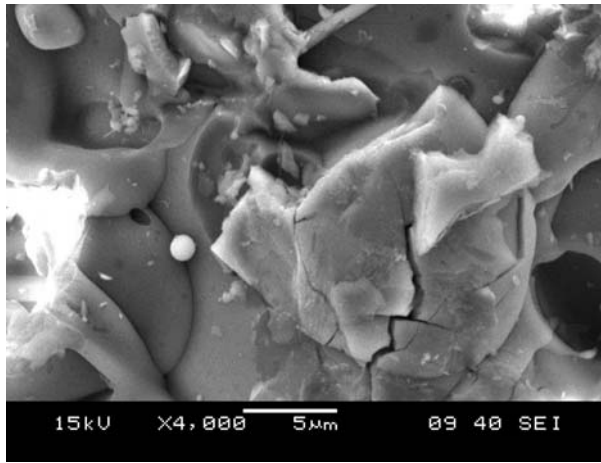
(b)

Fig.4.17 Surface Morphology of (a) dry silica sand and (b) silicon carbide erodent.

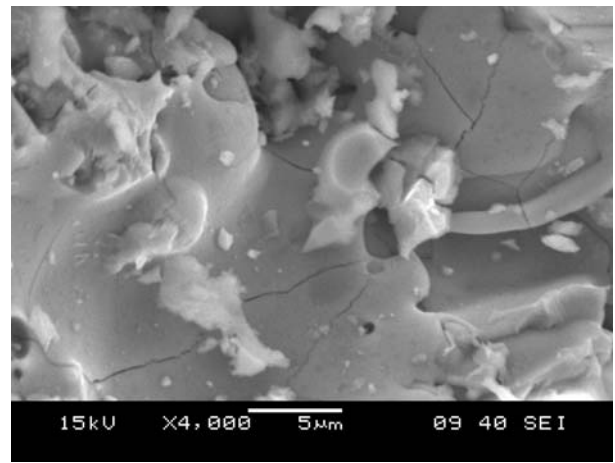
It can be visualized that, the sand particles are mostly spherical or rounded/equiaxed in shape with cleavage/quasi-cleavage edges, as observed in Fig.4.17 (a); while silicon carbide particles are having multiple angular facets and sharp edges, as seen in Fig.4.17 (b). This might be the cause of fast rate of removal of material through chipping/plowing of the surface when silicon carbide is used as erodent there by leading to higher amount of material loss (i.e. cumulative mass loss). Hence erosion rate is higher when SiC is used. So there is negligible crack initiation/formation, than minor chipping is observed on the eroded surfaces.

4.10.4 Worn surfaces

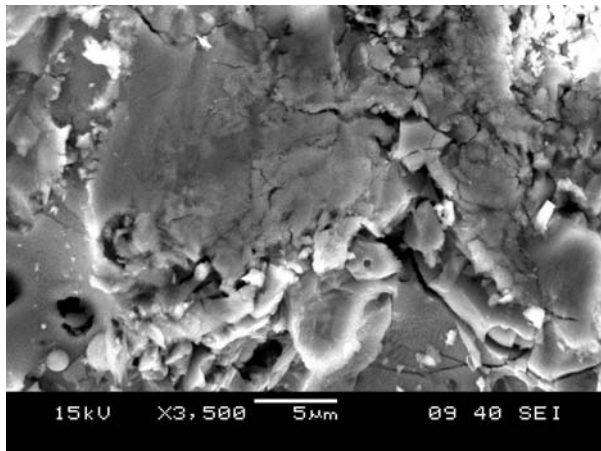
Surface morphology of fly ash-illmenite coating eroded (with dry silica sand) at different impact angles are shown in Fig.4.18.



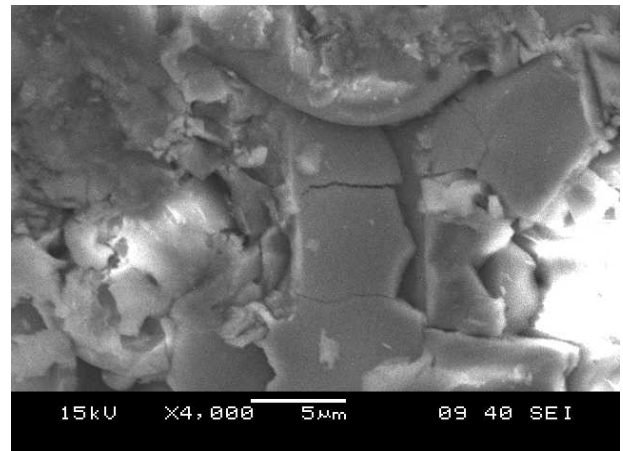
(a)



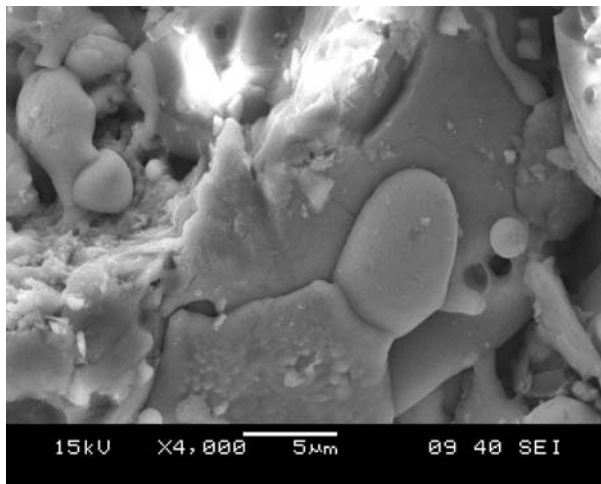
(b)



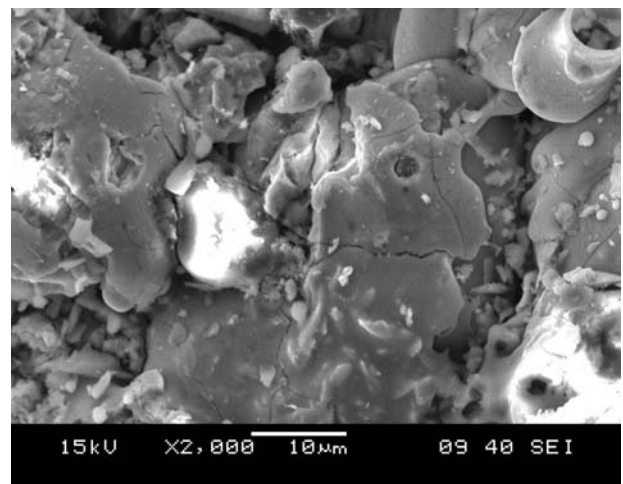
(c)



(d)



(e)



(f)

Fig.4.18 Micrographs of eroded surfaces of coatings deposited at (a) 11kW and (b) 18kW for 90° angle of impact; (c) 11 kW and (d) 18kW for 60° angle of impact and (e)11kW and (f)18kW for 30° angle of impact.

It can be seen from the Fig.4.15 (a) and (b) that when the erodent impacted at 90° the crack is initiated at a point, spreads from that point in all directions along the splats/grains. When the erodent impacts at 60° , Fig.4.15(c) & (d), the crack propagation is mainly at grain/splat boundaries. Load is transferred to lower layer and cracks have spread over there, instead of the top layer where the erodent has impacted; which may be due to the dominance of the tangential force component of the impinging particles/erodent. Similar type of structural evidence has also been observed by Westergard et al. [125]. They have reported that, the erosion rate is higher due to higher amount of plastic deformation which takes place at 60° . At an impact angle of 30° , chipping away of layers occurs and hence more cavities are formed. Some cracks are observed and appears to have originated and spread along grains/splats boundaries.

Chapter 5

CONCLUSIONS

CHAPTER 6

CONCLUSIONS

The conclusions drawn from the present work are as follows:

- Commercial grade fly ash-illmenite mixed powders in the size range 40 to 100 μ m is coatable on metal substrates employing thermal plasma spray technique. Coatings made with fly ash-illmenite possess desirable coating characteristics comparable to those of other conventional plasma sprayed ceramic coatings.
- Deposition efficiency for flyash-illmenite coatings ranges from 25% to 48% in case of mild steel substrate. It is interesting to note that the deposition efficiency has increased in a step up fashion with the increase in torch input power.
- Adhesion strength of the coating varies with operating power. Maximum adhesion strength of 6.732 MPa on mild steel substrate and of 5.842 Mpa on copper substrate is recorded on the coatings deposited at 18 kW. It is noted that, invariably in all cases, the interface bond strength increases with the input power to the torch up to a certain optimum power level and then shows a decreasing trend. Coating adhesion is better in case of mild steel substrate than of copper substrate.
- It is observed that the amount of porosity is more in case of the coatings made at lower (11kW) and higher (21kW) power levels. However; porosity is less for the coatings made at 18kW. The increased value of porosity may be the reason of low adhesion strength of the coatings deposited at low and at high power levels.
- The different phases observed in XRD studies, corroborates to the observation of different hardness values for (different) optically distinguished phases.

- Due to phase transformations and inter-oxide formation during plasma spraying at different power levels, changes in the coating characteristics such as hardness etc. are observed.
- Operating power level of the plasma torch influences the coating adhesion strength, deposition efficiency, coating thickness and coating hardness to a great extent. The coating morphology is also largely affected by the torch input power.
- The microstructures of the coatings are dependent on operating power level of the plasma torch, the physical characteristics such as coating porosity, phase transformation of the raw material during spraying.
- Initially the erosion rate increases sharply with time of impact and after certain time length of impacting, the erosion rate becomes lower in magnitude and finally reaches a steady state.
- The erosion wear rate is dependent on erodent dose, angle of attack, velocity of erodent, stand off distance and size of the erodent Taguchi experimental design identified impact angle and size of the erodent as the most significant parameters affecting the erosion wear rate of fly ash-illmenite coatings.
- The erosion rate is minimum at 30° angle of impact and is maximum at 90° when silica sand is used as erodent, while using silicon carbide as the erodent, the erosion wear is maximum at 60° impact angle.
- The erosion wear rate of the coatings is higher when eroded by SiC than that of by silica sand , which may be due not only to the morphology/structure but also to the hardness of the erodent material also.
- The mechanism of erosion wear at 90° impact angle is that, the abrasive particles impact and extrudes the surface of the coatings and produce indentations and extruded lips. The

lips become work hardened by repeated impact of the particles and eventually fall-off. Whereas, when erodent impact at acute angles erosion wear is dominated due to micro cutting, plowing and tunneling via pores and inter particle/grain boundaries.

- Erosion wear behavior is one of the main requirements of the coatings developed by plasma spraying for recommending specific application. In order to achieve tailored erosion wear rate accurately and repeatedly, the influence of the process parameters are to be controlled accordingly. The coating sustains erosion by solid particle impingement substantially and therefore fly ash-ilmenite can be considered as a potential coating material suitable for various tribological applications.

Scope for Future Work

The present work opens up a wide area for future investigators to explore many other aspects of fly ash-ilmenite coatings. Evaluation of thermal stability of these coatings is to be evaluated to find high temperature applications. Sliding wear behavior under different conditions can be investigated to identify suitable application areas. Post heat treatment of these coatings is to be made to ascertain further improvement in coating quality and properties.

REFERENCES

REFERENCES

1. Taylor P.R., Das A.K. - “Thermal Plasma Processing of Materials”— Power Beams and Materials Processing PBAMP, Mumbai, India:Allied Publishers Pvt. Ltd., (2002): pp.13-20 .
2. Bandopadhyaya P.P. – “Processing and Characterization of Plasma sprayed Ceramic coatings on Steel Substrate”—Ph.D.Thesis, IIT, Kharagpur, India (2000).
3. Mishra SC, et al. “Mineral processing recent advances and future trends”. New Delhi, India: Allied Publications, (1995):p. 837.
4. Thorpe, M.L., “Major Advances Noted in Thermal Spray Technology”, Advanced Materials and Processes, volume 1, (1993): p. 23-124
5. Lima C.R.C. and Trevisan R.E., “Graded plasma spraying of premixed metal ceramics powders on metallic substrates”, Journal of thermal spray technology, volume 6,(1997): p.199-204
- 6.Brown L.et al., Advances in Thermal Spraying , Oxford : Pergamon Press, (1986): p. 507.
7. Matejka.D., Benko B., Plasma Spraying of Metallic and Ceramic Materials, New York: Wiley Publication, (1989): p. 132.
- 8.. Heiman R.B ‘Plasma Spray Coating, Principle and Application’ , VCH, Weinheim, Germany, (1996).
9. Edwards R., “Cutting Tools”, The Institute of Materials, UK,(1993).
10. Budinski K. G., Surface Engg. For Wear Resistance, N.J., USA:,(1988).
11. Thorpe, M.L. Adv.Mater.Process.,143(5,50). (1993)
12. Metco Plasma Spraying Manual, Metco, USA,(1993).

13. Herman, H., plasma spray deposition processes MRS Bull., 13, 60-7, (1998)
14. Longo L. F., Thermal Spray Coatings, ASM, USA: (1985).
15. Meringolo V., Thermal Spray Coating, Tappi Press, Atlanta, USA (1983).
16. Wrigren J., Surf. Coat. Tech. Volume 45, (1991): p. 263.
17. Nicholas M. G. and Scott K. T., Surfacing Journal. Volume 12, (1981): p. 5.
18. Funk W. Goebe F., "Bond strength optimization of plasma-sprayed Cr_2O_3 layers by factorial two-level experiments." Thin Solid Film. Volume 128, (1985): p. 45.
19. Wielage B., Hofmann V., Steinhauser A., Zimmerman G., Wear. Volume 14, No. 2, (1998): P. 136.
20. Lee N. Y., Stinton D. P., Brandt C. C., Erdogan F., Lee Y. D. and Mutasim Z., J. Am. Cer. Soc., Volume 79, No. 12, (1996): P. 3003.
21. Nash A. R., Weare N. E. and Walker D. L., J. Metals. (1961), p. 473.
22. Ramchandran K. and Selvarajan P. A., Thin Solid Film. Volume 315, (1998): p. 149.
23. Ingham H. S. and Fabel A. J., Welding Journal. (1975): p. 101.
24. Hennaut J., Othmezzouri J. and Charlier J., Mat. Sc and Tech., Volume 11, (1995): p. 174.
25. Elvers B., Hawkins S. and Schultz G., Uhlmann's Encyclopedia of Industrial Chemistry, Volume 1/16, VCH, (1990): p. 433.
26. Tape N. A., Baker E. A. and Jackson B. C., Plating and Surface finishing, p. 30, 1976,.

27. Holm R., "The frictional force over the real area of Contact", Wiss. Vereoff. Siemens Werken, Volume17, No.4, (1938): p. 38-42.

28. Ashby M. F. and Lim S. C., "Wear - mechanism maps." Scripta Metallurgical et Materialia. Volume24, (1990): p. 805-810.

29. Wang Y., lei T.C. and Gao C.Q. "Influence of isothermal hardening on the sliding wear behaviour of 52100 bearing steel." Tribology International. Volume 23, No.1, (1990): p.47-63.

30. Soda N., "Wear of some F.F.C metals during unlubricated sliding part-1. Effects of load, velocity and atmospheric pressure on wear". Wear. Volume33, (1975):p. 1-16.

31. Burwell J.T. and Strang C.D, 'Metallic wear', Proc. Soc (London), 212A (1953), p. 470-477.

32. Burwell J .T. , "Survey of possible wear mechanisms." Wear. Volume1, (1957/58): p.119-141.

33. Zumgahr K.H., 'Microstructure and wear of materials' Elsevier , Amsterdam , (1987).

34. P.L.Ko, "Metallic wear-a review with special references to vibration-induced wear in power plant components." Tribology International. Volume 20, No. 1, (April 1987): p.66-78.

35. Eyre L.S., "Wear Characteristics of metals." Tribology International. (October 1976):p. 203-212.

36. Dowson, "Wear oh where." International Conference on wear of Materials, Vancouver Canada, April 14-18, (1985)

37. Peterson.M. B, "Advanced in tribo-materials I Achievements in Tribology", Amer. Soc. Mech. Eng., Volume1, New York, (1990):pp. 91-109.

38. Blau J., “Fifty years of research on the wear of metals.” Tribology International. Volume 30, No.5, (1997): p. 321-331.
39. Wang Y., “ Sliding wear behavior of ceramic, plasma sprayed on casting aluminum alloy against SiC ball.” Wear. Volume 161, (1993): p. 69.
40. Wang Y., Yuansheng J. and Shizhu W., “The tribological behaviour of various plasma-sprayed coatings against cast iron.” Wear. Volume 128, (1988): p. 265.
41. Jainjun W. and Qunji X., “Tribological properties of FeCl₃- graphite intercalation compound rubbed film on steel.” Wear. Volume 162 ,(1993): p. 229.
42. Lin J. F. and Li T. R., “Studies of Al₂O₃(p)- 6061 Al composites under dry sliding conditions using scanning electron microscopy, energy-dispersive spectrometry and X-ray diffractometry.” Wear. Volume 160, (1990): p. 201.
43. Ahn H.S. and Kwon O. K., “Classification of wear debris using a neural network.” Wear. Volume 225, (1999): p. 814.
44. Jainjun W., Qunji X. and Huiling W., Wear. Volume 152, (1992): p. 161.
45. L athabai S., Ottmuller M. , Fernandez I., “Solid particle erosion behaviour of thermal sprayed ceramic, metallic and polymer coatings.” Wear. Volume 221, (1998): p. 93.
46. Zhou L., Gao Y. M., Zhou J.E. , Zhou Q. D., “Corrosion wear behaviour of ion-implanted steel.” Wear. Volume 176, (1994): p. 39.
47. Ahn H. S. and Kwon O. K., “Wear behaviour of plasma-sprayed partially stabilized zirconia on a steel substrate.” Wear. Volume 162 – 164, (1993):p. 636.

48. Quinn T. F. J. and Winer W. O., “The thermal aspects of oxidational wear.” Wear. Volume 102, (1985): p. 67.
49. Kim A. Y., Lim D. S. and Ahn H. S., J. Kor. Cer. Soc, Volume 30, (1993): p. 1059.
50. Ahn H. S. , Kim J. Y. and Lim D. S., “A study on wear and erosion of sialon-SiN whisker ceramic composites.” Wear. Volume 203 – 204, (1997): p. 77.
51. Fu Y., Batchelor A. W., Xing H. and Gu Y., “ Failure mechanisms of plasma nitrided Inconel 718 film.” Wear. Volume 210, (1997): p. 157.
52. Sun Y., Li B., Yang D., Wang T., Sasaki Y. and Ishii K., Wear. Volume 215, (1998): p. 232.
53. Song Y. S., Han J. C. , Park M.H., Ro B.H., Lee K. H., Byun E. S., Sasaki S., Proc. 15th International Thermal Spray Conference, 25th – 29th May (1998) , France , pp. 225.
54. Mendelson M. I., Wear. Volume 50, (1978): p. 71.
55. Metco Technical Bulletin on TiO₂, Metco Inc., NY, USA;,(1971).
56. Dai W. W., Ding C. X., Li J. F., Zhang Y.F. and Zhang P. Y., “ Wear mechanism of plasma-sprayed TiO coating against stainless steel .” Wear. Volume 196, (1996): p. 238.
57. Suh N. P., “The delamination theory of wear”, Wear. Volume 25, (1973): p. 111.
58. H. So, “The mechanism of oxidational wear.” Wear. Volume 184, (1995): p. 161.
59. Eyre T. S., “ Effect of boronising on friction and wear of ferrous metals.”, Wear. Volume 34, (1975): p. 383.
60. Halling, Principles of Tribology, The Mcmillan Press Ltd, NY, USA, (1975).

61. Guilmad Y., Denape J. and Patil J. A., “ Friction and wear thresholds of alumina-chromium steel pairs sliding at high speeds under dry and wet conditions.” Trib. Int. Volume 26, (1993): p. 29.
62. Gee M. G., “The formation of aluminium hydroxide in the sliding wear of alumina.” Wear. Volume 153, (1992): p. 201.
63. Mcpherson R., J. Mat. Sc., Volume 8, (1973) : p. 859.
64. Mcpherson R., J. Mat. Sc., Volume 15, (1980) : p. 3141.
65. Lopez A. R. D. A ., Faber K. T. , J. Am. Cer. Soc., Volume 82, No.8, (1999): p. 2204.
66. Ono H., Teramoto T. and Shinoda T., Mat and Mfg. Processes. Volume 8(4&5), (1993): pp.451.
67. Musikant S., What Every Engineer Should Know About Ceramics, Marcell Dekker Inc, NY, USA:. (1991).
68. Wahi R. P. and Lischner B., J. Material Science. Volume 15, (1980): p. 875.
69. Yamamota T., Olsson M. ,Hogmark S., “Wear mechanisms and tribo mapping of AlO and SiC in dry sliding.” Wear. Volume 174,(1994): p. 21.
70. Ramachandran K., Selvarajan V., Ananthapadmanabhan P. V., Sreekumar K.P. “Microstructure, adhesion, microhardness, abrasive wear resistance of the plasma sprayed alumina and alumina – titania coatings.” Thin solid film. Volume 315, (1998): p. 144-152.

- 71.** Krishnakumar V. and Swarnamani S., “Tribological Behaviour of plasma sprayed Al_2O_3 and TiO_2 ceramic hard coating under dry contact.”, IIT Madras, department of applied Mechanics, (1996).
- 72.** Westergard R., Axen N., Wiklund U., Hogmark S., “An evaluation of plasma sprayed ceramic coatings by erosion, abrasion testing.” Wear. Volume 246, (2000): p.12-19.
- 73.** Normand B., Fervel V. , Coddet C. , Nikitine V. , “Tribological properties of plasma sprayed alumina–titania coatings:role and control of the microstructure.” surface and coatings technology. Volume123, (2000): p.278-287.
- 74.** Vijayakumar K., Sharma Apurbba Kr., Mayuram M.M., Krishnamurthy R., “Response of plasma sprayed alumina – titania ceramic composite to high frequency impact loading.”Materials letters. Volume 56, (2002): p. 252-262.
- 75.** Ananthapadmanabhana P. V. , Thiagarajana T .K., Sreekumara K. P., Satputea R.U., Venkatramania N., Ramachandran. K., “Co-spraying of alumina– titania: correlation of coating composition and properties with particle behaviour in the plasma jet.” Surface and coatings technology. Volume168, (2003): p.231-240.
- 76.** Bounazef Mokhtar, Guessasma Sofiane, Montavon Ghislain, Coddet Christian . “Effect of APS process parameters on wear behaviour of alumina – titania coatings.” Materials Letters. Volume 58, (2004): p. 2451-2455.
- 77.** Xinhua Lin , Yi Zeng, Xiaming Zhou , Chuanxian Ding ,” Microstructure of alumina /3wt.% titania coatings by plasma spraying with nanostructured powders.” Materials science and engineering. Volume357, (2003): p. 228-234.
- 78.** Sofiane Guessasma , Mokhtar Bounazef , Philippe Nardin , Tahar Sahraoui, “ Note on POD test parameters to study wear behaviour of alumina– titania coatings .” ceramics International. Volume52, (2006): p. 13-19.

- 79.** Okumus S. Cem, “ Microstructural and mechanical characterization of plasma sprayed Al_2O_3 – TiO_2 composite ceramic coating on Mo / cast iron substrates .” materials Letters. Volume59, (2005): p. 2314-3220.
- 80.** Habib K . A. , Saura J. J , Ferrer C. , Damra M. S. , Giménez E. , Cabedo L., “Comparison of flame sprayed Al_2O_3 / TiO_2 coatings: Their microstructure, mechanical properties and tribology behaviour.”surface and coatings technology. (2006).
- 81.** Sampath S, Herman H, Yazici RM,. Protective coatings processing and characterization. USA: The Mineral Metals and Materials Society; (1990). p. 145.
- 82.** Mishra SC, et al. Mineral processing recent advances and future trends. New Delhi, India: Allied Publications; (1995). p. 837.
- 83.** Tiwari S., Saxena M.. “Use of fly ash in high performance industrial coatings”. British Corrosion Journal, Volume 34, Number 3, (1999):pp. 184-191(8)
- 84.** Mishra S.C., Satpathy Alok, Singh K.P., Sethy Sangeeta, P.V.A., Padmanabham K.P. Sreekumar and Satpute R., “Plasma Spray Coating of Fly Ash on Metals for Tribological Application.” Proceedings of the International Seminar on Mineral Processing Technology Chennai, India. (2006):pp. 825 - 829.
- 85.** Mishra S. C.,. Rout K. C, Padmanabhan P. V. A. and Mills B., “Plasma spray coating of fly ash pre-mixed with aluminium powder deposited on metal substrates” Journal of Materials Processing Technology, Volume 102, Issues 1-3, (2000): Pages 9-13
- 86.** Sidhu Buta Singh, Singh Harpreet, Puri D. Prakash S. “Wear and oxidation behaviour of shrouded plasma sprayed fly ash coatings”. Tribology International, 40, (2007):p.800–808

- 87.** Satapathy Alok, Mishra S.C, Mohanty Umaprasad, Mishra Tapan Kumar and Raulo Pratyusha P. “plasma spraying of red mud-fly ash mixture on metals : an experimental study” .National Conference on Materials and Related Technology, TIET, Patiala, India (2003)

- 88.** Zhang Tiancheng , Luo Yichun , Li D.Y. , “ Erosion behavior of aluminide coating modified with yttrium addition under different erosion conditions.” Surface and Coatings Technology. Volume126, (2000):p.102-109.

- 89.** Herman H., Sampath S., “ Thermal Spray Coatings”, Metallurgical and Ceramic Protective Coatings, Chapman and Hall, London, UK,(1996) p. 261.

- 90.** Mishra S.B., Chandra K., Prakash S. , Venkataraman B. , “Characterisation and erosion Behaviour of a plasma sprayed Ni₃Al Coating on a Fe-based superalloy.” Materials Letters. Volume59, (2005): p.3694 – 3698.

- 91.** Westergard R., Erickson L. C., Axen N., Hawthorne H. M. , Hogmark S., Tribol. Int. Volume 31, No.5, (1998):p. 271.

- 92.** Pfender E., “Fundamental studies associated with the plasma spray process.” Surf. Coat. Technol. , Volume34 (1988) :p.1.

- 93.** O. Knotek , in: R.F. Bhushah (Ed.) , Handbook of Hard Coatings Deposition Technologies, Properties and Applications, p.92, (2001)

- 94.** Guo D.Z., Li F.L., Wang J.Y, Sun J.S., “Effects of post-coating processing on structure and erosive wear characteristics of flame and plasma spray coatings.” Surf. Coat. Technol. , Volume73, (1995):p. 73.

- 95.** Restall J. E., Proc. 3rd Conf. on Gas Turbine Materials in a Marine Environment, Bath, , Ministry of Defence, London, Session V, Paper 10, (1976)

- 96.** Galsworthy J. C., Restall J. E. and Booth G. C., Brunetaud in R., Coutsouradis D., Gibbons T. B., Lindblom Y., Meadowcroft D. B. and Stickler R. (eds.), Proc. Conf.on High Temperature Alloys for Gas Turbines, Liege, October 4 - 6, (1982), p. 207.

- 97.** Kosel T.H., Friction, Lubrication and Wear Technology, ASM Handbook, Volume 18, p. 199. (1992)

- 98.** Tabakoff W., “Erosion resistance of superalloys and different coatings exposed to particulate flows at high temperature.” Surf. Coat. Technol., Volume 120– 121, (1999): p.542.

- 99.** Levy A.V., “The erosion of carbide-metal composites”, Surf. Coat. Technol. ,Volume36, (1988):p. 387.

- 100.** Shipway P.H., Hutchings I.M., “Measurement of coating durability by solid particle Erosion.”, Surf. Coat. Technol.,Volume 71, (1995): p. 1.

- 101.** Brunton J.H., Rochester M.C., Preece C.M., ‘Erosion of solid surfaces by the impact of liquid drops.’ Erosion, Treatise on Materials Science and Technology, Volume 16,Academic Press, New York, (1979), p. 185–248.

- 102.** Lesser M.B., Field J.E., “The impact of compressible liquids.” Ann. Rev.Fluid Mech. Volume15 (1983):p. 97–122.

- 103.** Field J .E., ELSI conference: invited lecture—“liquid impact: theory, experiment, Applications.” Wear.Volume233–235, (1999): p. 1–12.

- 104.** Lee M.K., Kim W. W., Rhee C.K., Lee W.J., “ Liquid impact erosion mechanism and theoretical impact stress analysis in TiN- coated steam turbine blade materials.” Metal. Mater. Trans. VolumeA 30 (1999) : p.961–968.

- 105.** Angle P. A. Impact Wear of Materials, Elsevier; New York, (1976).

106. Tucker R.C. Jr., On the relationship between the microstructure and the wear characteristics of selected thermal spray coatings. Proceeding of ITSC, Kobe, Japan, (1995), pp. 477 – 482.

107. Alonso F., Fagoaga I. and Oregui P. :- “Erosion Protection of carbon – epoxy composites by plasma sprayed coatings.” Surface & Coatings Technology. Volume 49, Issues 1 – 3, 10 Dec, (1991): p.482 – 488.

108. Tabakoff W., Shanov. V. -- “Erosion rate testing at high temp. for turbo machinery use.” Surface & Coatings Technologies. Volume 76 – 77, Part I, Nov (1995), p. 75 – 80.

109. Hawthorne F. M, Erickson L. C., Ross D., Tan H. and Troczynski T., “The microstructural dependence of wear and indentation behaviour of some plasma- sprayed alumina coatings.” Wear. Volume 203 – 204, (1997): p. 709.

110. Zhang X. S., Clyne T. W. and Hutchings I. M., Surf. Engg., Volume 13, No.5, (1997): p.393.

111. Roberto Jose, Branco Tavares, Gansert Robert , Sampath Sanjay , Christopher C. Berndt , Herman Herbert –“ Solid Particle Erosion of Plasma Sprayed Ceramic Coatings. ”Materials Research. Volume 7, No.1. (2004): p. 147-153.

112. Chen H., Lee S.W., Du Hao, Ding Chuan X and Cho Chul Ho; “ Influence of feed stock and spraying parameters on the deposition efficiency. and microhardness of plasma sprayed zirconia coatings.” -- Materials Letter .Volume 58, Issues 7 – 8, (March 2004): p.241 – 1245.

113. Mishra S. C., Rout K. C., Ananthapadmanabhan P. V. and Mills B. , “ Plasma Spray Coating of Fly Ash Pre-Mixed with Aluminium Powder Deposited on Metal Substrates.”, J. Material Processing Technology.,Volume 102, 1 – 3 ,(2000): p. 9 – 13.

114. Lima C.R.C., Trevisan R.E., J.Themal Spray Tech.,Volume 62,(1997): p. 199.

- 115.** Lalleman G . – Tallaron, “ Study of Microstructure and adhesion of spinelles coatings formed by plasma spraying.”, Ph. D. Thesis No. 96 – 58 (1996) E.C. Lyon, France.
- 116.** Bullard D.E., Lynch D.C., Davenport W.G. Non-equilibrium Plasma Processing of ores, , Thermal Plasma Applications in Materials and Metallurgical Processing , N.El-Kaddah, The Minerals and Materials Society ,p.175 –191. (1992)
- 117.** Kitamura T., Shibata K., Takeda K., ‘In-flight reduction of Fe_2O_3 , Cr_2O_3 , TiO_2 and Al_2O_3 by Ar- H_2 plasma.’ Thermal Plasma Applications in Materials and Metallurgical Processing, N.El-Kaddah, The Minerals and Materials Society, p. 209-219. (1992)
- 118.** Sahin Y., “The Prediction of Wear Resistance Model for The Metal Matrix Composites.” Wear .Volume 258, (2005): p. 1717-1722.
- 119.** Levy A. V., “ The erosion corrosion behavior of protective coatings.” Surf. and Coating Technology, 36, (1988):p.387 – 406.
- 120.** Chabane Bousbaa, Abderrahim Madjoubi, Mohamed Hamidouche, Nourredine Bouaouadja,, “Effect of annealing and chemical strengthening on soda lime glass erosion wear by sand blasting.” Journal of European ceramic society, 23 , (2003):p.331-343.
- 121.** Bousid, S. and Bouaouadja, N., “Effects of impact angles on glass surface eroded by sand blasting.” J.Eur. Cer. Soc., 20(4), (2000):p.481-488.
- 122** Lishizhou, Dong XiangLin, Erosion wear and Fretting Wear of Materials (in Chinese), Publisher of Mechanical Industry, Beijing,(1987).
- 123.** Hutchings I. M., Tribology: Friction and Wear of Engineering Materials. Metallurgy & Material Science Series. (1992)
- 124.** Manish, R., Vishwanathan, B. and Sundarajan, G., “The solid particle of polymer matrix composites.” Wear, 171, (1994):149–161.

125. Westergard R., Erickson L.C, Axen N., Hawthornes H.M. and Hogmark S., “The erosion and abraision characteristics of alumina coatings plasma sprayed under different spraying conditions.” Tribology International. Vol.31, (1998):p.271-279

PUBLICATIONS

1. “ Plasma Spray Composite Coating on Metals Using Fly ash and Illmenite.” S.C.Mishra, Alok Satapathy, Satyabati Das, S.Sarkar, P.V.Ananthapadmanabhan, K.P.Sreekumar. Journal of Manufacturing Engineering,2008,vol.3,Issue.1,(in press)
2. “Investigation on Composite Coating of Low Grade Minerals.” S.C.Mishra, Satyabati Das, Alok Satapathy, S.Sarkar P.V.Ananthapadmanabhan , K.P.Sreekumar. Journal of Reinforced Plastics and Composites,2008,(in press)
3. “Erosion wear of plasma spray fly ash-illmenite composite coating” S.C.Mishra, Satyabati Das, Alok Satapathy P.V.Ananthapadmanabhan K.P.Sreekumar, Journal of Reinforced Plastics and Composites,2008,(accepted)
4. “Analysis of erosion wear of plasma sprayed ceramic coating using Taguchi Technique.” S.C.Mishra, Satyabati Das, Alok Satapathy P.V.Ananthapadmanabhan K.P.Sreekumar. Tribology Transactions,2008,(accepted)